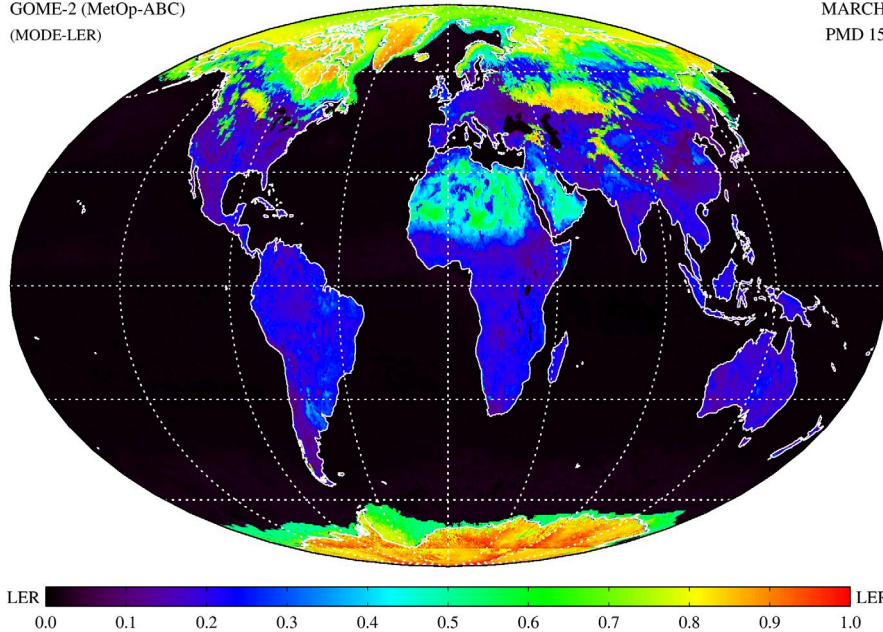


AC SAF VALIDATION REPORT

GOME-2 (MetOp-ABC)
(MODE-LER)

MARCH
PMD 15



GOME-2 surface DLER product

Product Identifier

O3M-402.1

Product Name

Directional Lambertian-equivalent reflectivity
(DLER) from GOME-2 / Metop-A+B+C

Authors

L.G. Tilstra
O.N.E. Tuinder
P. Stammes

Institute

Royal Netherlands Meteorological Institute (KNMI)
Royal Netherlands Meteorological Institute (KNMI)
Royal Netherlands Meteorological Institute (KNMI)

Document status sheet

Issue	Date	Page(s)	Modified Items / Reason for Change
1/2014	17-04-2014	all	first official version
2/2014	30-06-2014	all	changes and update after DRR
3/2014	11-07-2014	32,33	further changes after DRR
4/2014	13-11-2014	7	added “Heritage” section (1.2)
1/2017	23-02-2017	all	added new sections 1.4, 8 and 9 ; updated old sections 3–8 ; renamed old sections 3–6 ; updated old sections 1.3 and 1.6 ; updated tables 1 and 2 ; further textual changes
2/2017	02-05-2017	all	changes and update after DRR
1/2019	14-01-2019	all	extended and updated sections 1 and 2 ; updated sections 3–8 ; added figure 1 ; updated figures 2–27 and tables 1–10
2/2019	27-03-2019	all	changes and update after DRR ; added new sections 8 and 9
1/2022	02-12-2022	all	updated sections 1–10 ; updated figures 2–39 and tables 1–10
1/2023	05-01-2023	9,62	version created for the review of O3M-402.1
1/2024	19-11-2024	all	changes and update after DRR

Contents

– Introduction to EUMETSAT Satellite Application Facility on Atmospheric Composition monitoring (AC SAF)	8
1 Introduction	9
1.1 Document purpose and scope	9
1.2 Heritage	9
1.3 GOME-2 surface LER product	9
1.4 Changes w.r.t. previous versions of the products	10
1.5 Validation approach	11
1.6 Suggested reading material	11
1.7 Abbreviations and acronyms	12
2 Surface reflectivity databases for the UV-VIS	15
2.1 Introduction	15
2.2 Tables	16
3 MSC-LER: GOME-2ABC versus GOME-1	20
3.1 Global maps of the differences	20
3.2 Statistical analysis of the differences	22
3.3 Conclusion of the comparison with GOME-1	26
4 MSC-LER: GOME-2ABC versus OMI	27
4.1 Global maps of the differences	27
4.2 Statistical analysis of the differences	29

4.2.1	MIN-LER product	29
4.2.2	MODE-LER product	29
4.3	Conclusion of the comparison with OMI	36
5	MSC-LER: GOME-2ABC versus MERIS	37
5.1	Global maps of the differences	37
5.2	Conclusion of the comparison with MERIS	37
6	PMD-LER: GOME-2ABC versus OMI	41
6.1	Global maps of the differences	41
6.2	Statistical analysis of the differences	41
6.3	Conclusion of the comparison with OMI	45
7	PMD-LER versus MSC-LER	47
7.1	Global maps of the differences	47
7.2	Statistical analysis of the differences	50
7.3	Conclusion of the PMD-LER versus MSC-LER comparison	50
8	Comparing DLER with MODIS BRDF	57
8.1	Case 1: Amazonia (vegetation)	57
8.2	Case 2: Equatorial Africa (vegetation)	59
8.3	Case 3: Libyan desert	60
8.4	Summary	61
9	Comparison with previous version of the database	62
9.1	v4.1 versus v3.1 – Main Science Channels	62
9.2	v4.1 versus v3.1 – PMD bands	64
9.3	Summary	66

10 Summary and conclusions	67
A Tables with extended validation results	69
References	84

Introduction to EUMETSAT Satellite Application Facility on Atmospheric Composition monitoring (AC SAF)

Background

The monitoring of atmospheric chemistry is essential due to several human caused changes in the atmosphere, like global warming, loss of stratospheric ozone, increasing UV radiation, and pollution. Furthermore, the monitoring is used to react to the threads caused by the natural hazards as well as follow the effects of the international protocols.

Therefore, monitoring the chemical composition and radiation of the atmosphere is a very important duty for EUMETSAT and the target is to provide information for policy makers, scientists and general public.

Objectives

The main objectives of the AC SAF is to process, archive, validate and disseminate atmospheric composition products (O₃, NO₂, SO₂, BrO, HCHO, H₂O, OClO, CO, NH₃), aerosol products and surface ultraviolet radiation products utilising the satellites of EUMETSAT. The majority of the AC SAF products are based on data from the GOME-2 and IASI instruments onboard MetOp satellites.

Another important task besides the near real-time (NRT) and offline data dissemination is the provision of long-term, high-quality atmospheric composition products resulting from reprocessing activities.

Product categories, timeliness and dissemination

NRT products are available in less than three hours after measurement. These products are disseminated via EUMETCast, WMO GTS or internet.

- Near real-time trace gas columns (total and tropospheric O₃ and NO₂, total SO₂, total HCHO, CO) and ozone profiles
- Near real-time absorbing aerosol indexes from main science channels and polarisation measurement detectors
- Near real-time UV indexes, clear-sky and cloud-corrected

Offline products are available within two weeks after measurement and disseminated via dedicated web services at EUMETSAT and AC SAF.

- Offline trace gas columns (total and tropospheric O₃ and NO₂, total SO₂, total BrO, total HCHO, total H₂O) and ozone profiles
- Offline absorbing aerosol indexes from main science channels and polarisation measurement detectors
- Offline surface UV, daily doses and daily maximum values with several weighting functions

Data records are available after reprocessing activities from the EUMETSAT Data Centre and/or the AC SAF archives.

- Data records generated in reprocessing
- Surface Lambertian-equivalent reflectivity
- Total OClO

Users can access the AC SAF offline products and data records (free of charge) by registering at the AC SAF web site.

More information about the AC SAF project, products and services: <https://acsaf.org/>

AC SAF Helpdesk: helpdesk@acsaf.org

X/Twitter: https://x.com/Atmospheric_SAF

1 Introduction

1.1 Document purpose and scope

This document is the Validation Report (VR) for the GOME-2 surface LER products developed at KNMI in the framework of the AC SAF (Satellite Application Facility on Atmospheric Composition Monitoring). The aim of this VR is to present the validation approach, to present the results from the validation, and to report to the users the quality that they may expect.

1.2 Heritage

The GOME-2 surface LER product is the Lambertian-equivalent reflectivity (LER) of the Earth's surface observed by the GOME-2 instruments. It is the improved follow-up of earlier surface LER databases based on observations performed by GOME-1 (on the ERS-2 satellite) [Koelemeijer *et al.*, 2003] and OMI (on the Aura satellite) [Kleipool *et al.*, 2008].

The GOME-2 surface LER products are developed at KNMI in the framework of the AC SAF (Satellite Application Facility on Atmospheric Composition Monitoring). The algorithm described in the ATBD [Tilstra *et al.*, 2024a] is the direct continuation of the algorithms that were developed by Koelemeijer *et al.* [2003] and Kleipool *et al.* [2008]. Also see Tilstra *et al.* [2017, 2021].

1.3 GOME-2 surface LER product

Only one GOME-2 surface LER product is produced. Previously, separate products were produced for each GOME-2 instrument. The current product is based on the combination of level-1 data from the GOME-2 instruments on the Metop-A, Metop-B, and Metop-C satellites:

Product ID	Satellite	Platforms	Surface LER versions
O3M-402.1	GOME-2	Metop-A + Metop-B + Metop-C	MSC & PMD

The input consists of GOME-2 level-1b orbits (or PDUs) of version 6.3 (R3) and 7.0 (NRT). The data processor can process level-1b files from the GOME-2A, GOME-2B, and GOME-2C instruments, without discriminating much between these. The data from GOME-2A are taken from the period 4 January 2007 to 15 July 2013 (MSC-LER) or from the period 13 March 2008 to 15 July 2013 (PMD-LER). The data from GOME-2B are from the period 1 November 2012 to 31 August 2022. The data from GOME-2C are from the period 29 January 2019 to 31 August 2022.

The GOME-2A/-B/-C surface LER product consists of two surface LER versions: one version based on GOME-2 observations by the Main Science Channels (MSCs) and one version based on GOME-2 observations by the Polarisation Measurement Devices (PMDs). The PMD-based version has the advantage over the MSC-based version that the surface LER is based on eight times as many observations, each with an eight times smaller footprint. This makes the retrieved surface LER less susceptible to residual cloud contamination, statistically more stable, and therefore more reliable. It also allows a higher spatial resolution of the intrinsic surface LER database grid.

On the other hand, the surface LER of the PMD-based version is available only for a fixed list of wavelength bands. The wavelengths of the PMD bands are given in Table 3. This limitation is not an issue for the MSC-based surface LER. Here the list of wavelength bands could be determined based on user needs, taking into account that the wavelength bands have to be positioned in the continuum, avoiding strong absorption bands. The selected wavelength bands are given in Table 2.

1.4 Changes w.r.t. previous versions of the products

The GOME-2 surface LER database studied in this version of the VR carries version number 4.1 and is the improved follow-up of database version number 3.1 that was studied in VR version 2/2019 and of database version number 2.1 that was studied in VR version 2/2017.

Version 2.1 was an improvement on the preceding official version 1.1 that was studied in VR version 4/2014. The improvements were an improved detection and handling of cloud contamination due to residual clouds, an improved method of filling in empty grid cell resulting from polar night, access to collocated (level-2) ozone products instead of assimilated total ozone fields, and a much improved error calculation. However, the most important improvement was the increased spatial resolution near coastlines. The method that was used to achieve this adopts the concept of dynamic gridding and is/was described extensively in the ATBD [Tilstra *et al.*, 2024a].

Version 3.1 was based on a combination of GOME-2A and GOME-2B data. The resulting surface LER database covered a period of more than 10 years (2007–2018). The largest improvement, however, was the introduction of the directionally dependent surface LER (DLER) which was developed specifically to provide viewing-geometry dependent surface reflectivity information for the Metop satellites and for other polar satellites with similar equator crossing times. A number of new wavelength bands were added, most notably those at 685, 697 and 712 nm which were specifically meant to support O₂-B band retrievals. This required updating the atmospheric correction to include water vapour (H₂O) dependence. Other improvements were a higher spatial resolution for certain mountain ranges and deserts and a 2D interpolation/smoothing scheme to better accommodate the different intrinsic spatial resolutions in the database grid. Next to this, the overall data consistency was improved by recalibrating GOME-2A reflectance data relative to GOME-2B reflectance data.

Version 4.1 is based on a combination of GOME-2 data from all three Metop satellites (A, B, C). The time range was extended to the year 2022, thereby covering more than 15 years. However, because of the overlap of the three instruments in time, more than 20 years of data were combined. The larger amount of data leads to a reduction of cloud contamination and a higher stability of the resulting surface LER fields. Other improvements are the addition of a new wavelength band at 747 nm, better performance at coastlines, and a more stable and more complete statistical error field. A more detailed overview of all processor versions is given in the PUM [Tilstra *et al.*, 2024b].

1.5 Validation approach

Validation of the retrieved GOME-2 surface LER databases is performed by comparison with other surface LER databases that are discussed in section 2. From these, the GOME surface LER database [Koelemeijer *et al.*, 2003] makes most sense as a reference, because of the orbital and instrumental similarities between GOME and GOME-2, and their overlapping set of LER wavelength bands. Note that the GOME surface LER database was essentially retrieved using the MIN-LER approach (as explained in the ATBD), so a comparison with the GOME surface LER will in principle only allow validation of the GOME-2 surface LER determined using the MIN-LER approach.

The OMI surface LER database [Kleipool *et al.*, 2008] may be used for validation of the wavelengths below 500 nm. The OMI surface LER database is important as a reference because it uses the same surface LER retrieval approach as the one described in the ATBD. That is, both the GOME-2 MIN-LER and the GOME-2 MODE-LER products can be compared to their OMI counterparts and this will provide information on the correctness of the GOME-2 surface LER algorithm and database.

Additionally, we compare the GOME-2 surface LER database with the MERIS black-sky albedo (BSA) database [Popp *et al.*, 2011]. This is strictly speaking not correct, because the BSA is the integral of the bidirectional reflectance distribution function (BRDF) over the entire hemisphere whereas the LER is derived from the much smaller range of viewing angles of the satellite's observation geometry. Also, the LER approach by definition assumes a direction-independent surface albedo. Note that the comparison only makes sense over land, because the MERIS surface LER values over sea are not retrieved from MERIS observations. They were taken directly from the GOME surface LER database. As a result, the MERIS database only offers limited importance as a reference.

1.6 Suggested reading material

Herman, J. R., and E. A. Celarier (1997), Earth surface reflectivity climatology at 340–380 nm from TOMS data, *J. Geophys. Res.*, 102(D23), 28,003–28,011, doi:10.1029/97JD02074.

Koelemeijer, R. B. A., J. F. de Haan, and P. Stammes (2003), A database of spectral surface reflectivity in the range 335–772 nm derived from 5.5 years of GOME observations, *J. Geophys. Res.*, *108*(D2), 4070, doi:10.1029/2002JD002429.

Gao, F., C. B. Schaaf, A. H. Strahler, A. Roesch, W. Lucht, and R. Dickinson (2005), MODIS bidirectional reflectance distribution function and albedo Climate Modeling Grid products and the variability of albedo for major global vegetation types, *J. Geophys. Res.*, *110*, D01104, doi:10.1029/2004JD005190.

Kleipool, Q. L., M. R. Dobber, J. F. de Haan, and P. F. Levelt (2008), Earth surface reflectance climatology from 3 years of OMI data, *J. Geophys. Res.*, *113*, D18308, doi:10.1029/2008JD010290.

Popp, C., P. Wang, D. Brunner, P. Stammes, Y. Zhou, and M. Grzegorski (2011), MERIS albedo climatology for FRESCO+ O2 A-band cloud retrieval, *Atmos. Meas. Tech.*, *4*, 463–483, doi:10.5194/amt-4-463-2011.

Tilstra, L. G., O. N. E. Tuinder, P. Wang, and P. Stammes (2017), Surface reflectivity climatologies from UV to NIR determined from Earth observations by GOME-2 and SCIAMACHY, *J. Geophys. Res. Atmos.*, *122*, 4084–4111, doi:10.1002/2016JD025940.

Tilstra, L. G., O. N. E. Tuinder, P. Wang, and P. Stammes (2017), Surface albedo databases determined from PMD measurements performed by the GOME-2 instrument, *Proceedings of the 2017 EUMETSAT Meteorological Satellite Conference*, EUMETSAT, Rome, Italy, 2017.

Tilstra, L. G., O. N. E. Tuinder, P. Wang, and P. Stammes (2021), Directionally dependent Lambertian-equivalent reflectivity (DLER) of the Earth’s surface measured by the GOME-2 satellite instruments, *Atmos. Meas. Tech.*, *14*, 4219–4238, doi:10.5194/amt-14-4219-2021.

1.7 Abbreviations and acronyms

AAH	Absorbing Aerosol Height
AAI	Absorbing Aerosol Index
AC SAF	Satellite Application Facility on Atmospheric Composition Monitoring
AOT	Aerosol Optical Thickness
ATBD	Algorithm Theoretical Basis Document
BBA	Biomass Burning Aerosol
BRDF	Bidirectional Reflectance Distribution Function
BSA	Black-Sky Albedo
CDOP	Continuous Development & Operations Phase
COT	Cloud Optical Thickness

DAK	Doubling-Adding KNMI
DDA	Desert Dust Aerosols
DOAS	Differential Optical Absorption Spectroscopy
DU	Dobson Units, 2.69×10^{16} molecules cm^{-2}
ENVISAT	Environmental Satellite
EOS-Aura	Earth Observing System – Aura satellite
ERS	European Remote Sensing Satellite
ESA	European Space Agency
ETOPO-4	Topographic & Bathymetric data set from the NGDC, 4 arc-min. resolution
EUMETSAT	European Organisation for the Exploitation of Meteorological Satellites
FOV	Field-of-View
FRESCO	Fast Retrieval Scheme for Clouds from the Oxygen A band
FWHM	Full Width at Half Maximum
GMTED2010	Global Multi-resolution Terrain Elevation Data 2010
GOME	Global Ozone Monitoring Experiment
HDF	Hierarchical Data Format
IT	Integration Time
KNMI	Koninklijk Nederlands Meteorologisch Instituut
LER	Lambertian-Equivalent Reflectivity
LUT	Look-Up Table
MERIS	Medium Resolution Imaging Spectrometer
MetOp	Meteorological Operational Satellite
MLS	Mid-Latitude Summer
MSC	Main Science Channel
NetCDF	Network Common Data Form, NetCDF
NGDC	NOAA's National Geophysical Data Center (Boulder, Colorado, USA)
NISE	Near-real-time Ice and Snow Extent
NOAA	National Oceanic and Atmospheric Administration
NRT	Near-Real-Time
OMI	Ozone Monitoring Instrument
O3M SAF	Satellite Application Facility on Ozone and Atmospheric Chemistry Monitoring
PMD	Polarisation Measurement Device
PSD	Product Specification Document
PUM	Product User Manual
RAA	Relative Azimuth Angle
RMSE	Root-Mean-Square Error
RTM	Radiative Transfer Model

SAA	Solar Azimuth Angle
SCIAMACHY	Scanning Imaging Absorption Spectrometer for Atmospheric Chartography
SZA	Solar Zenith Angle
S5	Sentinel-5 mission
S5P	Sentinel-5 Precursor mission
TBA	To be Added
TBC	To be Confirmed
TBD	To be Defined
TEMIS	Tropospheric Emission Monitoring Internet Service
TOA	Top-of-Atmosphere
TOMS	Total Ozone Mapping Spectrometer
TROPOMI	Tropospheric Monitoring Instrument
UTC	Coordinated Universal Time
UV	Ultraviolet
VAA	Viewing Azimuth Angle
VIS	Visible
VR	Validation Report
VZA	Viewing Zenith Angle

2 Surface reflectivity databases for the UV-VIS

2.1 Introduction

Surface reflectivity databases are needed for cloud, aerosol and trace gas retrievals. One of the first surface reflectivity databases retrieved using UV satellite remote sensing techniques is the Total Ozone Mapping Spectrometer (TOMS) [Heath *et al.*, 1975] surface LER database [Herman and Celarier, 1997]. The retrieved reflectivity is the Lambertian-equivalent reflectivity (LER) of the surface found from scenes which are assumed to be cloud free. The retrieval method relies on the removal of the (modelled) atmospheric contribution from the (observed) top-of-atmosphere (TOA) reflectance. In this approach the surface is defined to behave as a Lambertian reflector. The TOMS surface LER database ($1.25^\circ \times 1^\circ$) was retrieved for 340 and 380 nm only, which limits its usefulness.

The GOME [Burrows *et al.*, 1999] surface reflectivity database provides the surface LER on a $1^\circ \times 1^\circ$ grid for 11 wavelength bands between 335 and 772 nm [Koelemeijer *et al.*, 2003]. Although this is already quite an improvement with respect to the TOMS surface LER database, the database is still limited in quality by the low number of measurements from which the surface LER had to be extracted and the large GOME footprint size (see Table 1). In particular, pixels over sea are often affected by residual cloud contamination. In these cases the surface LER was retrieved from scenes which were not sufficiently cloud free. In other cases, e.g. snow surfaces, the surface LER was retrieved from a few measurements which were not representative for the entire month.

A large improvement on these points is the OMI surface reflectivity database [Kleipool *et al.*, 2008]. First, the OMI instrument [Levelt *et al.*, 2006] has a much smaller footprint size ($24 \times 13 \text{ km}^2$ at nadir) combined with a larger global coverage (see Table 1). This leads to better statistics and results in a higher accuracy for the surface LER retrieval. Second, the higher number of measurements allows for inspecting the distribution of scene LERs for each grid cell, and for making a more sophisticated selection of representative (cloud-free) scenes instead of directly taking the minimum scene LER value like in the case of the TOMS and GOME databases. Third, the provided OMI surface LER database has a higher spatial resolution ($0.5^\circ \times 0.5^\circ$ grid). The limiting factor is the OMI wavelength range. The longest wavelength in the OMI surface LER database is 499 nm.

The GOME-2 series of satellite instruments does not have some of the limitations of the satellite instruments mentioned above and can be used to create a better, more reliable surface LER database [Tilstra *et al.*, 2017]. To be more specific, it has the spectral range of GOME but a much smaller footprint ($80 \times 40 \text{ km}^2$) which is constant over the full swath width. Additionally, the number of measurements that are available per longitude/latitude cell is smaller than that of OMI, but enough to perform a statistical analysis on the distribution of retrieved scene LERs. Developing the GOME-2 surface LER retrieval the approach used for the OMI surface LER database was followed.

The main advantage of the GOME-2 surface LER database with respect to the OMI surface LER database is the wider wavelength range of the GOME-2 instrument. Additionally, the retrieval algorithm uses aerosol information, available via the GOME-2 Absorbing Aerosol Index (AAI) product, to filter out scenes with large aerosol loadings, as these scenes can result in inaccurate values of the retrieved surface LER. This filtering is especially important for locations over desert areas.

2.2 Tables

In Table 1 we summarise the properties of the discussed surface reflectivity databases. For GOME-2 we provide the specifications for the MSC-based and PMD-based algorithms. In Table 2 we list the wavelength bands of the surface reflectivity databases, and their application. In Table 3 we provide the wavelengths of the GOME-2 PMD bands, relevant to the PMD-based algorithm. The selection of the wavelength bands for the GOME-2 MSC-LER was influenced largely by the already existing surface LER databases. Below 325 nm the surface contribution to the TOA reflectance is low, which prevents an accurate retrieval of the surface LER below this wavelength. For the GOME-2 PMD-LER this means that the surface LER for PMDs 1–3 cannot be retrieved, as indicated.

instrument	TOMS	GOME	OMI	MSC - GOME-2 - PMD	
satellite	Nimbus-7	ERS-2	Aura	MetOp-A/B/C	
equator crossing time (LT)	12:00	10:30	13:45	09:30	
dayside flight direction	S→N	N→S	S→N	N→S	
number of days for global coverage	1	3	1	1.5	
pixel size at nadir (km × km)	50 × 50	320 × 40	24 × 13	80 × 40	10 × 40
number of usable pixels per orbit	~12000	~1300	~83000	~11000	~88000
dataset time range (*)	1978–1993	1995–2000	2004–2007	2007–2022	2008–2022
selected wavelength bands	2	11	23	27	12
wavelength range covered (nm)	340–380	335–772	328–499	328–772	333–799
band width (nm)	1.0	1.0	1.0	1.0	see text
spatial resolution (°lon × °lat)	1.25 × 1.0	1.0 × 1.0	0.5 × 0.5	1.0 × 1.0	0.5 × 0.5
reference	HC1997	KHS2003	KDHL2008	TTWS2017/2021	

Table 1: Characteristics and properties of the UV-VIS surface LER databases, and of the satellite instruments from which they are derived. Wavelength band information can be found in Tables 2/3.

(*)The longer the time period covered, the higher the number of times a certain region has been observed. This increases the chances of having observed this region under clear sky conditions. Occasional reprocessing over longer time periods therefore increases the quality, stability, and reliability of the surface LER product. GOME-2A data are available from January 2007; GOME-2B data are available from November 2012; GOME-2C data are available from January 2019.

Table 2: Wavelength bands of the four monochromatic surface LER databases, and their applications. All wavelength bands are located outside strong gaseous absorption bands in order to avoid complicated modelling of the radiative transfer. The number of wavelength bands is also given.

λ (nm)	TOMS	GOME	OMI	GOME-2	application / relevance
328			+	+	LER, ozone, HCHO, SO ₂
335		+	+	+	LER, ozone, HCHO
340	+			+	LER, aerosol, HCHO, BrO
342			+		LER, aerosol, HCHO, BrO
345			+		LER, aerosol, HCHO, BrO
354			+	+	LER, aerosol, HCHO, BrO, OCIO
367			+	+	LER, aerosol, OCIO
372			+		LER, aerosol, OCIO
376			+		LER, aerosol, OCIO
380	+	+	+	+	LER, aerosol, OCIO
388			+	+	LER, aerosol, OCIO
406			+		LER, aerosol
416		+	+	+	LER, aerosol
418			+		LER, aerosol
425			+	+	LER, aerosol, NO ₂
440		+	+	+	LER, aerosol, NO ₂
442			+		LER, aerosol, NO ₂
452			+		LER, aerosol, NO ₂
463		+	+	+	LER, aerosol, NO ₂ , O ₂ -O ₂
471			+		LER, aerosol, NO ₂ , O ₂ -O ₂
477			+		LER, aerosol, NO ₂ , O ₂ -O ₂
488			+		LER, aerosol, NO ₂ , O ₂ -O ₂
494		+	+	+	LER, aerosol, NO ₂ , O ₂ -O ₂
499			+		LER, aerosol
510				+	LER, aerosol
526				+	LER, aerosol, vegetation
546				+	LER, aerosol, vegetation
555		+		+	LER, aerosol, vegetation
564				+	LER, aerosol, vegetation, O ₂ -O ₂

585				+	LER, aerosol, vegetation, O ₂ -O ₂ , H ₂ O
610		+		+	LER, aerosol, H ₂ O
640				+	LER, aerosol, H ₂ O
670		+		+	LER, aerosol, H ₂ O, O ₂ -B
685				+	LER, aerosol, H ₂ O, O ₂ -B
697				+	LER, aerosol, H ₂ O, O ₂ -B
712				+	LER, aerosol, H ₂ O, O ₂ -B
747				+	LER, aerosol, O ₂ -A
758		+		+	LER, aerosol, O ₂ -A
772		+		+	LER, aerosol, O ₂ -A
Total:	2	11	23	27	

Table 2: Wavelength bands of the four monochromatic surface LER databases, and their applications. All wavelength bands are located outside strong gaseous absorption bands in order to avoid complicated modelling of the radiative transfer. The number of wavelength bands is also given.

The widths of the PMD bands are not provided in Table 3, but these (and other information) can be found in the “GOME-2 Factsheet” [EUMETSAT, 2021]. Additionally, Figure 1 provides a graphical representation of the spectral response functions of the PMD bands. The spectral response functions were determined using the slit functions of the individual detector pixels that make up the PMD bands. Note that we use the data from the PMD-p detector, not from the PMD-s detector. Ideally, PMD-p and PMD-s detectors should provide the same reflectance. In practice, they do not.

PMD	λ (nm)	application / relevance	PMD	λ (nm)	application / relevance
01	313	not retrieved	09	461	LER, aerosol, NO ₂ , O ₂ -O ₂
02	318	not retrieved	10	520	LER, aerosol
03	325	not retrieved	11	555	LER, aerosol, vegetation
04	333	LER, ozone, HCHO	12	590	LER, aerosol
05	338	LER, aerosol, HCHO, BrO	13	640	LER, aerosol, H ₂ O
06	369	LER, aerosol, OCIO	14	757	affected by O ₂ absorption
07	382	LER, aerosol, OCIO	15	799	LER, aerosol
08	414	LER, aerosol	PMD band definition v3.1, PMD-p detector		

Table 3: Wavelength information for the PMD bands used in the PMD-based surface LER algorithm. The wavelength definition follows PMD band definition v3.1, so the information applies to MetOp-A PMD data from after 11 March 2008 as well as to all MetOp-B and MetOp-C PMD data.

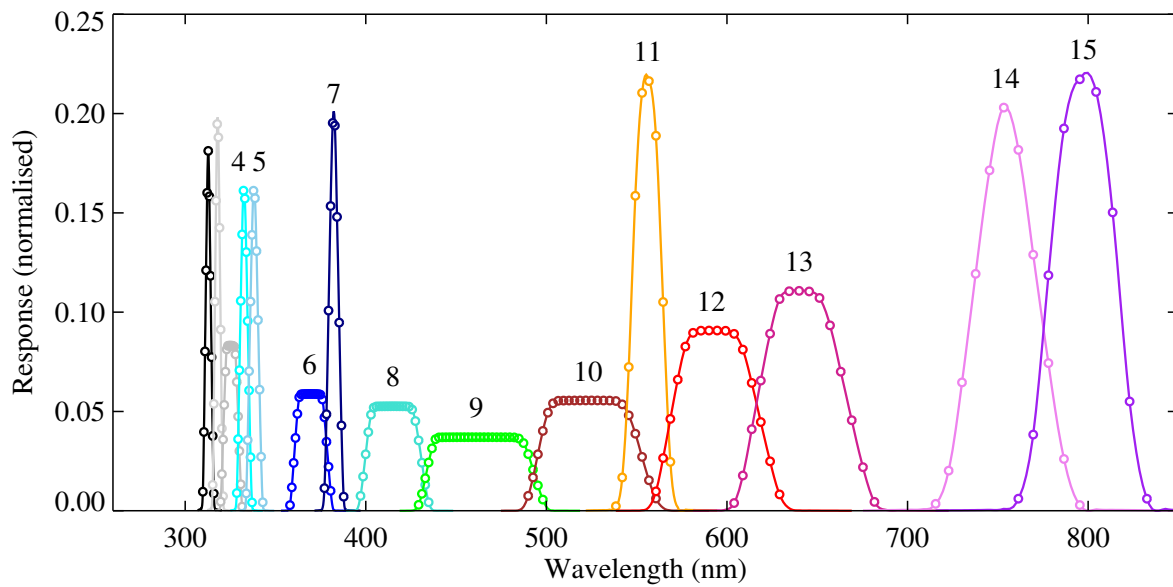


Figure 1: Spectral response functions of the fifteen GOME-2 PMD bands, determined using the slit functions of the underlying detector pixels of the PMD band. Only PMD bands 4–15 are labelled.

For some of the PMD bands the relatively broad wavelength range covered leads to inference with absorption bands. For instance, PMD 14 overlaps with the oxygen-A absorption band and this affects the retrieved surface LER. Likewise, PMD 15 is affected somewhat by water vapour absorption.

3 MSC-LER: GOME-2ABC versus GOME-1

In this section, we compare the GOME-2ABC surface LER product with the GOME-1 surface LER product. Because of the orbital and instrumental similarities between GOME-1 and GOME-2, the GOME-1 surface LER product should, at least on paper, be the ideal reference. Note, however, that the GOME-1 surface LER database was retrieved only using the MIN-LER approach (as explained in the ATBD). As a result, the GOME-1 surface LER database can only be used to validate the GOME-2ABC surface LER database determined using the MIN-LER approach.

All eleven wavelength bands of the GOME-1 surface LER database were included in the GOME-2 surface LER databases. We can, therefore, analyse the entire wavelength range covered.

3.1 Global maps of the differences

For each month of the year and for each wavelength band in the GOME-1 surface LER database (see Table 2) we calculate the difference in surface LER provided by the GOME-2ABC and GOME-1 surface LER databases. A typical outcome is shown in Figure 2, which presents a global map of the surface LER difference at the 772-nm wavelength band for the month March. The overall quality is good, but the GOME-2ABC surface LER is lower than the GOME-1 surface LER. The difference clearly depends on surface type. For surfaces with a higher surface reflectivity (land, snow, ice) the bias is more negative than for surfaces with a lower surface reflectivity (ocean).

There are a few regions where the surface LER difference is found to be positive (indicated by the red areas in Figure 2). At a first glance, some of these red areas appear to be partly caused by differences in snow/ice presence. Such differences could be related to actual differences in the snow/ice situation during the observed periods (GOME-1: 1995–2000; GOME-2ABC: 2007–2022). Note, however, that most of the “red” regions are located close to land/sea boundaries. This is rather suspicious and the large pixel size of the GOME-1 measurements (see Table 1) has had a hand in the appearance of these features (see, for instance, the discussion in *Popp et al.* [2011]). In fact, now that the spatial resolution of the GOME-2 surface LER database has been increased near the coastline, the differences that are found are more prominent. In the comparisons with higher resolution databases, such as the OMI surface LER database (see section 4), the differences have become smaller. This indicates that the attempt to increase the resolution near the coastlines was in fact successful.

Also notice that the correction for cloud contamination in the GOME-1 surface LER retrieval produces certain features in Figure 2. To be a bit more explicit, as an example we mention that the $5^\circ \times 5^\circ$ box near 80°N , 0°E coincides with one of the $5^\circ \times 5^\circ$ boxes used in the GOME-1 surface LER algorithm to search for replacement values [*Koelemeijer et al.*, 2003].

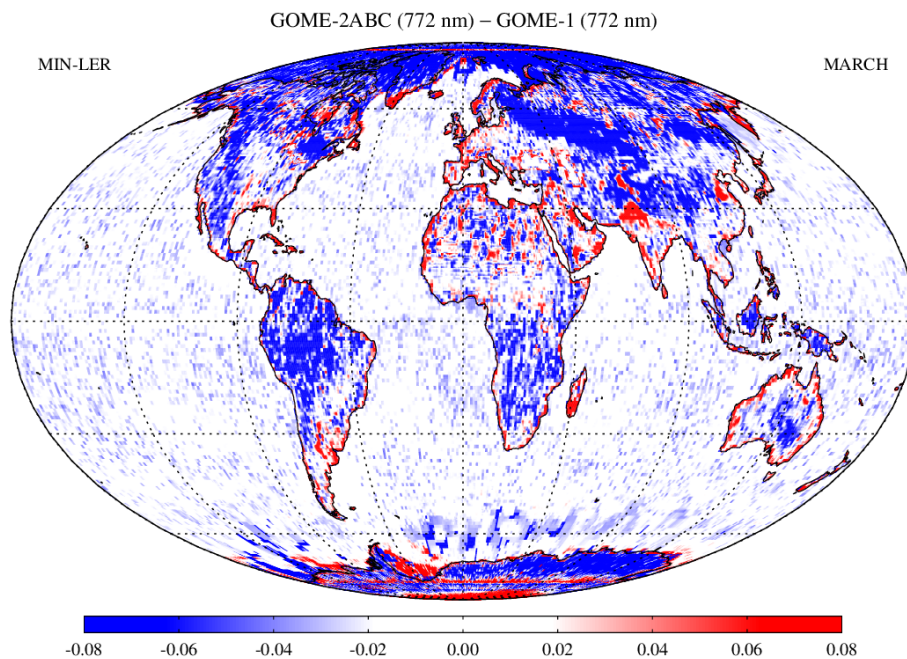


Figure 2: Map of the difference between the 772-nm surface LER from the GOME-2ABC and GOME-1 surface LER databases. The MIN-LER is used here. Over the ocean, the agreement is fair, but there clearly is a negative offset. Over land, this negative bias can go up to as much as 0.06.

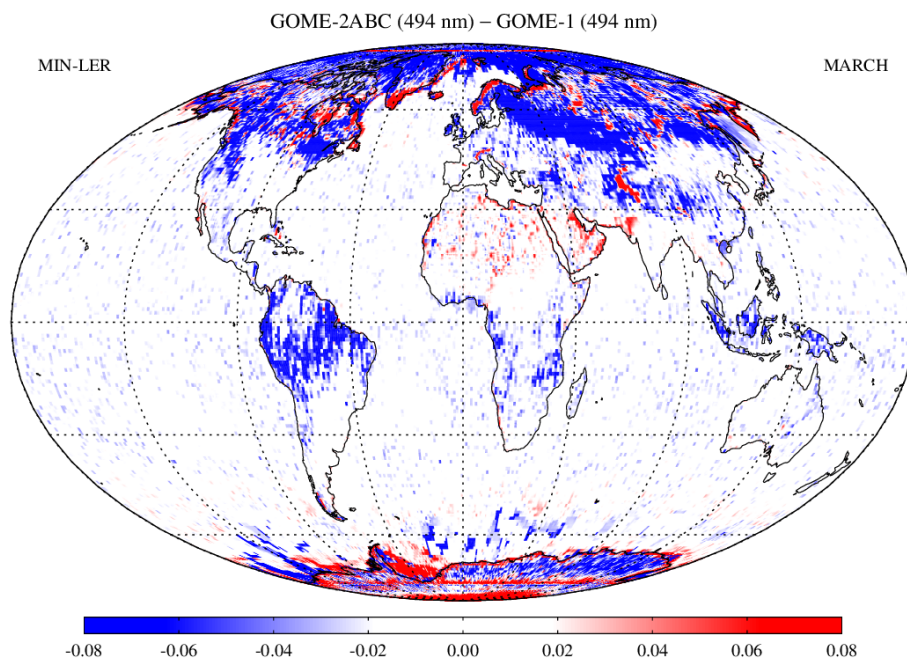


Figure 3: Map of the difference between the 494-nm surface LER from the GOME-2ABC and GOME-1 surface LER databases. Over the ocean, the agreement is good, but also for this wavelength there is an offset. Over land, the agreement is good, apart from a negative bias.

In Figure 3 we present a similar plot for the same month of the year (March) but for the 494-nm wavelength band. For this wavelength band the agreement between the GOME-2ABC and GOME-1 surface LER appears to be better. Over the ocean the absolute difference is lower than at 772 nm and well within the 0.01 level, despite the fact that the surface LER at 494 nm is normally larger than at 772 nm (and larger differences could be expected). The remaining larger negative values can be related to remaining cloud contamination in the GOME-1 surface LER. Over land the negative bias found earlier at 772 nm is again present, albeit less pronounced than for the 772-nm wavelength band. The agreement seems to be better at 494 nm compared to 772 nm, but this may also be caused by the fact that the surface LER values over land are also typically lower at 494 nm than at 772 nm. For snow/ice surfaces the negative bias is maximal, which again points to a dependence of the surface LER difference on surface type. All in all the agreement is good also for this wavelength band.

3.2 Statistical analysis of the differences

To provide a more statistical analysis of the differences between the GOME-2ABC and GOME-1 surface LER databases, we present in Figure 4 histograms of the surface LER differences. We only consider surface LER data with latitudes between 60°N and 60°S, thereby excluding data measured for extreme solar zenith angles as well as data located near the polar regions. The black histograms represent all possible scenes, the blue histograms are based on scenes over water, the green histograms are based on scenes over land and/or snow/ice. The histograms are provided for each month of the year, for the 494-nm wavelength band. The mean of the distribution is represented by the dashed vertical line, the mode of the distribution is given by the dotted vertical line. The histograms in Figure 4 confirm the lower values already reported in the previous section.

In Figure 5 we present the result for the same month for the 772-nm wavelength band. The results are different in the sense that the distributions are somewhat more asymmetric. This may be a result of the correction for cloud contamination in the GOME-1 surface LER retrieval. This correction basically copies the surface LER from a potentially single “clear-sky” ocean grid cell to many “cloud contaminated” ocean grid cells. This procedure can alter the shape of the distribution considerably. In any case, the result confirms the lower values for the GOME-2ABC surface LER reported earlier.

To provide more quantitative information, we tabulate in Table 4 the results for all months and all wavelengths. Looking at the data we see that the mean difference is only slightly dependent on the month of the year. No clear seasonal variation can be extracted. The same can be said about the spread (FWHM) of the distribution: it does not depend much on the month of the year.

Note that the wavelength bands at 335 and 380 nm seem to be showing slightly different behaviour than the other wavelength bands. For instance, the biases are much larger than those of the others nearby wavelength bands. The spread (FWHM) of the distribution is also larger for the 335 and 380-

GOME-2ABC MIN-LER (494 nm) versus GOME-1 MIN-LER (494 nm)

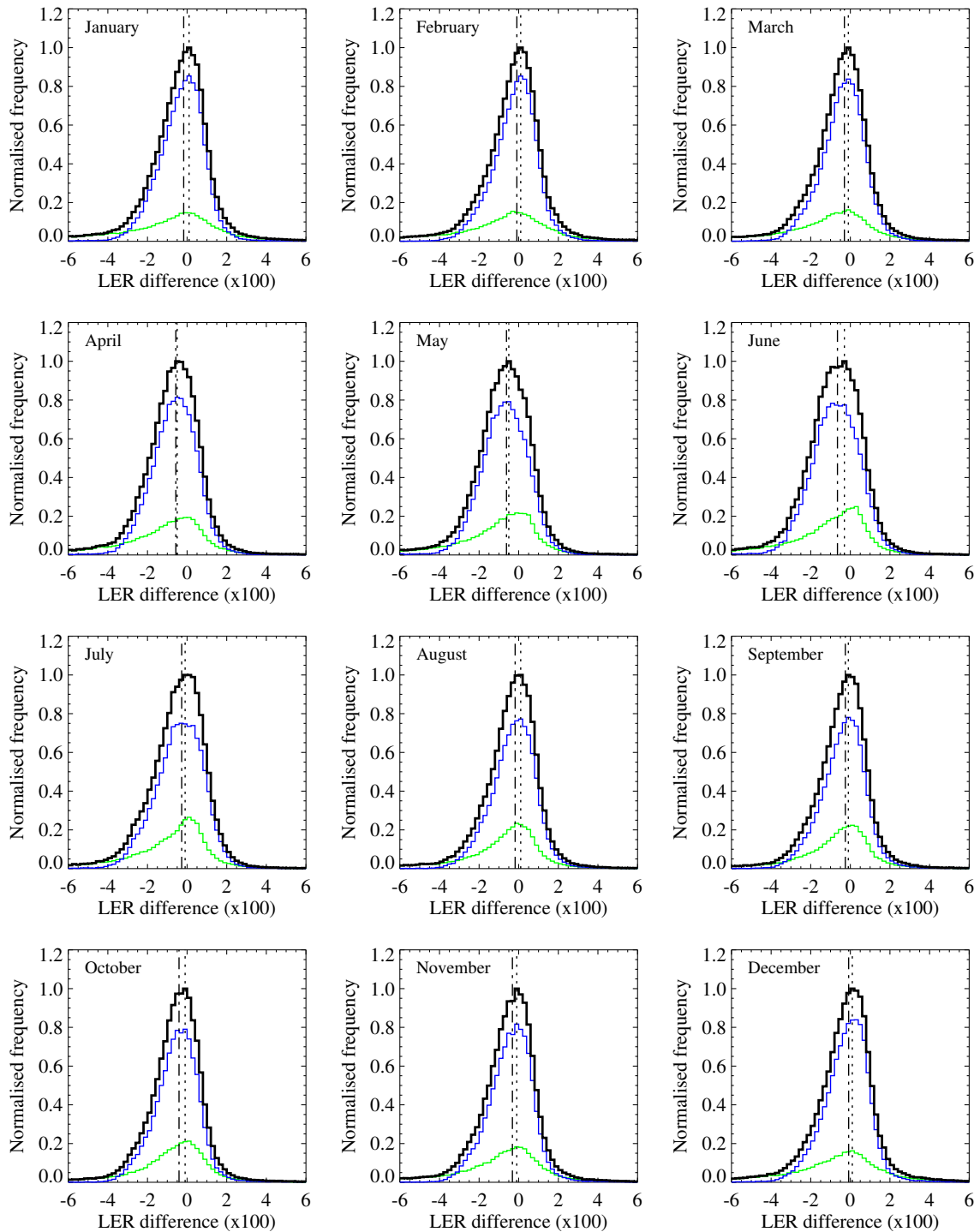


Figure 4: Histogram of the differences in the surface LER databases of GOME-2ABC and GOME-1 at 494 nm. The GOME-1 surface LER database was determined according to the MIN-LER approach, which means that we can only validate the GOME-2ABC MIN-LER product. The vertical lines indicate the mean (dashed line) and the mode (dotted line) of the distribution.

GOME-2ABC MIN-LER (772 nm) versus GOME-1 MIN-LER (772 nm)

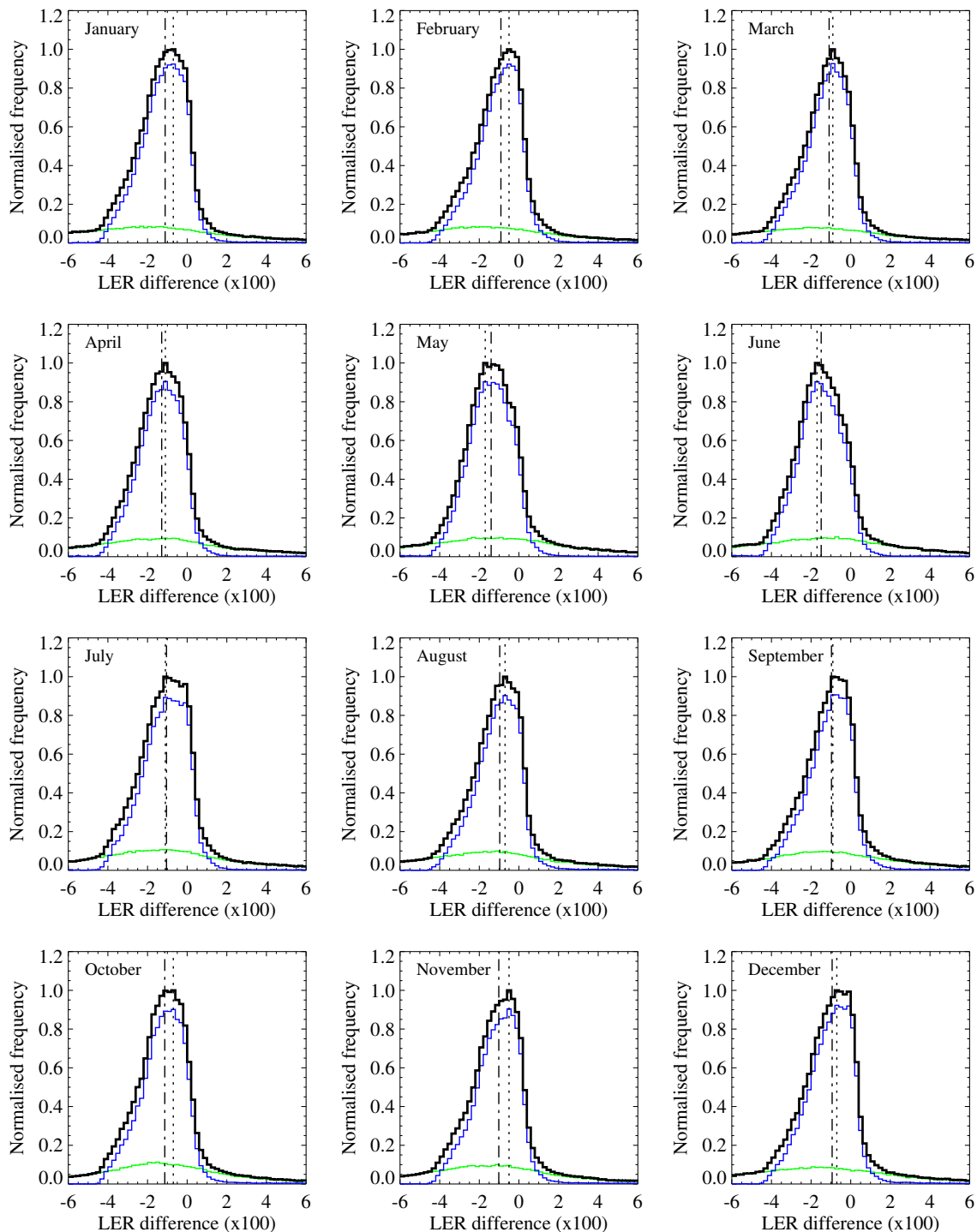


Figure 5: Histogram of the differences in the surface LER databases of GOME-2ABC and GOME-1 at 772 nm. For this wavelength the histograms are somewhat asymmetric. This might be related to the correction for cloud contamination over the ocean (either for GOME-1, GOME-2ABC, or both). The vertical lines indicate the mean (dashed line) and the mode (dotted line) of the distribution.

GOME-2ABC versus GOME-1 (MIN-LER)												
Mean surface LER difference ($\times 100$)												
λ (nm)	JAN	FEB	MAR	APR	MAY	JUN	JUL	AUG	SEP	OCT	NOV	DEC
335	0.70	0.79	0.80	-0.22	-0.52	-0.87	0.18	0.28	0.51	0.41	0.50	0.98
380	1.69	1.80	1.64	1.11	0.90	0.82	1.36	1.54	1.55	1.41	1.50	1.74
416	0.35	0.36	0.15	-0.35	-0.36	-0.38	-0.05	0.01	0.06	-0.05	-0.05	0.32
440	0.09	0.20	0.01	-0.38	-0.42	-0.44	-0.12	-0.02	-0.01	-0.13	-0.10	0.19
463	0.01	0.12	-0.10	-0.41	-0.45	-0.47	-0.13	-0.04	-0.06	-0.20	-0.15	0.09
494	-0.17	-0.09	-0.30	-0.57	-0.62	-0.65	-0.27	-0.18	-0.25	-0.41	-0.32	-0.09
555	-0.58	-0.44	-0.64	-0.86	-0.99	-1.06	-0.61	-0.50	-0.51	-0.67	-0.60	-0.45
610	-0.69	-0.53	-0.73	-0.92	-1.00	-1.07	-0.62	-0.58	-0.61	-0.77	-0.66	-0.53
670	-0.86	-0.69	-0.88	-1.10	-1.19	-1.26	-0.79	-0.75	-0.77	-0.95	-0.83	-0.69
758	-1.09	-0.89	-1.08	-1.28	-1.40	-1.49	-1.04	-0.96	-0.96	-1.11	-1.01	-0.92
772	-1.11	-0.91	-1.09	-1.29	-1.40	-1.49	-1.04	-0.97	-0.97	-1.13	-1.02	-0.94
FWHM of distribution ($\times 100$)												
λ (nm)	JAN	FEB	MAR	APR	MAY	JUN	JUL	AUG	SEP	OCT	NOV	DEC
335	3.85	3.94	4.03	3.66	4.07	4.40	4.40	4.55	4.43	4.07	4.13	4.19
380	3.03	3.01	3.01	2.94	3.07	3.16	3.05	2.88	2.93	2.87	3.00	3.12
416	2.85	2.82	2.82	2.90	3.02	3.08	3.00	2.72	2.67	2.66	2.77	2.76
440	2.77	2.71	2.70	2.81	2.90	3.00	2.91	2.61	2.56	2.54	2.65	2.69
463	2.69	2.60	2.60	2.75	2.84	2.96	2.85	2.54	2.49	2.48	2.57	2.61
494	2.62	2.52	2.54	2.72	2.81	2.94	2.81	2.50	2.46	2.47	2.54	2.55
555	2.69	2.58	2.56	2.67	2.76	2.87	2.79	2.51	2.52	2.55	2.60	2.62
610	2.71	2.60	2.59	2.70	2.73	2.79	2.74	2.51	2.53	2.60	2.66	2.65
670	2.74	2.61	2.62	2.74	2.77	2.81	2.78	2.54	2.57	2.66	2.69	2.68
758	2.83	2.68	2.69	2.82	2.90	2.94	2.94	2.70	2.71	2.77	2.77	2.78
772	2.87	2.73	2.73	2.84	2.91	2.95	2.96	2.73	2.74	2.81	2.80	2.82

Table 4: Mean difference in the surface LER of the GOME-2ABC and GOME-1 surface LER databases. The FWHM of the distribution is also given. The numbers have been multiplied by 100.

nm wavelength bands. An explanation for the bias is the impact of instrument degradation on the GOME-1 surface LER database, as reported by *Koelemeijer et al.* [2003]. This had an impact on the 335 and 380-nm results. Note that a correction for instrument degradation had been applied to the GOME-1 surface LER database. However, this correction was not sufficient for the 335 and 380-nm wavelength bands [*Koelemeijer et al.*, 2003]. An imperfect correction for instrument degradation for the GOME-1 surface LER database cannot not, however, explain the increase in the spread of the distribution. The increase of the spread of the distribution is presumably a result of the increased difficulty of observing the surface at the shorter wavelengths.

Appendix A presents tables with results from the intercomparisons that were presented earlier, but now for land and water surfaces separately.

3.3 Conclusion of the comparison with GOME-1

The main result of the analysis is that the agreement between the GOME-2ABC and GOME-1 surface LER databases is in principle quite good, but that the GOME-2ABC surface LER values are in general lower (typically 0.01 in magnitude) than the GOME-1 surface LER values. Exceptions are the surface LER values at 335 and 380 nm, which are higher for GOME-2ABC. The magnitude of the difference seems to be dependent on the surface type (and on the surface LER). This could point to differences due to differences in the radiometric calibration of the instruments. Despite this, the magnitude of the reported bias is relatively small, and the agreement is in general good.

4 MSC-LER: GOME-2ABC versus OMI

In this section, we compare the GOME-2ABC surface LER with the OMI surface LER database. The orbital parameters for GOME-2 and OMI are quite different (see Table 1) which makes the comparison less than ideal from this point of view. Also, the time periods covered by the two database are very different (GOME-2ABC: 2007–2022; OMI: 2004–2007). On the other hand, we can perform the comparison for both the MIN-LER and the MODE-LER products because the OMI surface LER product contains both of these surface LER types. Unfortunately, because of the limited wavelength range of OMI, only the wavelength bands from 335 to 494 nm can be compared in this study.

4.1 Global maps of the differences

In Figure 6 we present the difference between the 494-nm surface LER for the month March from the GOME-2ABC MIN-LER and OMI MIN-LER databases. The agreement is in general rather good. Over the ocean the differences are very close to zero. For some areas over the ocean there are slightly negative or slightly positive differences. These differences are clearly caused by case-to-case differences in the correction for cloud contamination for the GOME-2ABC and OMI surface LER algorithms. The differences are in any case very small. Over land the differences are close to zero for most non-snow/ice surfaces. We find negative values (for parts of Australia, South America, the Himalaya, and the African continent) but also positive values (for parts of Asia, South America, and desert areas like the Sahara). The differences are, in general, to be considered small.

Larger differences are found for the snow/ice covered surfaces. In fact, for most of the snow/ice related surfaces the GOME-2ABC surface LER is smaller by values approaching -0.06 compared to the OMI surface LER. For some areas, the differences are positive, reaching values of $+0.06$. This behaviour is clearly related to the snow/ice situation in the scene. As the MIN-LER is based on the minimum LER found in the time period used, changes in the actual snow/ice situation will have a large impact. For that reason, the switching from blue to red seems to be correct behaviour, considering the differences in the time period covered. Nevertheless, there appears to be a negative bias for the snow/ice surfaces in the polar regions. This bias could be the result of the different overpass times, or different observation geometries (surface BRDF), but it could also be the result of differences in the radiometric calibration of the two instruments.

In Figure 7 we present the global map of the differences between the MODE-LER of GOME-2ABC and OMI, again for the month March. The plot is comparable to the one in Figure 6. A red-coloured feature is present in Northern Africa, close to the equator. This feature is caused by the fact that the switch from 1% accumulated value to the mode of the scene LER distribution takes place at a different location. This is the result of a difference between the two algorithms. The OMI surface

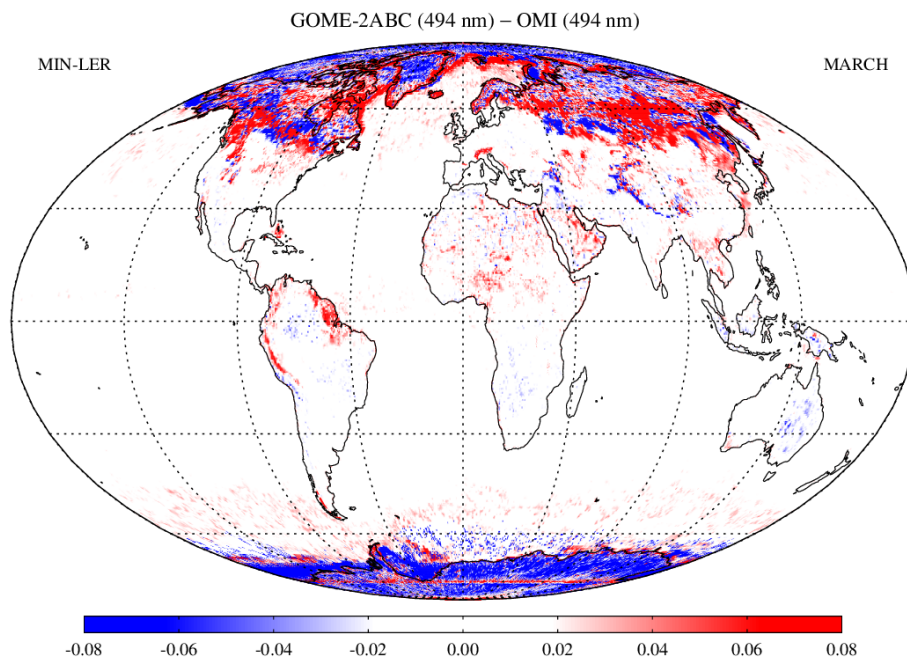


Figure 6: Map of the difference between the 494-nm surface LER from the GOME-2ABC and OMI MIN-LER databases, for the month March. Over the ocean, the agreement is good with deviations generally far below the 0.01 level. Above snow/ice areas, the deviations are systematically larger.

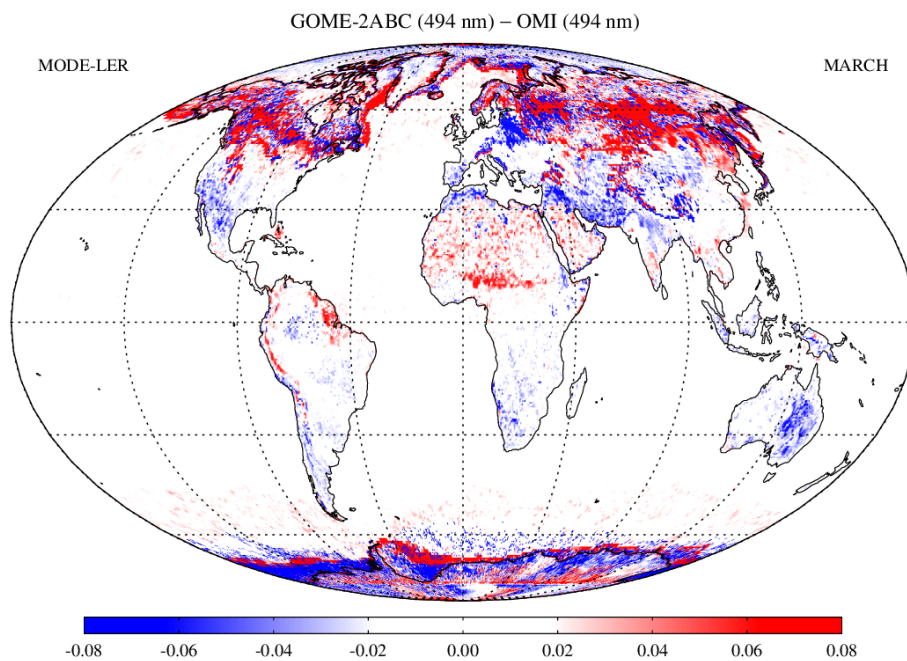


Figure 7: Map of the difference between the 494-nm surface LER from the GOME-2ABC and OMI MODE-LER databases, for the month March. Over the ocean, the agreement is good. Above land, the agreement is generally good, apart from differences related to snow/ice cover and extent.

LER retrieval uses the FWHM of the scene LER distribution to determine whether or not the mode should be used. The GOME-2 surface LER retrieval on the other hand uses the standard deviation of the scene LER distribution. In general, the MODE-LER over land is a bit more negative than the MIN-LER. For the snow/ice surfaces near the North and South poles, there appears to be a bit more “white” in the MODE-LER difference as compared to the MIN-LER difference.

4.2 Statistical analysis of the differences

We calculate the distributions of the differences for each month of the year, for each of the OMI surface LER wavelength bands that coincide with the GOME-2 surface LER wavelength bands (see Table 2). This is done for the MIN-LER and MODE-LER surface LER products.

4.2.1 MIN-LER product

In Figure 8 we present the results for the MIN-LER product. The histograms are histograms of the distribution of the differences between GOME-2ABC and OMI for 380 nm. As can be seen, the histograms are symmetric but do not have their mean and mode values close to zero. The bias is on the order of 0.016. This is the case for all months of the year. In Figure 9 we present the same result, but then for the 494 nm wavelength band. The bias is negligible. The width of the distribution is smaller than at 380 nm. This is to be expected because the majority of the grid cells are located over the ocean and for these cases the surface LER itself is smaller at 494 nm than at 380 nm.

In Table 5 we present the numerical results of the histogram analyses. The table presents the mean surface MIN-LER difference for each month of the year and for each of the ten wavelength bands that could be compared. It also lists the spread (FWHM) of the distribution. All numbers were multiplied by 100. Note that especially for the wavelength bands of 416 nm and above the agreement is very good. Also notice that the spread of the difference distribution is much smaller than that found for the GOME-2ABC versus GOME-1 comparison (as reported in Table 4).

4.2.2 MODE-LER product

In Figures 10 and 11 and we again present plots of the histograms of the differences for the 380 and 494 nm wavelength bands, but this time for the MODE-LER. From the 380-nm result we conclude that the results are comparable to the MIN-LER result shown before in Figure 8. The shape of the distribution is similar, and the mean and mode of the distributions are close to zero. Also for the 494-nm result the distributions are very similar to the MIN-LER result shown before in Figure 9.

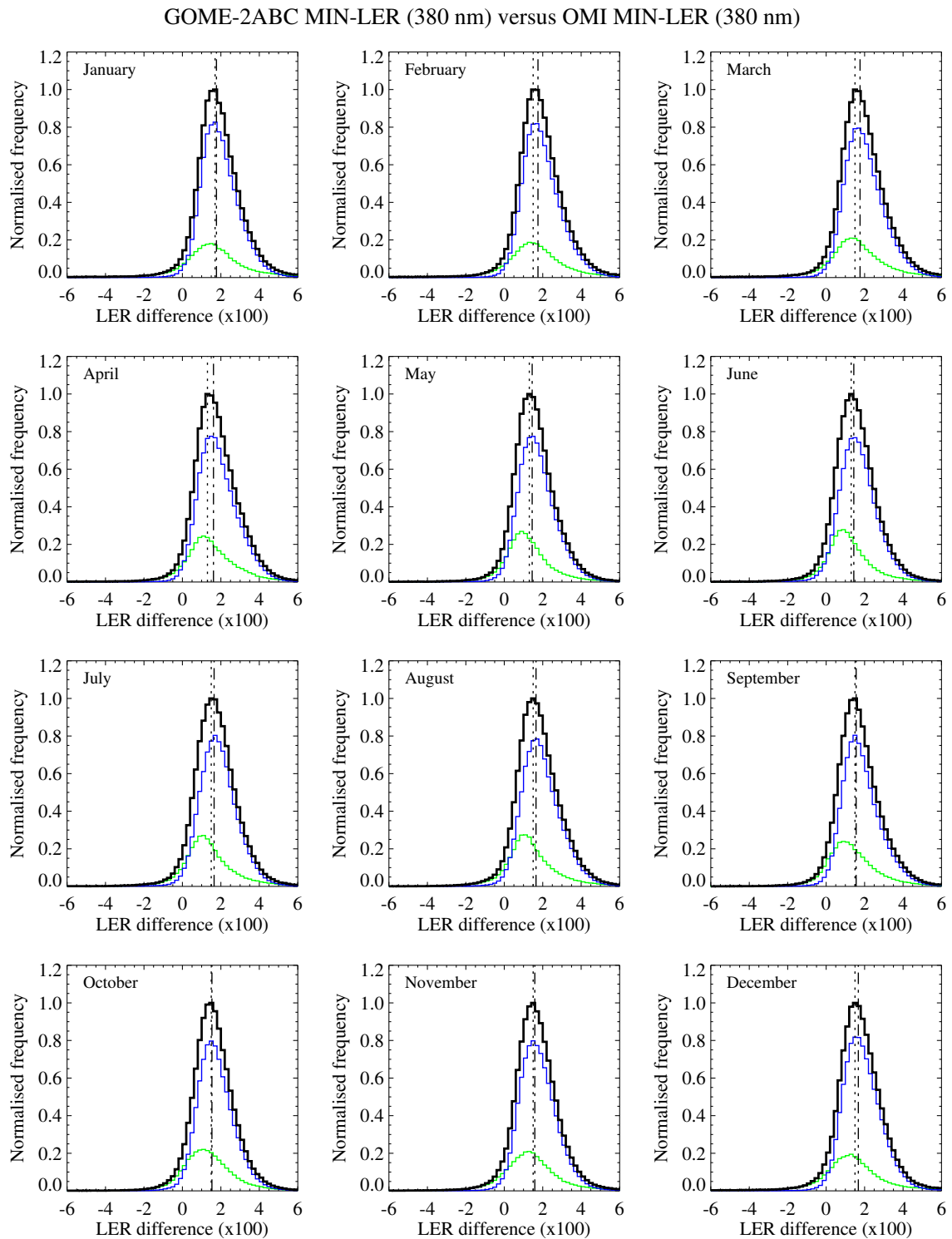


Figure 8: Histogram of the differences in the surface LER databases of GOME-2ABC and OMI at 380 nm. The MIN-LER products are compared. There seems to be a small systematic offset. The vertical lines indicate the mean (dashed line) and the mode (dotted line) of the distribution.

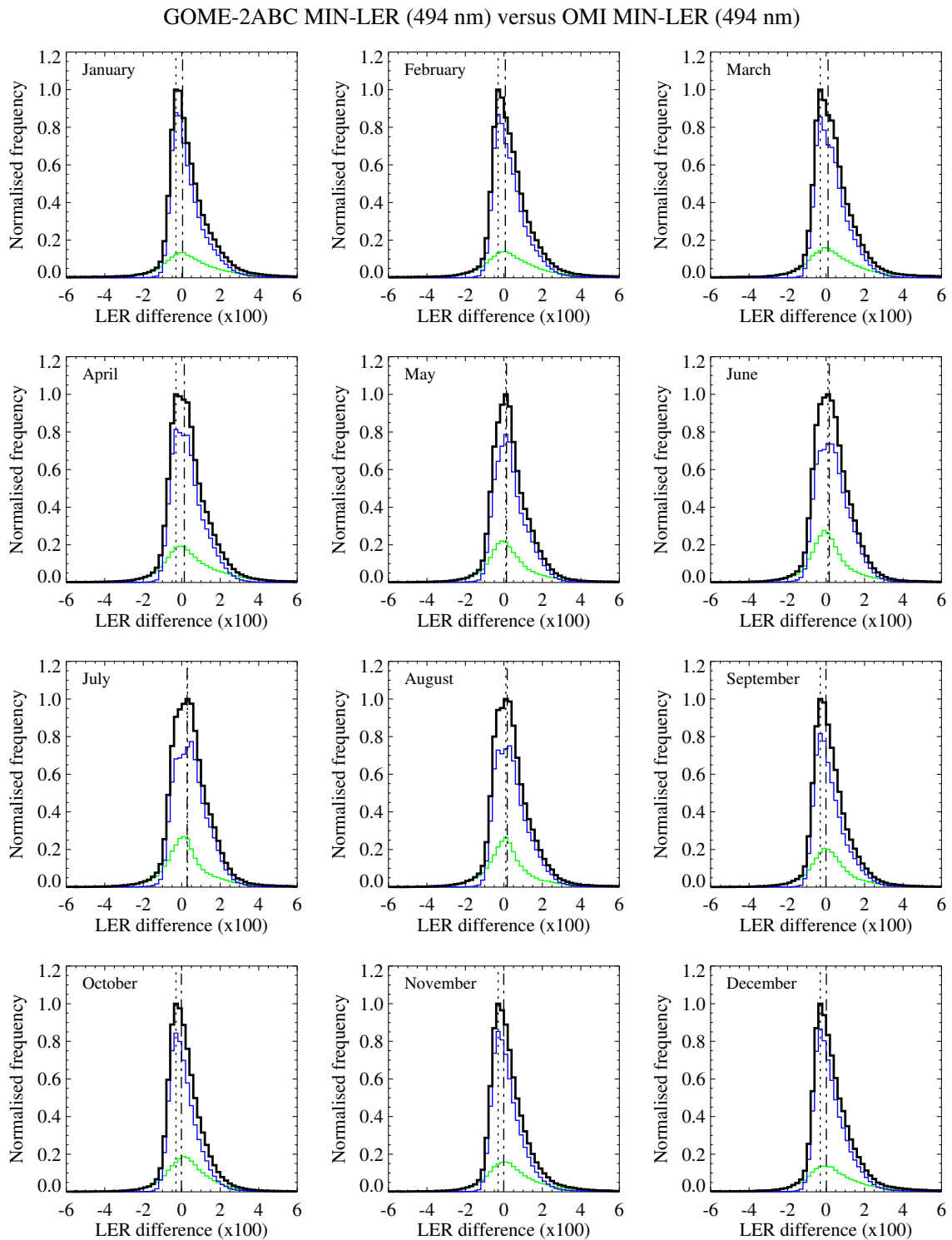


Figure 9: Histogram of the differences in the surface LER databases of GOME-2ABC and OMI at 494 nm. The MIN-LER products are compared. The agreement is very good for all the months. The vertical lines indicate the mean (dashed line) and the mode (dotted line) of the distribution.

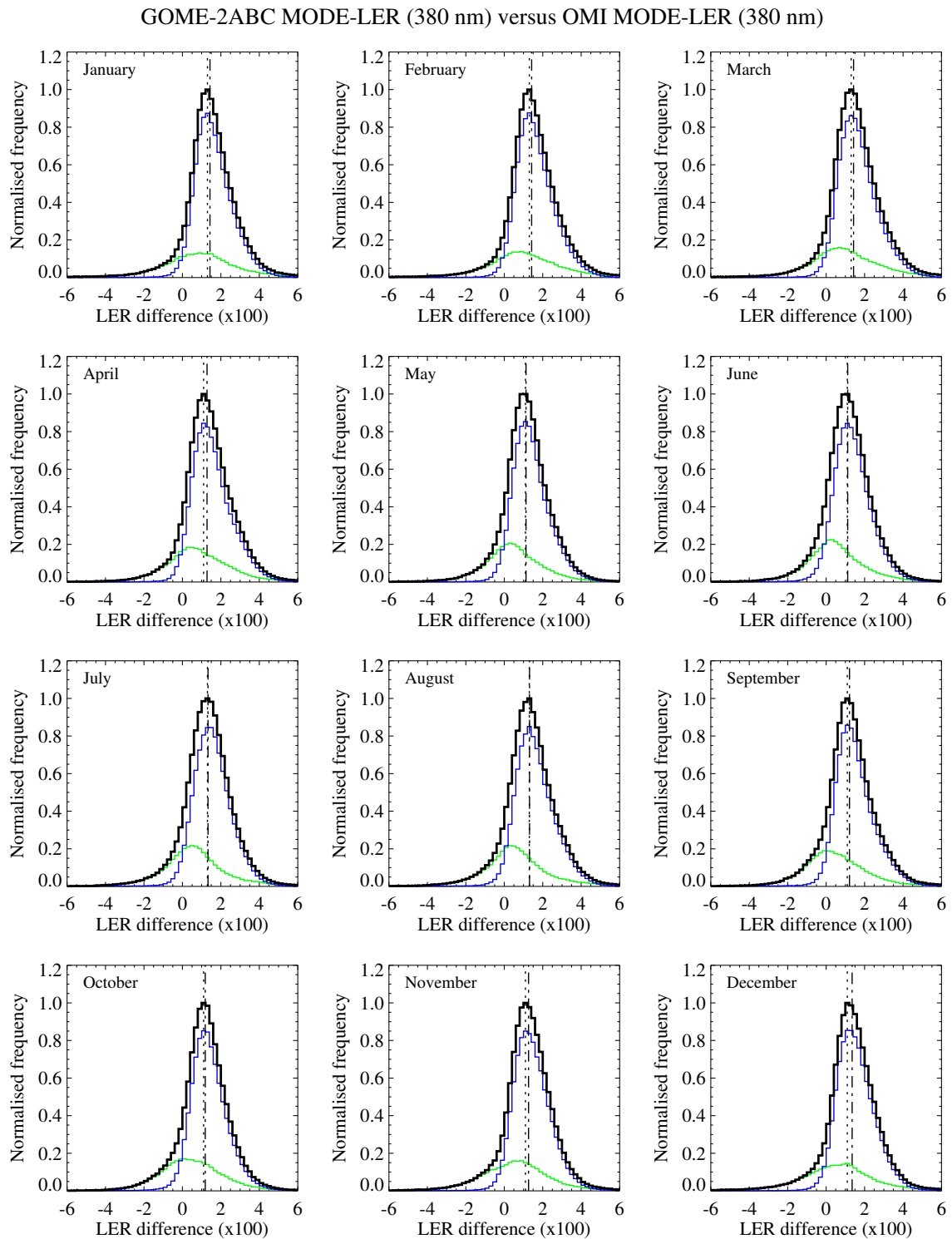


Figure 10: Histogram of the differences in the surface LER databases of GOME-2ABC and OMI at 380 nm. This time the MODE-LER products are compared. The agreement is good for all the months. The vertical lines indicate the mean (dashed line) and the mode (dotted line) of the distribution.

GOME-2ABC MODE-LER (494 nm) versus OMI MODE-LER (494 nm)

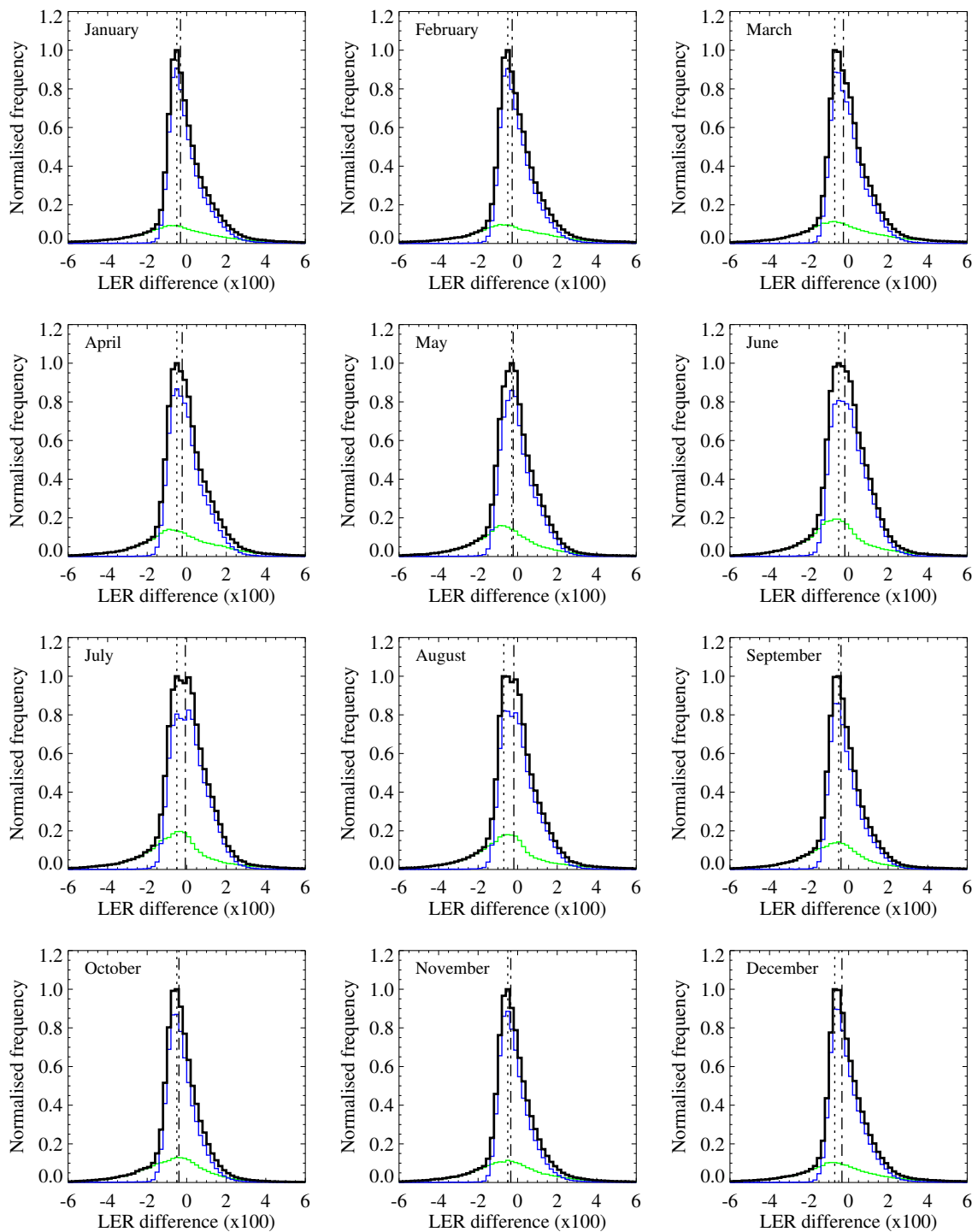


Figure 11: Histogram of the differences in the surface LER databases of GOME-2ABC and OMI at 494 nm. The MODE-LER products are compared. The agreement is very good. The vertical lines indicate the mean (dashed line) and the mode (dotted line) of the distribution.

GOME-2ABC versus OMI (MIN-LER)												
Mean surface LER difference ($\times 100$)												
λ (nm)	JAN	FEB	MAR	APR	MAY	JUN	JUL	AUG	SEP	OCT	NOV	DEC
335	2.91	2.82	2.72	2.15	1.72	1.62	1.91	2.14	2.37	2.53	2.62	2.79
354	2.12	2.09	2.03	1.66	1.32	1.23	1.49	1.67	1.77	1.86	1.94	2.02
367	1.69	1.67	1.65	1.42	1.14	1.07	1.29	1.42	1.44	1.46	1.52	1.61
380	1.77	1.75	1.77	1.62	1.45	1.44	1.65	1.65	1.56	1.54	1.59	1.67
388	1.37	1.35	1.39	1.25	1.12	1.09	1.28	1.28	1.19	1.16	1.20	1.28
416	0.40	0.40	0.42	0.33	0.24	0.23	0.39	0.36	0.25	0.25	0.27	0.32
425	0.39	0.38	0.40	0.36	0.26	0.27	0.43	0.39	0.26	0.24	0.25	0.31
440	0.25	0.26	0.30	0.26	0.20	0.21	0.35	0.29	0.15	0.14	0.16	0.19
463	0.18	0.20	0.23	0.23	0.20	0.23	0.35	0.26	0.10	0.08	0.09	0.12
494	0.04	0.08	0.11	0.13	0.14	0.17	0.28	0.17	-0.01	-0.02	-0.01	0.02
FWHM of distribution ($\times 100$)												
λ (nm)	JAN	FEB	MAR	APR	MAY	JUN	JUL	AUG	SEP	OCT	NOV	DEC
335	2.40	2.30	2.32	2.36	2.57	2.62	2.51	2.35	2.44	2.38	2.45	2.53
354	2.26	2.22	2.25	2.23	2.30	2.35	2.29	2.23	2.34	2.28	2.32	2.37
367	2.19	2.22	2.27	2.20	2.05	2.07	2.05	2.12	2.19	2.18	2.23	2.29
380	2.20	2.22	2.30	2.33	2.16	2.22	2.27	2.30	2.23	2.18	2.22	2.27
388	2.11	2.14	2.22	2.24	2.06	2.09	2.11	2.14	2.13	2.11	2.15	2.19
416	1.96	2.02	2.10	2.05	1.81	1.82	1.85	1.89	1.87	1.91	1.97	2.01
425	1.93	1.98	2.06	2.05	1.81	1.85	1.88	1.90	1.83	1.88	1.93	1.99
440	1.87	1.92	2.02	2.01	1.82	1.91	1.95	1.89	1.78	1.82	1.86	1.92
463	1.71	1.78	1.87	1.90	1.76	1.92	1.96	1.82	1.65	1.67	1.70	1.77
494	1.60	1.68	1.77	1.83	1.72	1.90	1.95	1.78	1.57	1.57	1.58	1.67

Table 5: Mean difference in the surface LER of the GOME-2ABC and OMI surface LER databases. The FWHM of the distribution is also given. The numbers have been multiplied by 100.

In Table 6 we present, in the usual manner, the numerical results of the comparison. Comparing with the results presented earlier in Table 5 we see that the values are very comparable. This is especially the case for the width (FWHM) of the distributions, but also the mean and mode of the distributions

GOME-2ABC versus OMI (MODE-LER)												
Mean surface LER difference ($\times 100$)												
λ (nm)	JAN	FEB	MAR	APR	MAY	JUN	JUL	AUG	SEP	OCT	NOV	DEC
335	2.65	2.57	2.47	1.90	1.48	1.37	1.66	1.90	2.12	2.27	2.37	2.53
354	1.86	1.84	1.79	1.42	1.09	1.01	1.27	1.43	1.52	1.60	1.69	1.77
367	1.36	1.36	1.33	1.10	0.83	0.77	1.00	1.11	1.10	1.12	1.21	1.29
380	1.43	1.42	1.43	1.28	1.13	1.12	1.33	1.31	1.21	1.19	1.26	1.35
388	1.02	1.01	1.04	0.91	0.78	0.76	0.95	0.93	0.83	0.79	0.86	0.95
416	0.01	0.02	0.02	-0.05	-0.14	-0.14	0.03	-0.03	-0.16	-0.17	-0.11	-0.06
425	0.00	0.01	0.01	-0.03	-0.12	-0.10	0.07	0.01	-0.15	-0.17	-0.12	-0.07
440	-0.13	-0.11	-0.09	-0.12	-0.18	-0.17	-0.02	-0.10	-0.25	-0.26	-0.22	-0.19
463	-0.19	-0.16	-0.15	-0.14	-0.17	-0.14	-0.00	-0.12	-0.29	-0.30	-0.26	-0.24
494	-0.32	-0.28	-0.26	-0.23	-0.22	-0.19	-0.07	-0.19	-0.39	-0.39	-0.35	-0.34
FWHM of distribution ($\times 100$)												
λ (nm)	JAN	FEB	MAR	APR	MAY	JUN	JUL	AUG	SEP	OCT	NOV	DEC
335	2.27	2.19	2.17	2.25	2.53	2.55	2.43	2.25	2.31	2.25	2.33	2.38
354	2.16	2.14	2.14	2.14	2.26	2.31	2.23	2.15	2.27	2.21	2.25	2.26
367	2.18	2.24	2.29	2.20	2.07	2.08	2.05	2.15	2.25	2.24	2.28	2.29
380	2.24	2.29	2.38	2.41	2.26	2.36	2.39	2.44	2.35	2.27	2.29	2.32
388	2.15	2.21	2.29	2.31	2.15	2.21	2.22	2.26	2.24	2.19	2.22	2.23
416	2.01	2.08	2.16	2.14	1.92	1.96	1.97	2.03	2.00	1.99	2.05	2.06
425	1.99	2.05	2.12	2.14	1.95	2.00	2.02	2.06	1.97	1.96	2.01	2.05
440	1.92	1.99	2.09	2.12	1.97	2.11	2.12	2.06	1.91	1.89	1.93	1.98
463	1.76	1.85	1.94	2.02	1.93	2.15	2.16	1.99	1.77	1.73	1.76	1.81
494	1.63	1.75	1.84	1.94	1.88	2.12	2.14	1.94	1.66	1.61	1.63	1.70

Table 6: Mean difference in the surface LER of the GOME-2ABC and OMI surface LER databases. The FWHM of the distribution is also given. The numbers have been multiplied by 100.

are very comparable. This is a clear indication that the differences in the surface LER are mostly the result of differences in the two instruments, in the observation geometries, and in the time periods covered, but not so much in the retrieval approaches that are used. Note, however, that the differences

are small. We conclude that the GOME-2ABC and OMI MODE-LER products are in agreement.

Appendix A presents tables with results from the intercomparisons that were presented earlier, but now for land and water surfaces separately.

4.3 Conclusion of the comparison with OMI

The comparison with the OMI surface LER product indicates that the GOME-2ABC surface LER product is of good quality. Deviations are found, but these are small over the ocean and over most of the land. Near snow/ice borders we see differences, which may be explained by real differences in the actual snow/ice situation observed in the two observation periods (OMI: 2004–2007; GOME-2ABC: 2007–2022). A bias in the surface LER difference is found over snow/ice surfaces. The bias is small and one cannot judge from the results whether the bias is caused by GOME-2ABC, by OMI, or by the differences in overpass time and observation geometry. The wavelength bands below 400 nm show a bias of about +0.015 in the GOME-2ABC surface LER which may be due to radiometric calibration problems. In summary, the GOME-2ABC MSC surface LER product is of good quality.

5 MSC-LER: GOME-2ABC versus MERIS

In this section, we compare the GOME-2ABC surface LER product with the MERIS black-sky albedo (BSA) product. Because a BSA is fundamentally different from a LER, differences are to be expected. Note that the MERIS BSA is only delivered for land surfaces. Over sea, the MERIS surface reflectivity that is present in the database is actually taken from the GOME-1 surface LER product. Nevertheless, the MERIS BSA may be useful as an independent reference.

We compare the MERIS BSA with the GOME-2ABC MIN-LER and MODE-LER products, because it is not clear to us whether the MERIS surface reflectivity should be related to one or the other.

5.1 Global maps of the differences

In Figure 12 we plotted the difference between the GOME-2ABC MIN-LER and the MERIS BSA for the 772-nm wavelength band for the month March. In Figure 13 we do the same but here for GOME-2ABC the MODE-LER is used instead of the MIN-LER. For the sea surface, the conclusion is as expected: the differences are exactly the same as found in the comparison with the GOME-1 surface LER. This is because the MERIS database is filled with GOME-1 surface albedo over the ocean. For the land surfaces we see in the MIN-LER case that the difference is negative almost everywhere. For the MODE-LER case in Figure 13, there are also red areas (positive differences).

In Figures 14 and 15 we repeat this but now for the 494-nm wavelength band. Here the differences are near-zero for large parts of the land surfaces. For the snow/ice covered land surfaces, however, the differences are negative. The MODE-LER comparison presented in Figure 15 reveals quite a few red areas, where the differences are positive. These areas have desert or snow/ice surfaces.

The conclusion is that we cannot draw much quantitative information from the comparison with the MERIS BSA. A statistical analysis will therefore not be presented. Note that a statistical analysis, when it would be performed, would be dominated by the sea surface.

5.2 Conclusion of the comparison with MERIS

The comparison with the MERIS BSA does not provide much additional information on the accuracy of the GOME-2ABC surface LER product. First of all, over sea the surface reflectivity values in the MERIS database are just those of the GOME-1 surface LER database. We compared the MERIS BSA with the GOME-2ABC MIN-LER and MODE-LER databases. The MERIS BSA over land appears to be systematically higher than the GOME-2ABC MIN-LER surface LER. On the other hand, for desert and snow/ice surfaces, the GOME-2ABC MODE-LER shows higher values than the

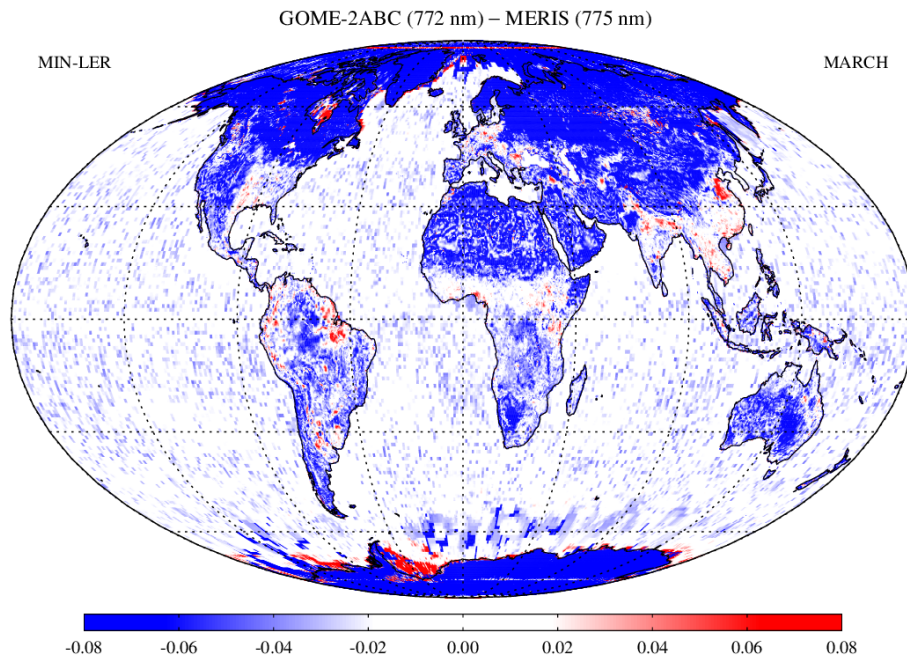


Figure 12: Map of the difference between the GOME-2ABC surface LER at 772 nm and the MERIS BSA at 775 nm for calendar month March. The GOME-2ABC MIN-LER field was used here. Please note that over the ocean, the MERIS database is filled with GOME-1 surface LER values.

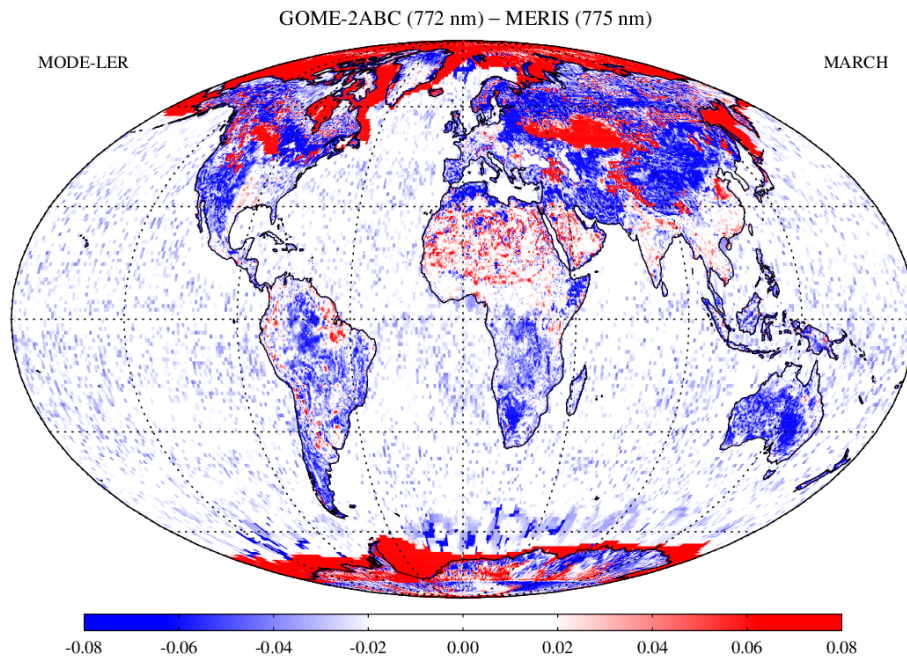


Figure 13: Map of the difference between the GOME-2ABC surface LER at 772 nm and the MERIS BSA at 775 nm for calendar month March. The GOME-2ABC MODE-LER field was used here. Please note that over the ocean, the MERIS database is filled with GOME-1 surface LER values.

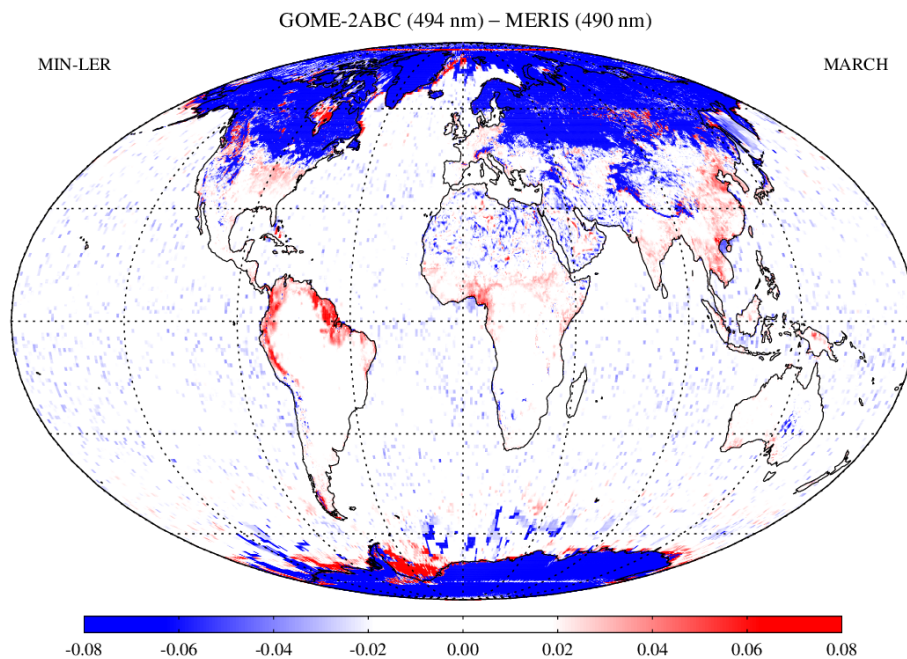


Figure 14: Map of the difference between the GOME-2ABC surface LER at 494 nm and the MERIS BSA at 490 nm for calendar month March. The GOME-2ABC MIN-LER field was used here. Please note that over the ocean, the MERIS database is filled with GOME-1 surface LER values.

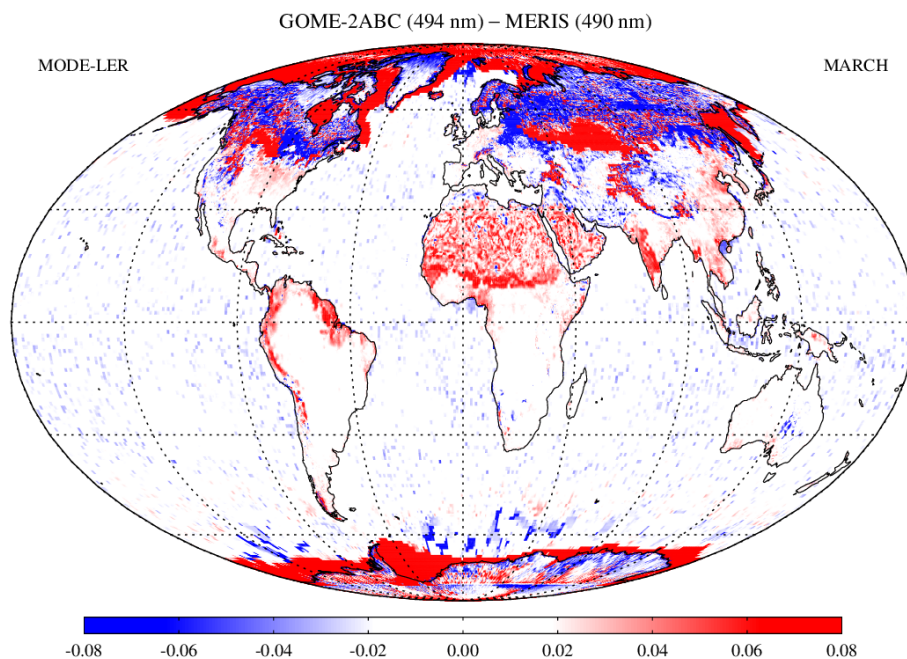


Figure 15: Map of the difference between the GOME-2ABC surface LER at 494 nm and the MERIS BSA at 490 nm for calendar month March. The GOME-2ABC MODE-LER field was used here. Please note that over the ocean, the MERIS database is filled with GOME-1 surface LER values.

MERIS database. A statistical analysis was not presented, because it would be dominated by the sea surface. As explained before, MERIS albedo of the ocean originates from the GOME-1 surface LER database.

6 PMD-LER: GOME-2ABC versus OMI

For the GOME-2 PMD-LER product we do not perform a comparison with the GOME-1 surface LER product, for a number of reasons. First of all, the GOME-1 surface LER product is only available in the MIN-LER form. Secondly, the 335-nm and 380-nm GOME-1 surface LER wavelength bands are known to be affected by instrument degradation [Koelemeijer *et al.*, 2003]. Thirdly, the GOME-1 surface LER database has a lower spatial resolution (see Table 1). Fourthly, the GOME-1 surface LER wavelength bands are generally not close enough to the PMD wavelength bands.

Using the OMI surface LER database as a reference makes more sense. It has the same intrinsic spatial resolution as the GOME-2 PMD surface LER product, is available in MIN-LER and MODE-LER versions, and has wavelength bands close enough to all PMD wavelength bands. The downside, unfortunately, is that the list of wavelength bands in the OMI surface LER database only goes up to 499 nm. This means that we can only validate the PMD bands 4–9.

6.1 Global maps of the differences

Global maps of the difference in surface LER are presented in Figures 16 and 17. Figure 16 presents the MIN-LER comparison for PMD 9. Figure 17 presents the MODE-LER comparison. The figures are very similar to the figures presented in section 4. A bias of roughly 0.01 in the values over the ocean, which was present in version 2.1 of the database, disappeared in the previous version 3.1. The explanation that was given for this bias was a difference in the radiometric calibration of the PMD band reflectance with respect to the MSC reflectance. Note that such differences had been reported in the past [Tilstra *et al.*, 2011]. The recalibration of GOME-2A reflectance to GOME-2B reflectance removed the bias. The bias remains absent in the current version 4.1 of the database.

Over land the behaviour is not much different than over the ocean, except for the desert areas and the snow/ice areas. The behaviour over land is more or less in line with the behaviour over land that was seen for the MSC surface LER (see Figures 6 and 7). Note, however, that the closest wavelength band shown in these two figures was the 494 nm wavelength band whereas PMD 9 is centred around 461 nm and was compared with OMI wavelength band 463 nm. This difference of about 30 nm in wavelength may explain some of the differences between MSC-based LER and PMD-based LER.

6.2 Statistical analysis of the differences

In Figure 18 we present histograms of the difference between the GOME-2ABC MIN-LER product (for PMD 9) and the OMI MIN-LER (for the 463-nm wavelength band). In Figure 19 the same is

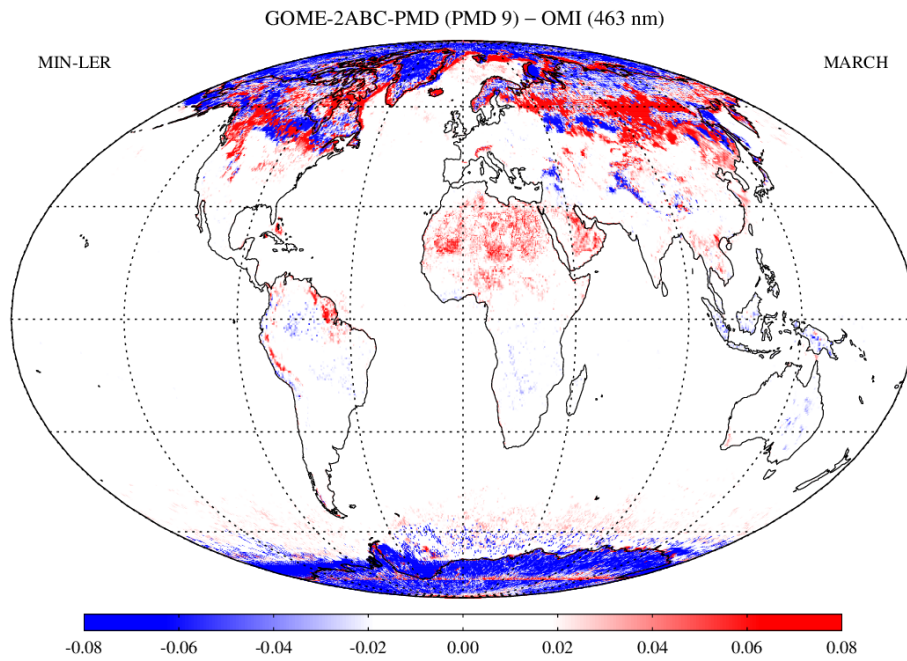


Figure 16: Map of the difference between the surface LER from GOME-2ABC (PMD 9) and OMI (463 nm). The MIN-LER is used here. Over the ocean, the agreement is good but with a negative bias of magnitude 0.01. Above snow/ice areas, the deviations are systematically larger.

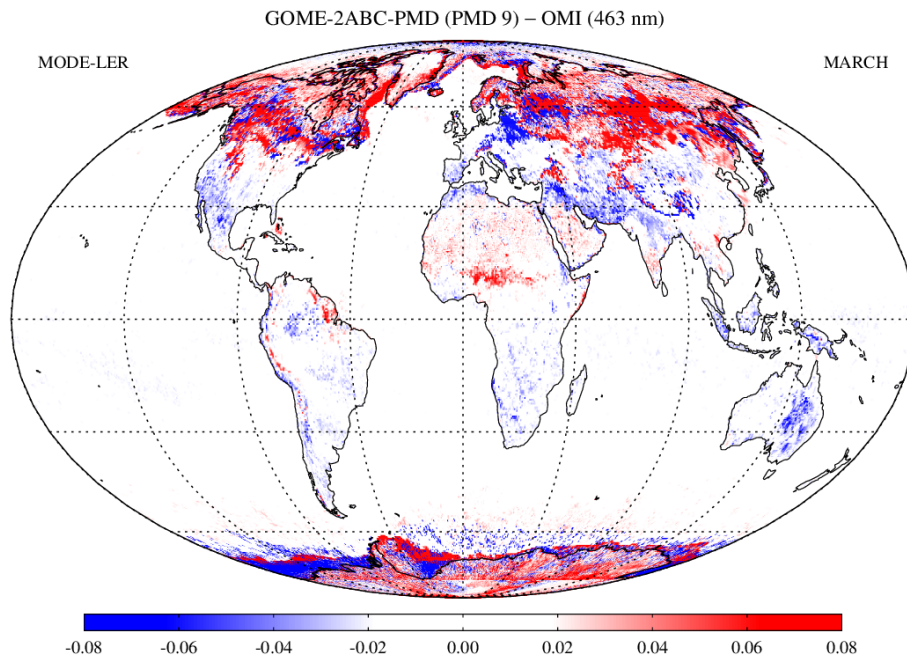


Figure 17: Map of the difference between the surface LER from GOME-2ABC (PMD 9) and OMI (463 nm). The MODE-LER is used here. Over the ocean, the agreement is good. Above land, the agreement is generally good, apart from differences related to snow/ice cover and extent.

GOME-2ABC-PMD MIN-LER (PMD 9) versus OMI MIN-LER (463 nm)

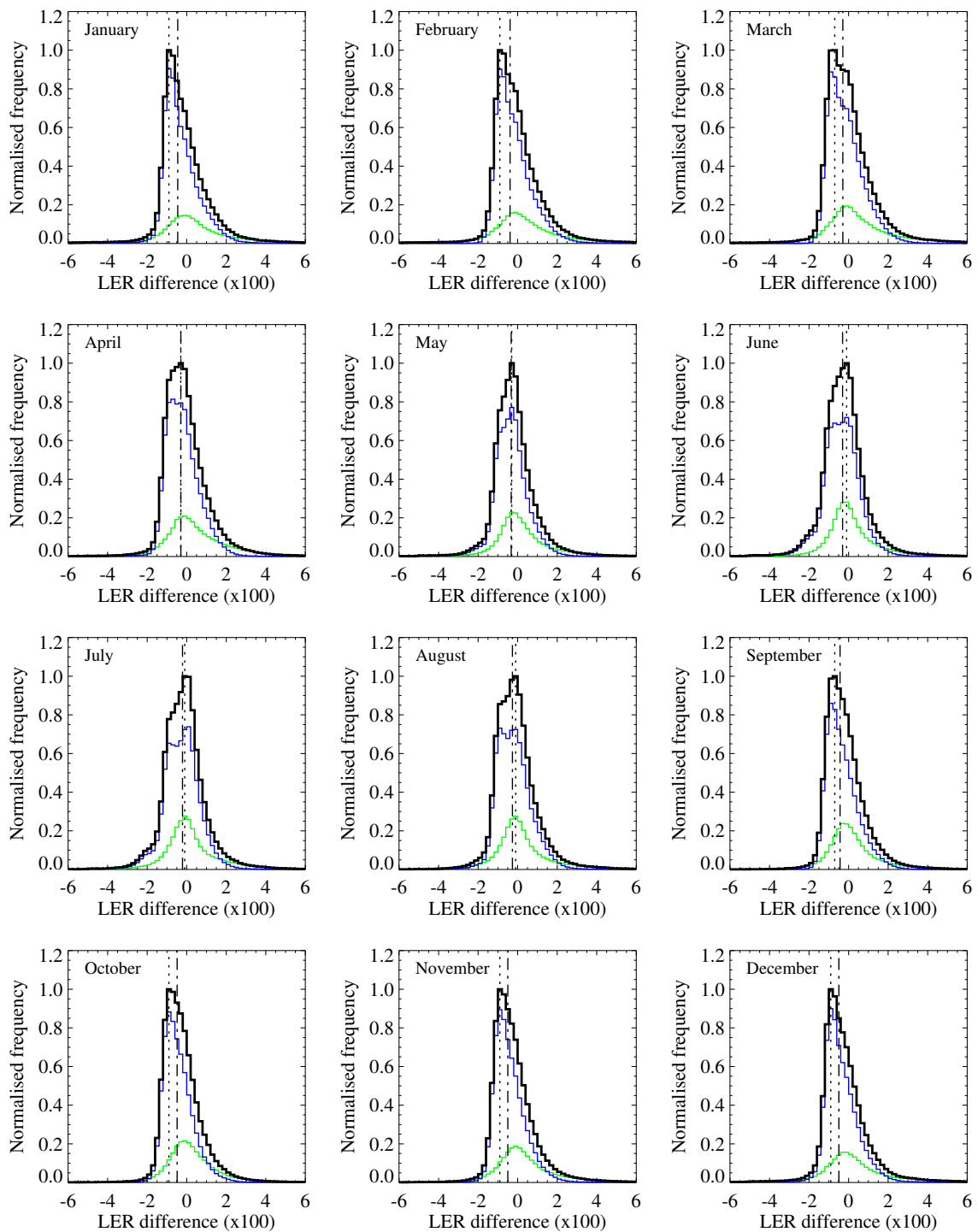


Figure 18: Histogram of the difference between the surface LER from GOME-2ABC (PMD 9) and OMI (463 nm). The MIN-LER products are compared. The agreement is good for all the months. The vertical lines indicate the mean (dashed line) and the mode (dotted line) of the distribution.

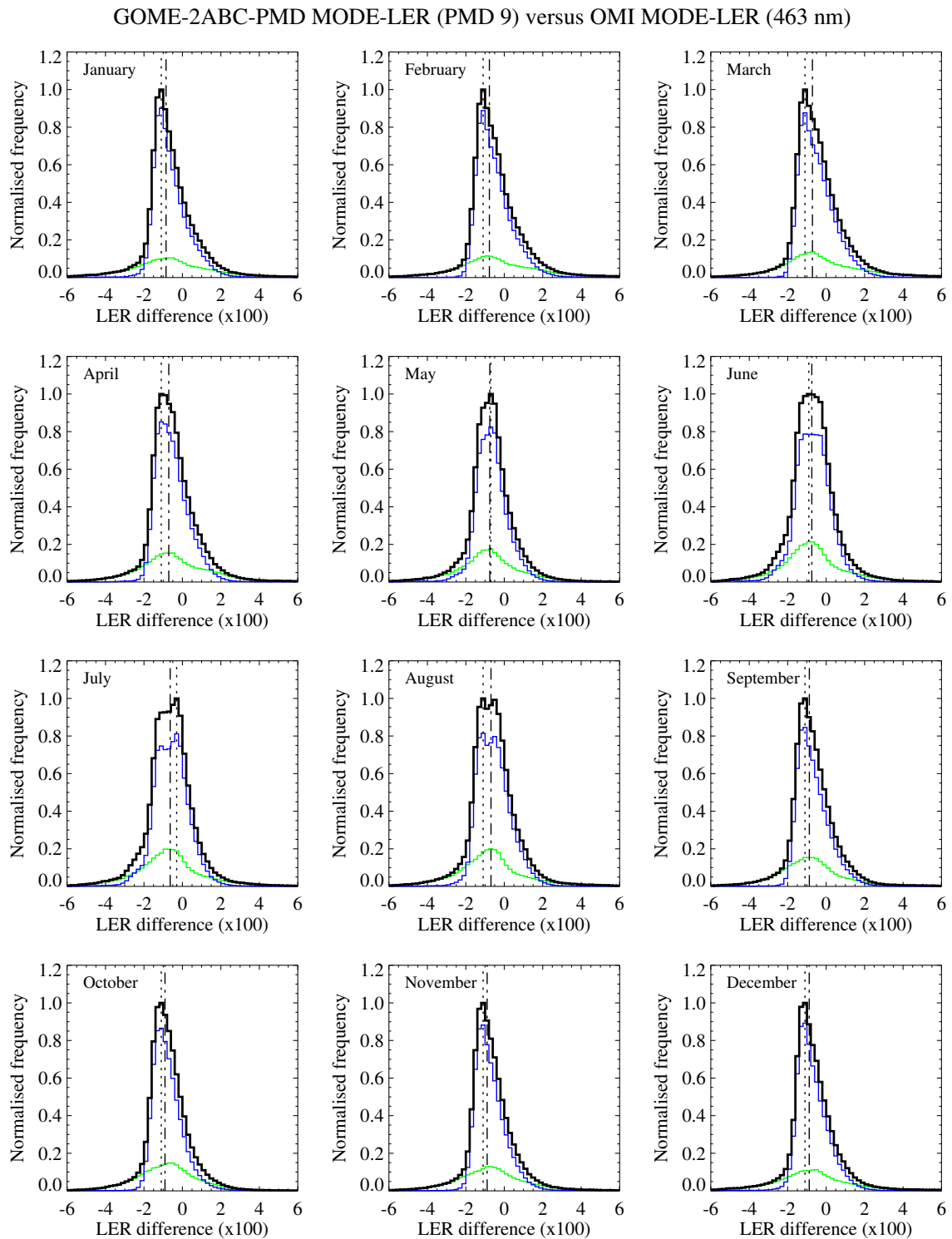


Figure 19: Histogram of the difference between the surface LER from GOME-2ABC (PMD 9) and OMI (463 nm). The MODE-LER products are compared. The agreement is good for all the months. The vertical lines indicate the mean (dashed line) and the mode (dotted line) of the distribution.

presented, but then for the MODE-LER product. The mean and the width of the distributions for all PMD bands that could be validated (PMDs 4–9) are summarised in Tables 7 and 8. The differences are quite small and the FWHM values are slightly smaller compared to the previous version 3.1.

GOME-2ABC-PMD versus OMI (MIN-LER)												
Mean surface LER difference ($\times 100$)												
PMD	JAN	FEB	MAR	APR	MAY	JUN	JUL	AUG	SEP	OCT	NOV	DEC
4	-0.27	-0.42	-0.51	-0.94	-1.24	-1.42	-1.15	-1.01	-0.88	-0.75	-0.59	-0.34
5	-0.76	-0.87	-0.99	-1.34	-1.62	-1.77	-1.51	-1.41	-1.28	-1.17	-1.03	-0.83
6	0.59	0.59	0.61	0.39	0.13	0.02	0.23	0.32	0.39	0.40	0.46	0.55
7	-0.97	-0.94	-0.89	-1.11	-1.28	-1.35	-1.17	-1.14	-1.11	-1.12	-1.10	-1.05
8	-0.16	-0.10	-0.02	-0.10	-0.22	-0.24	-0.10	-0.11	-0.21	-0.25	-0.24	-0.23
9	-0.46	-0.38	-0.29	-0.30	-0.33	-0.30	-0.21	-0.26	-0.43	-0.48	-0.50	-0.49
FWHM of distribution ($\times 100$)												
PMD	JAN	FEB	MAR	APR	MAY	JUN	JUL	AUG	SEP	OCT	NOV	DEC
4	1.98	1.97	2.14	2.35	2.61	2.77	2.59	2.25	2.25	2.23	2.18	2.06
5	1.99	1.96	2.12	2.29	2.53	2.66	2.50	2.21	2.17	2.17	2.16	2.06
6	2.03	2.05	2.09	2.00	2.03	2.12	2.07	1.95	1.95	1.93	1.99	2.03
7	1.80	1.83	1.82	1.77	1.79	1.85	1.80	1.65	1.62	1.71	1.78	1.78
8	1.86	1.95	2.04	1.90	1.72	1.82	1.85	1.80	1.75	1.78	1.83	1.83
9	1.76	1.85	1.96	1.87	1.69	1.87	1.90	1.86	1.73	1.70	1.71	1.71

Table 7: Mean difference in the surface LER of the GOME-2ABC-PMD and OMI surface LER databases. The FWHM of the distribution is also given. The numbers have been multiplied by 100.

Appendix A presents tables with results from the intercomparisons that were presented earlier, but now for land and water surfaces separately.

6.3 Conclusion of the comparison with OMI

The PMD-based version of the GOME-2ABC surface LER database compares well to the OMI surface LER database. This holds for both the MIN-LER and MODE-LER products. In the comparison a small mismatch between the wavelengths of the PMD bands and the OMI wavelength bands has to be accepted. This, and the different wavelength width of the PMD bands, will have had an impact

GOME-2ABC-PMD versus OMI (MODE-LER)												
Mean surface LER difference ($\times 100$)												
PMD	JAN	FEB	MAR	APR	MAY	JUN	JUL	AUG	SEP	OCT	NOV	DEC
4	-0.53	-0.66	-0.75	-1.21	-1.53	-1.71	-1.43	-1.29	-1.14	-1.01	-0.84	-0.60
5	-1.02	-1.11	-1.23	-1.61	-1.90	-2.05	-1.79	-1.68	-1.54	-1.43	-1.29	-1.10
6	0.28	0.29	0.31	0.09	-0.18	-0.28	-0.06	0.02	0.09	0.08	0.16	0.24
7	-1.32	-1.28	-1.24	-1.48	-1.66	-1.73	-1.53	-1.50	-1.47	-1.49	-1.44	-1.39
8	-0.52	-0.45	-0.39	-0.48	-0.60	-0.63	-0.48	-0.49	-0.60	-0.64	-0.61	-0.59
9	-0.85	-0.77	-0.71	-0.71	-0.75	-0.75	-0.64	-0.69	-0.87	-0.91	-0.89	-0.88
FWHM of distribution ($\times 100$)												
PMD	JAN	FEB	MAR	APR	MAY	JUN	JUL	AUG	SEP	OCT	NOV	DEC
4	1.80	1.83	1.99	2.30	2.69	2.90	2.66	2.29	2.19	2.12	2.03	1.88
5	1.82	1.82	1.98	2.23	2.59	2.77	2.54	2.23	2.11	2.07	2.03	1.90
6	2.01	2.04	2.07	1.96	2.05	2.19	2.10	1.98	1.96	1.96	2.01	2.01
7	1.81	1.85	1.84	1.76	1.81	1.92	1.88	1.71	1.69	1.77	1.82	1.79
8	1.94	2.06	2.15	2.00	1.85	2.01	2.03	1.97	1.92	1.89	1.93	1.90
9	1.77	1.88	2.01	1.94	1.79	2.06	2.10	2.01	1.80	1.72	1.71	1.71

Table 8: Mean difference in the surface LER of the GOME-2ABC-PMD and OMI surface LER databases. The FWHM of the distribution is also given. The numbers have been multiplied by 100.

on the outcome of the comparison. Nevertheless, the results indicate that the PMD-LER is in general of good quality. Over sea, negligible differences are found in comparison to OMI. Over snow/ice surfaces there are larger differences, which are still acceptable, however, and may be explained by imperfections in radiometric calibration of the PMDs. The existence of such calibration issues is not speculative as these have already been reported in the past [Tilstra *et al.*, 2011].

7 PMD-LER versus MSC-LER

In this section we compare the GOME-2 PMD-LER database to the GOME-2 MSC-LER database. As both algorithms are to a high degree equal, differences found must be attributed to differences related to performance (footprint size, number of observations per month), differences related to the time periods covered, differences related to the wavelength mismatch between PMD band and MSC wavelength band, or to differences related to the radiometric calibration of PMD and MSC.

As a result of too large wavelength mismatches between some of the PMD bands and their MSC counterparts, we can only reliably validate PMD bands 4–11 and 13–14.

7.1 Global maps of the differences

In Figure 20 we present a global map of the difference between the MIN-LER of the PMD-LER and the MIN-LER of the MSC-LER, for the month March. Here we compare the PMD-LER from PMD 11 (centred around 555 nm) with the MSC-LER wavelength band at 555 nm. Note that PMD 11 is a relatively thin PMD band (see Figure 1), which makes the comparison more accurate. From Figure 20 we conclude that there is a high agreement between the PMD-LER and the MSC-LER. Only for areas that may be linked to high values of the surface albedo (snow/ice areas) there is a clear negative difference. The difference goes up to 0.04 in magnitude. The most likely explanation is difference between the calibration of PMD bands and the main science channels.

Other differences that are worth noting are the appearance of features related to residual cloud contamination (over the seas surrounding Antarctica) and features related to snow/ice presence and extent. The residual cloud features are very modest for the current versions of the databases, with differences up to 0.01 in magnitude. In the previous version of the database (v3.1), there were “red” areas in Eurasia related to snow/ice presence. This difference was caused by the different time periods used for the PMD-LER and the MSC-LER. Now that the time period that is covered has been extended, the red features have disappeared completely. In Figure 21, which presents the surface LER difference based using the MODE-LER approach, the agreement between PMD-LER and MSC-LER over snow/ice surfaces seems to be somewhat better. On the whole, Figures 20 and 21 indicate that there is a good agreement between PMD-LER and MSC-LER.

In Figures 22 and 23 we present similar plots but now based on the comparison between PMD 7 (centred around 382 nm) and the MSC wavelength band located at 380 nm. This time the differences are larger over both sea and land. Note that PMD 7 was selected here mainly because of its thin bandwidth (see Figure 1). The difference (going up to 0.04 in magnitude) must be caused by differences in radiometric calibration. Note that relative errors of up to 4% were reported in the past

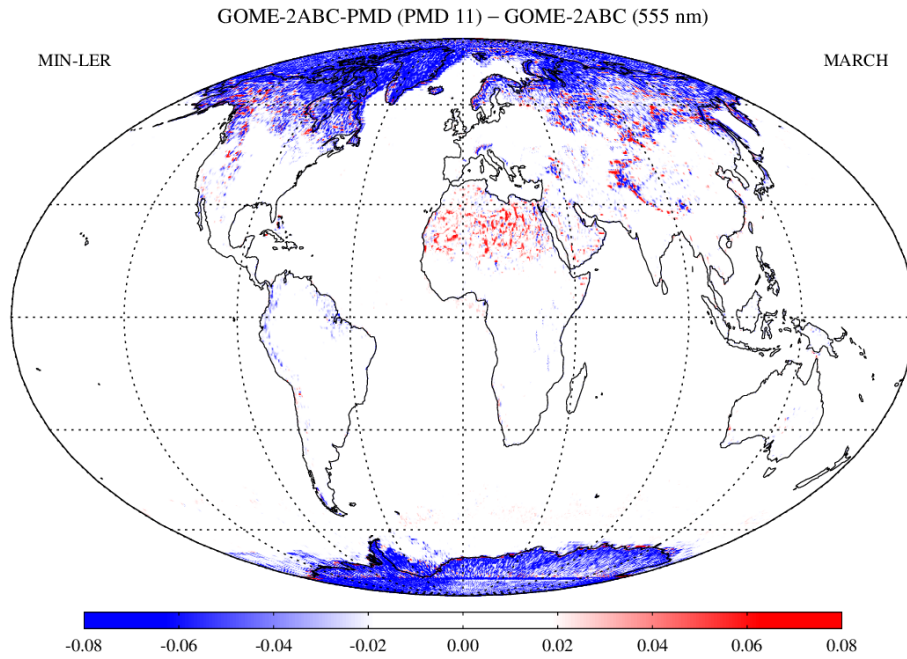


Figure 20: Map of the difference between the surface LER from the GOME-2ABC PMD-LER (PMD 11) and the GOME-2ABC MSC-LER (555 nm). The MIN-LER is plotted here, for March.

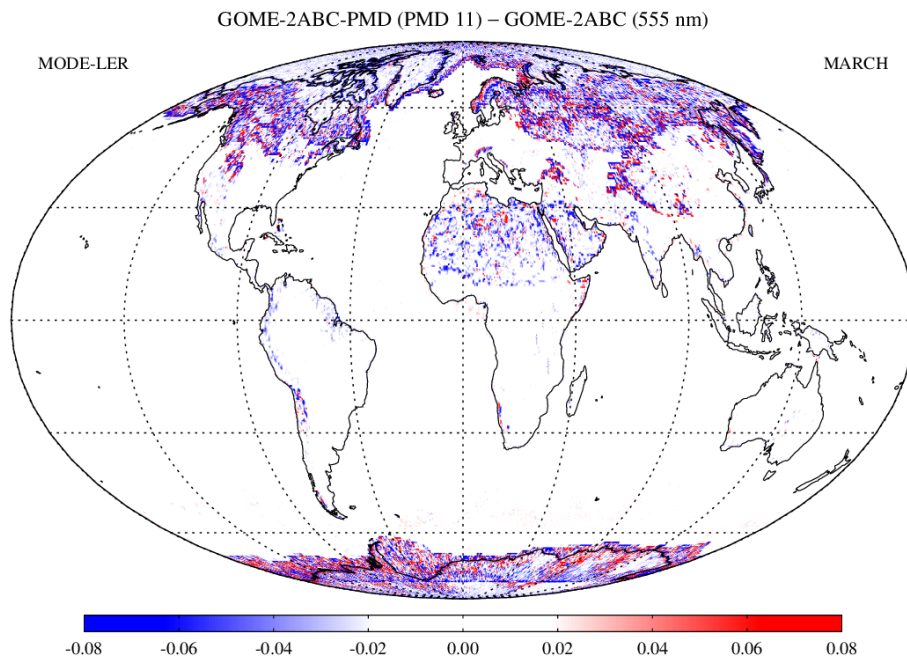


Figure 21: Map of the difference between the surface LER from the GOME-2ABC PMD-LER (PMD 11) and the GOME-2ABC MSC-LER (555 nm). The MODE-LER is plotted here, for March.

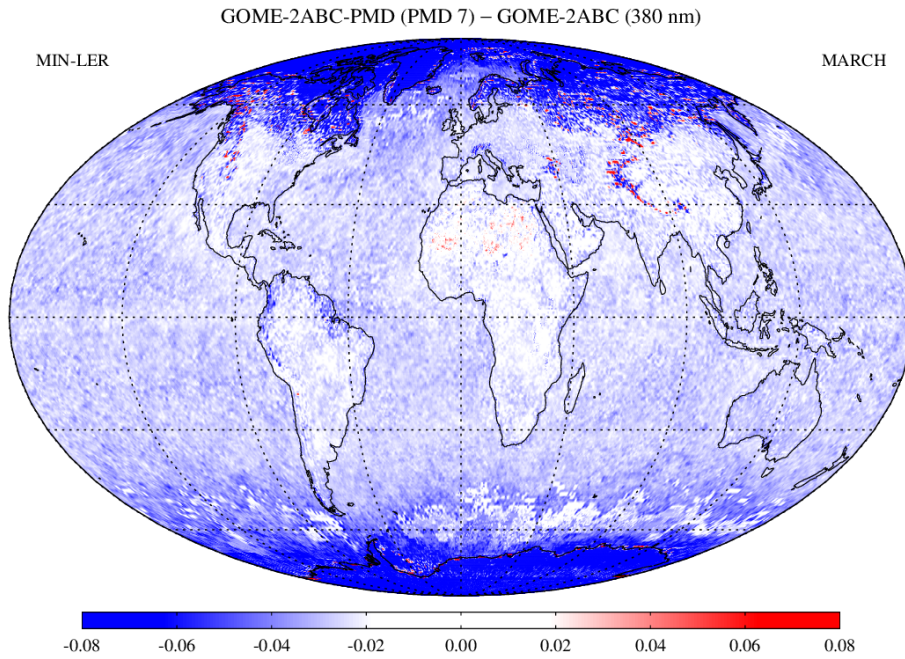


Figure 22: Map of the difference between the surface LER from the GOME-2ABC PMD-LER (PMD 7) and the GOME-2ABC MSC-LER (380 nm). The MIN-LER is plotted here, for March.

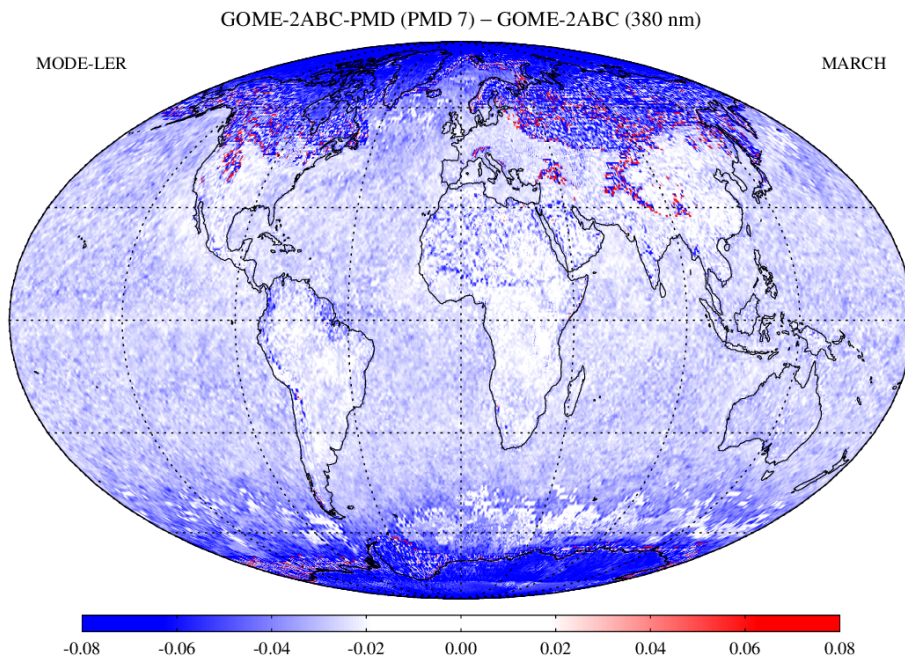


Figure 23: Map of the difference between the surface LER from the GOME-2ABC PMD-LER (PMD 7) and the GOME-2ABC MSC-LER (380 nm). The MODE-LER is plotted here, for March.

for the PMD bands [Tilstra *et al.*, 2011]. To be more precise, for PMD 7 the “transformation” from MSC to PMD that was found was $R_{\text{PMD7}} \approx 0.98 \cdot R_{\text{MSC}} - 0.01$. Such a relationship between MSC reflectance and measured PMD reflectance would explain a surface LER difference of -0.03 for snow surfaces (assuming an albedo of 0.8). For the desert areas (albedo around 0.2), the error explained would be around -0.014 . For the ocean (albedo around 0.03), the error explained would be around -0.01 . These numbers are in the range of what we see in Figures 22 and 23. Note that the PMD-LER may also be partly lower than the MSC-LER because of the better statistics involved, i.e., the higher chances of finding cloud-free scenes may lead to somewhat lower values for the PMD-LER.

7.2 Statistical analysis of the differences

In Figures 24 and 25 we present histograms of the surface LER differences for PMD 11 for all twelve months of the year. The MIN-LER differences are presented in Figure 24 and the MODE-LER differences are presented in Figure 25. The agreement is high. No seasonal dependence is observed. In Figures 26 and 27 we present the results for PMD 7. Here we find, as expected and as discussed earlier, larger differences. A large seasonal variation is again not present.

In Tables 9 and 10 we present the difference between PMD-LER and MSC-LER for all PMD bands that could be compared and for all months. The results for the MIN-LER comparison are presented in Table 9 and the ones for the MODE-LER comparison are presented in Table 10. Compared to the previous version of the database (v3.1), the performance is more or less the same. Only the reported FWHM values are smaller for all wavelength bands, which suggests that the PMD-LER database (and/or the MSC-LER database) is statistically more stable than before.

Appendix A presents tables with results from the intercomparisons that were presented earlier, but now for land and water surfaces separately.

7.3 Conclusion of the PMD-LER versus MSC-LER comparison

In general, the agreement between PMD-LER and MSC-LER is high. For the shorter wavelengths the differences that we find are larger. We attribute the differences between PMD-LER and MSC-LER mainly to imperfections in the radiometric calibration of the PMD bands. From earlier studies [Tilstra *et al.*, 2011] we know of the existence of such calibration issues for the PMD band reflectances. When we take the reported calibration errors of the PMD bands into account and calculate the impact for the different surface types we can reproduce the differences that were found between PMD-LER and MSC-LER. Therefore, differences in radiometric calibration explain most of the differences found. Note that the PMD-LER and MSC-LER retrieval codes are for the largest part identical.

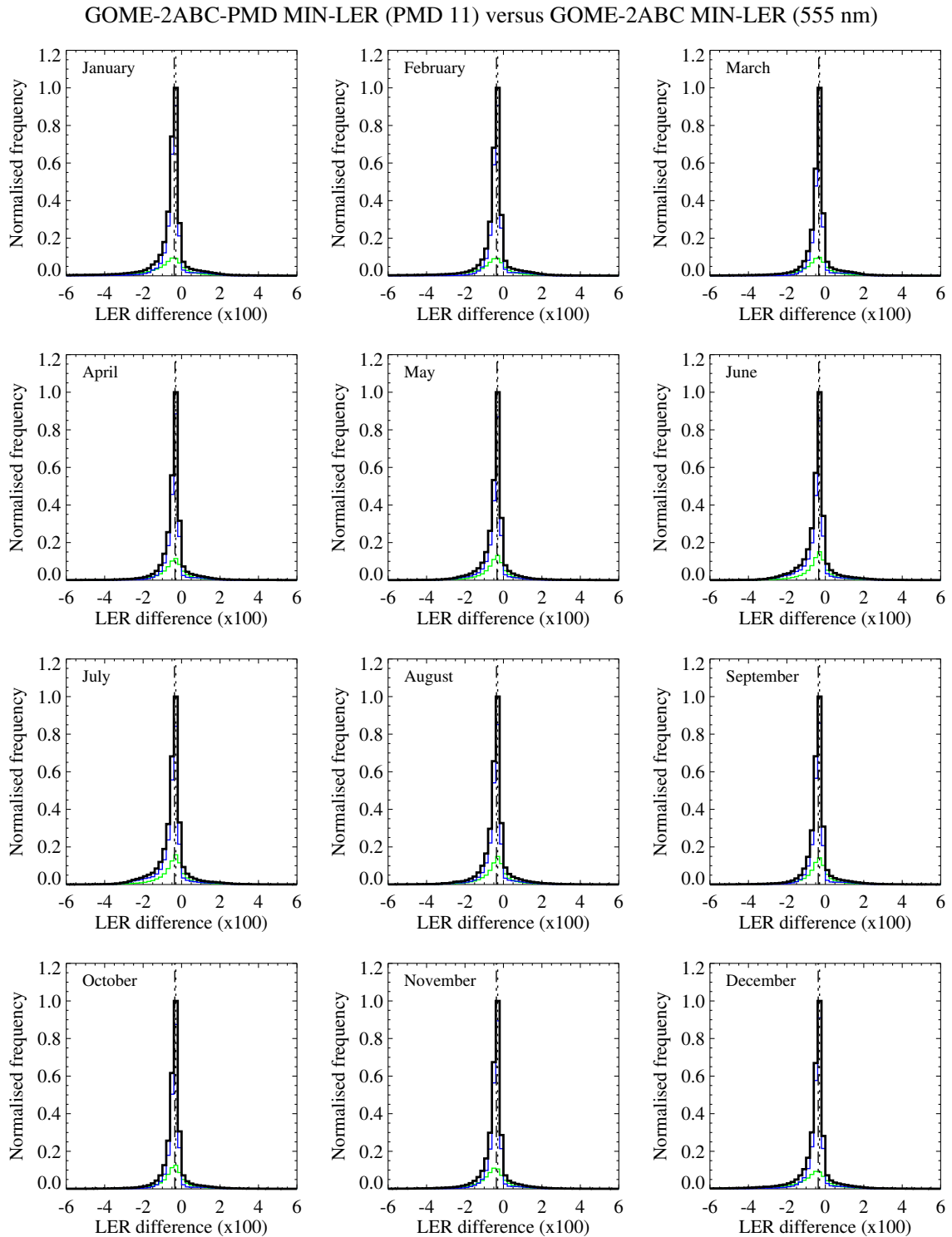


Figure 24: Histogram of the difference between the surface LER from the GOME-2ABC PMD-LER (PMD 11) and the GOME-2ABC MSC-LER (555 nm). The MIN-LER products are compared. The vertical lines indicate the mean (dashed line) and the mode (dotted line) of the distribution.

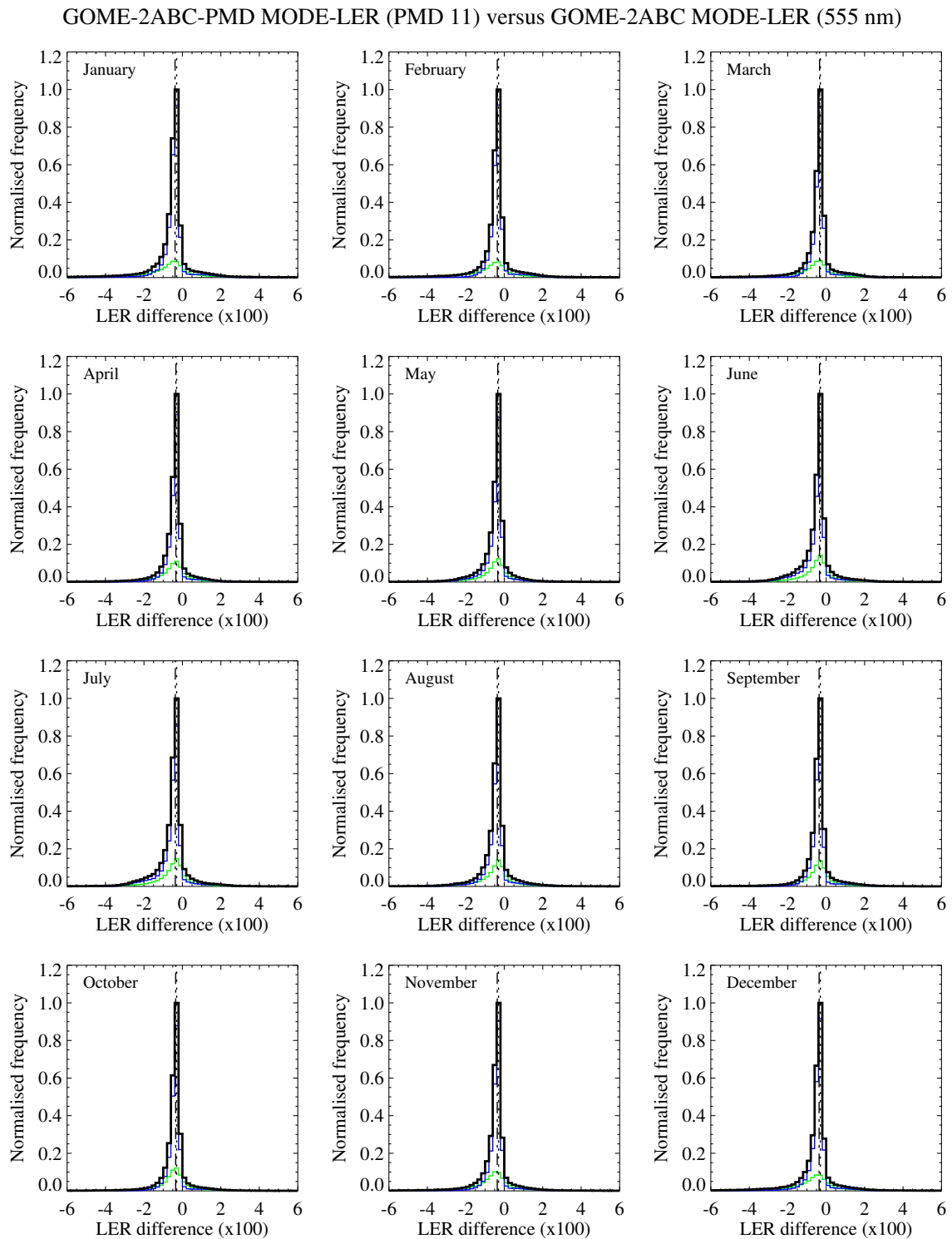


Figure 25: Histogram of the difference between the surface LER from the GOME-2ABC PMD-LER (PMD 11) and the GOME-2ABC MSC-LER (555 nm). The MODE-LER products are compared. The vertical lines indicate the mean (dashed line) and the mode (dotted line) of the distribution.

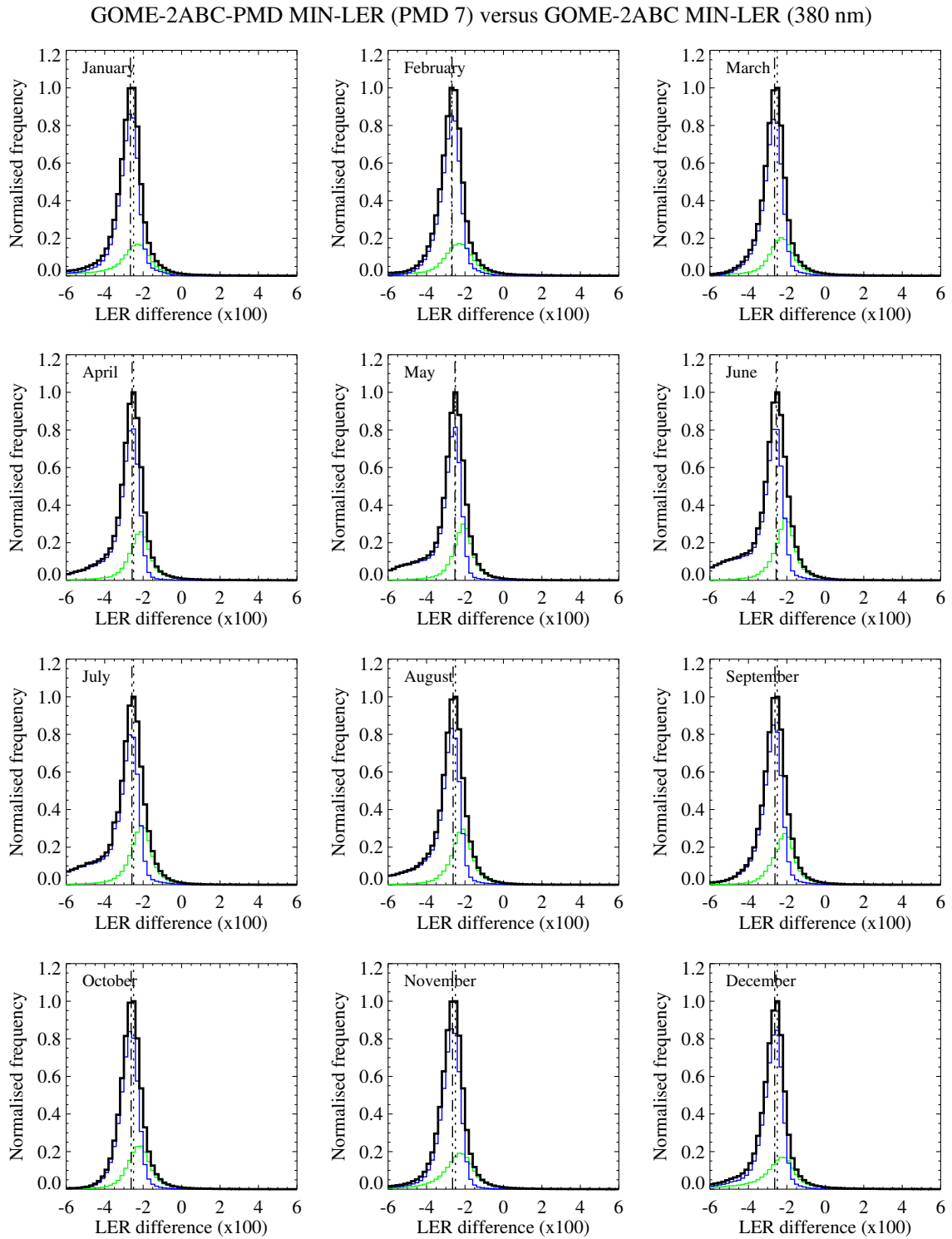


Figure 26: Histogram of the difference between the surface LER from the GOME-2ABC PMD-LER (PMD 7) and the GOME-2ABC MSC-LER (380 nm). The MIN-LER products are compared. The vertical lines indicate the mean (dashed line) and the mode (dotted line) of the distribution.

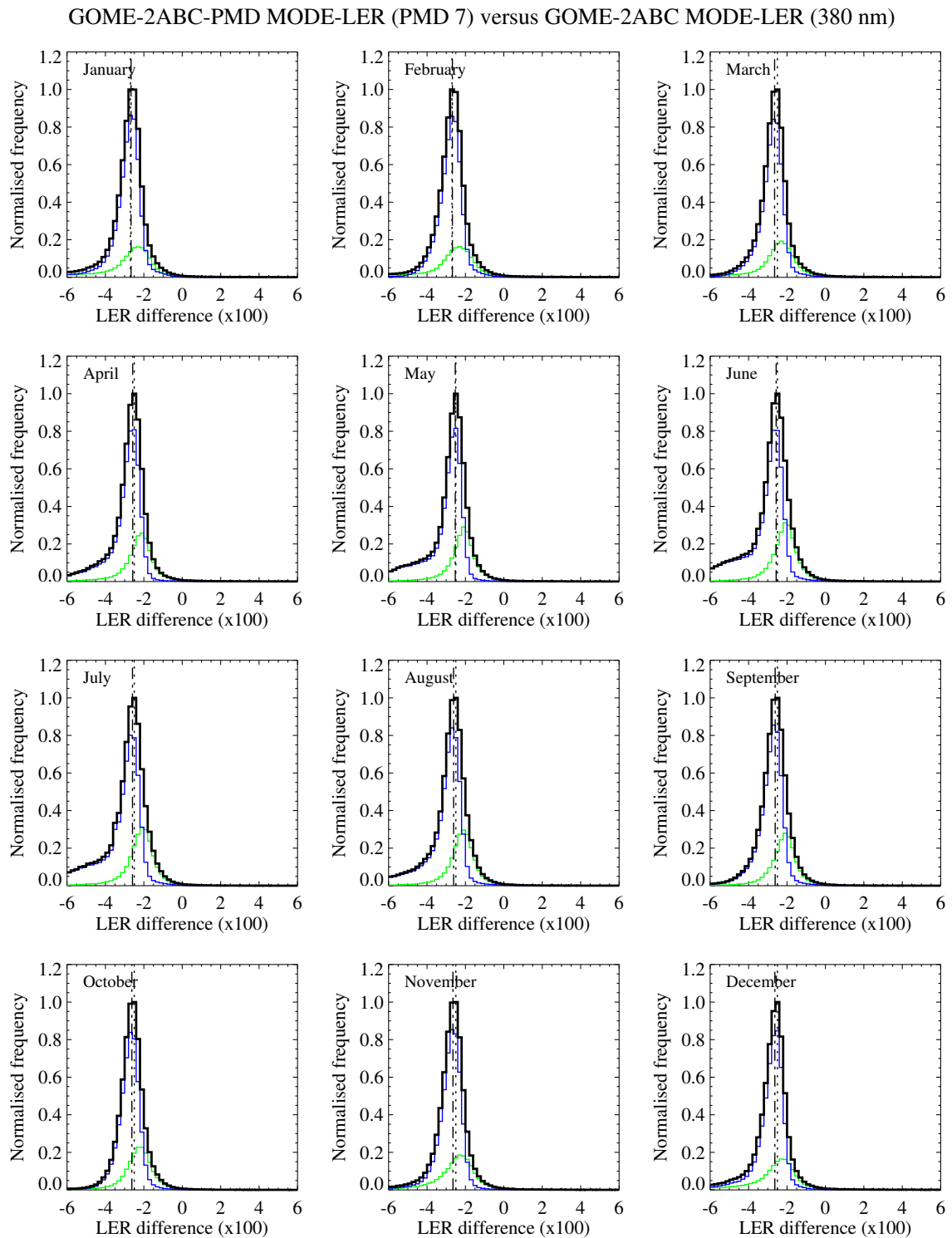


Figure 27: Histogram of the difference between the surface LER from the GOME-2ABC PMD-LER (PMD 7) and the GOME-2ABC MSC-LER (380 nm). The MODE-LER products are compared. The vertical lines indicate the mean (dashed line) and the mode (dotted line) of the distribution.

GOME-2ABC-PMD versus GOME-2ABC (MIN-LER)												
Mean surface LER difference ($\times 100$)												
PMD	JAN	FEB	MAR	APR	MAY	JUN	JUL	AUG	SEP	OCT	NOV	DEC
4	-3.21	-3.25	-3.16	-3.08	-3.04	-3.07	-3.08	-3.12	-3.15	-3.20	-3.20	-3.14
5	-3.07	-3.10	-3.07	-2.97	-2.92	-2.94	-2.96	-3.02	-3.03	-3.07	-3.07	-3.03
6	-1.09	-1.10	-1.07	-1.01	-0.97	-0.99	-1.00	-1.06	-1.04	-1.05	-1.04	-1.03
7	-2.66	-2.68	-2.64	-2.57	-2.52	-2.56	-2.59	-2.62	-2.62	-2.63	-2.65	-2.63
8	-0.54	-0.50	-0.45	-0.41	-0.40	-0.41	-0.42	-0.44	-0.46	-0.49	-0.50	-0.51
9	-0.68	-0.64	-0.59	-0.56	-0.54	-0.54	-0.57	-0.58	-0.60	-0.60	-0.63	-0.64
10	-0.71	-0.68	-0.65	-0.66	-0.65	-0.66	-0.68	-0.68	-0.69	-0.67	-0.69	-0.69
11	-0.38	-0.36	-0.34	-0.34	-0.34	-0.34	-0.37	-0.36	-0.37	-0.35	-0.37	-0.37
13	-0.10	-0.10	-0.10	-0.10	-0.11	-0.11	-0.13	-0.12	-0.11	-0.10	-0.10	-0.11
14	-0.25	-0.26	-0.26	-0.26	-0.26	-0.28	-0.29	-0.28	-0.26	-0.24	-0.25	-0.25
FWHM of distribution ($\times 100$)												
PMD	JAN	FEB	MAR	APR	MAY	JUN	JUL	AUG	SEP	OCT	NOV	DEC
4	1.70	1.78	1.65	1.57	1.67	1.87	1.82	1.60	1.57	1.59	1.71	1.68
5	1.61	1.66	1.56	1.46	1.50	1.71	1.71	1.53	1.51	1.51	1.60	1.60
6	1.12	1.13	1.07	1.02	1.03	1.14	1.12	1.06	1.05	1.05	1.08	1.11
7	1.25	1.29	1.22	1.22	1.20	1.37	1.42	1.32	1.32	1.22	1.26	1.24
8	0.84	0.83	0.77	0.74	0.74	0.79	0.81	0.78	0.78	0.78	0.82	0.83
9	0.70	0.69	0.67	0.66	0.68	0.75	0.77	0.74	0.72	0.67	0.69	0.68
10	0.55	0.54	0.53	0.55	0.56	0.56	0.57	0.56	0.53	0.52	0.54	0.55
11	0.48	0.46	0.42	0.42	0.42	0.45	0.50	0.47	0.46	0.43	0.46	0.46
13	0.39	0.39	0.37	0.36	0.36	0.38	0.42	0.39	0.39	0.38	0.39	0.38
14	0.43	0.42	0.41	0.43	0.46	0.49	0.49	0.47	0.43	0.41	0.43	0.44

Table 9: Mean difference in the surface LER of the GOME-2ABC-PMD and GOME-2ABC surface LER databases. The FWHM of the distribution is also given. The numbers have been multiplied by 100.

GOME-2ABC-PMD versus GOME-2ABC (MODE-LER)												
Mean surface LER difference ($\times 100$)												
PMD	JAN	FEB	MAR	APR	MAY	JUN	JUL	AUG	SEP	OCT	NOV	DEC
4	-3.21	-3.25	-3.15	-3.07	-3.03	-3.06	-3.07	-3.10	-3.14	-3.19	-3.19	-3.14
5	-3.07	-3.10	-3.07	-2.96	-2.91	-2.93	-2.95	-3.00	-3.01	-3.06	-3.07	-3.03
6	-1.09	-1.10	-1.06	-1.00	-0.97	-0.99	-0.99	-1.05	-1.03	-1.04	-1.04	-1.03
7	-2.66	-2.68	-2.65	-2.58	-2.53	-2.56	-2.59	-2.62	-2.62	-2.62	-2.65	-2.63
8	-0.54	-0.50	-0.45	-0.41	-0.40	-0.41	-0.43	-0.44	-0.46	-0.48	-0.49	-0.51
9	-0.68	-0.64	-0.60	-0.57	-0.54	-0.54	-0.57	-0.59	-0.60	-0.60	-0.63	-0.65
10	-0.70	-0.67	-0.65	-0.66	-0.65	-0.66	-0.69	-0.68	-0.68	-0.67	-0.68	-0.69
11	-0.38	-0.36	-0.34	-0.34	-0.34	-0.35	-0.37	-0.36	-0.37	-0.35	-0.37	-0.37
13	-0.10	-0.10	-0.10	-0.10	-0.11	-0.11	-0.13	-0.12	-0.11	-0.10	-0.10	-0.10
14	-0.25	-0.26	-0.26	-0.26	-0.26	-0.28	-0.29	-0.28	-0.26	-0.24	-0.25	-0.25
FWHM of distribution ($\times 100$)												
PMD	JAN	FEB	MAR	APR	MAY	JUN	JUL	AUG	SEP	OCT	NOV	DEC
4	1.69	1.78	1.66	1.59	1.69	1.89	1.84	1.62	1.58	1.59	1.70	1.67
5	1.60	1.66	1.57	1.48	1.52	1.72	1.72	1.54	1.52	1.51	1.59	1.58
6	1.12	1.13	1.08	1.03	1.04	1.15	1.13	1.06	1.04	1.05	1.08	1.11
7	1.24	1.28	1.23	1.23	1.21	1.38	1.44	1.34	1.34	1.22	1.25	1.22
8	0.84	0.82	0.77	0.74	0.74	0.79	0.82	0.78	0.78	0.77	0.82	0.82
9	0.69	0.69	0.66	0.65	0.67	0.74	0.76	0.73	0.72	0.67	0.68	0.67
10	0.55	0.53	0.52	0.55	0.56	0.56	0.57	0.56	0.53	0.51	0.53	0.54
11	0.48	0.46	0.42	0.42	0.42	0.45	0.50	0.47	0.45	0.42	0.45	0.45
13	0.38	0.38	0.36	0.36	0.36	0.38	0.41	0.39	0.38	0.37	0.39	0.38
14	0.43	0.42	0.41	0.43	0.47	0.49	0.49	0.47	0.43	0.41	0.43	0.44

Table 10: Mean difference in the surface LER of the GOME-2ABC-PMD and GOME-2ABC surface LER databases. The FWHM of the distribution is also given. The numbers have been multiplied by 100.

8 Comparing DLER with MODIS BRDF

In this section we compare the GOME-2 surface DLER database with MODIS surface BRDF data. The DLER product is by definition a Lambertian product, meaning that it will describe surface reflection optimally when it is used in a radiative transfer model that includes Lambertian surface reflection. The MODIS BRDF product, on the other hand, has to be used when the radiative transfer model can handle surface BRDF. Surface DLER and BRDF by definition are different properties.

Because DLER and BRDF are fundamentally different properties, we cannot compare the two *and* expect to find a good agreement between the two. For the UV wavelength range, where the Rayleigh optical thickness is high, we will have substantial multiple scattering. In these circumstances there will be quite some light paths which visit the surface more than once. In these cases, the (directional) Lambertian model cannot be expected to agree with the BRDF. But, for the longest wavelengths most light paths are only scattered once (and only at the surface). In these cases the DLER and BRDF should be much more alike. We will compare the two for a number of cases.

8.1 Case 1: Amazonia (vegetation)

In Figure 28 we compare the GOME-2 surface DLER product with the established MODIS BRDF product [Schaaf and Wang, 2015] for a 1×1 degree latitude/longitude box in the Amazon region. The MODIS kernel coefficients (f_{iso} , f_{vol} , f_{geo}) are taken from the MODIS MCD43C1 product, which has a spatial resolution of 0.05×0.05 degrees. We downloaded the MCD43C1 product for 15 March 2008, so it can be compared to the DLER result of the month March. To simulate the scanning motion of GOME-2, we let the viewing angle run from -55 to $+55$ degrees, and set realistic SZA and RAA, which both depend on the viewing angle. This is to simulate the fact that east-viewing and west-viewing directions for the same location will in general have been measured at different solar positions. The geometric and volumetric kernels K_{vol} and K_{geo} are calculated from the viewing and solar angles and the BRDF can be calculated from the kernels and the kernel coefficients.

The left window presents the comparison for MODIS band 4, which is centred around 555 nm. This band can be compared well to the 555-nm DLER wavelength band. In the right window MODIS band 1, centred around 645 nm, is compared to the 640-nm DLER wavelength band. For both wavelengths, there is quite a good agreement between the MODIS BRDF and GOME-2 surface DLER. This is to be expected, because for the wavelengths involved (555 nm and 645 nm) there should not be a large difference between BRDF and surface DLER. This is because the optical thickness of the atmosphere is relatively low at these wavelengths, and light paths involving multiple surface reflections are rare. In any case, the agreement is a strong indication that the GOME-2 surface DLER product is found to exhibit the expected directional behaviour when compared to MODIS BRDF.

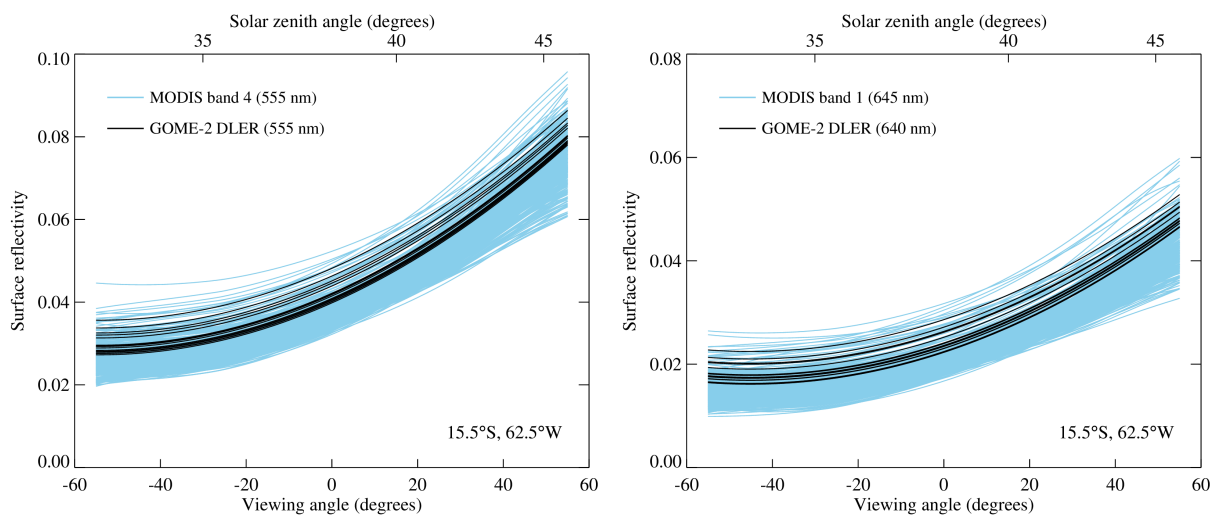


Figure 28: MODIS BRDF versus GOME-2 MSC-DLER for a 1×1 degree latitude/longitude box in Amazonia. The scanning motion of GOME-2 is simulated by letting the viewing angle run from -55 (east-viewing) to $+55$ degrees (west-viewing), with SZA and RAA depending on the viewing angle.

In Figure 29 we present a similar plot as shown in Figure 28, but this time the PMD-based surface DLER product is compared with the MODIS surface BRDF. The blue MODIS BRDF curves have not changed, the black curves, which now represent the PMD-DLER, have changed slightly. We can conclude that there is good agreement between the PMD-DLER and the MODIS BRDF. Note that the black PMD-DLER curves show more variability amongst themselves than the black MSC-DLER curves do in Figure 29. This is both normal and as expected, because the PMD-based (D)LER database has a higher internal spatial resolution than the MSC-based (D)LER database.

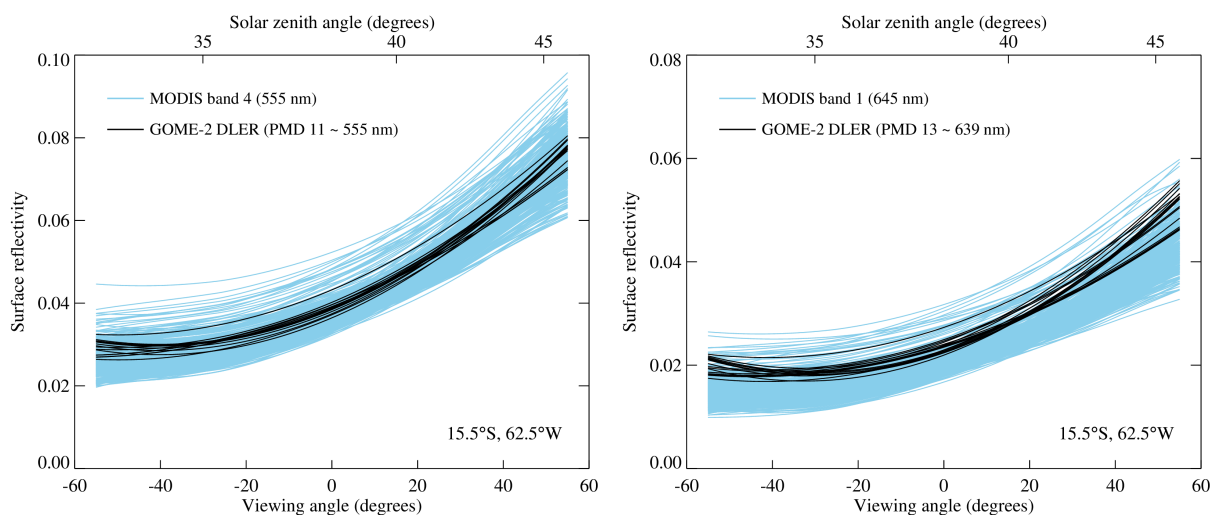


Figure 29: MODIS BRDF versus GOME-2 PMD-DLER for Amazonia. Compare with Figure 28. Note that the PMD-DLER has a higher internal spatial resolution than the MSC-DLER.

8.2 Case 2: Equatorial Africa (vegetation)

In Figures 30 and 31 we perform the same analyses as before, but now for a region in Equatorial Africa. The main surface type in the 1×1 degree latitude/longitude box is “vegetation”. While searching for scenes to study we tried to find homogeneous scenes, but there is still quite some variability in the surface as evidenced by the blue MODIS BRDF curves. The agreement that we find between the MSC-DLER/PMD-DLER on the one side and the MODIS BRDF on the other is again good, but slightly less good than found in Figures 28 and 29 for the Amazonia case.

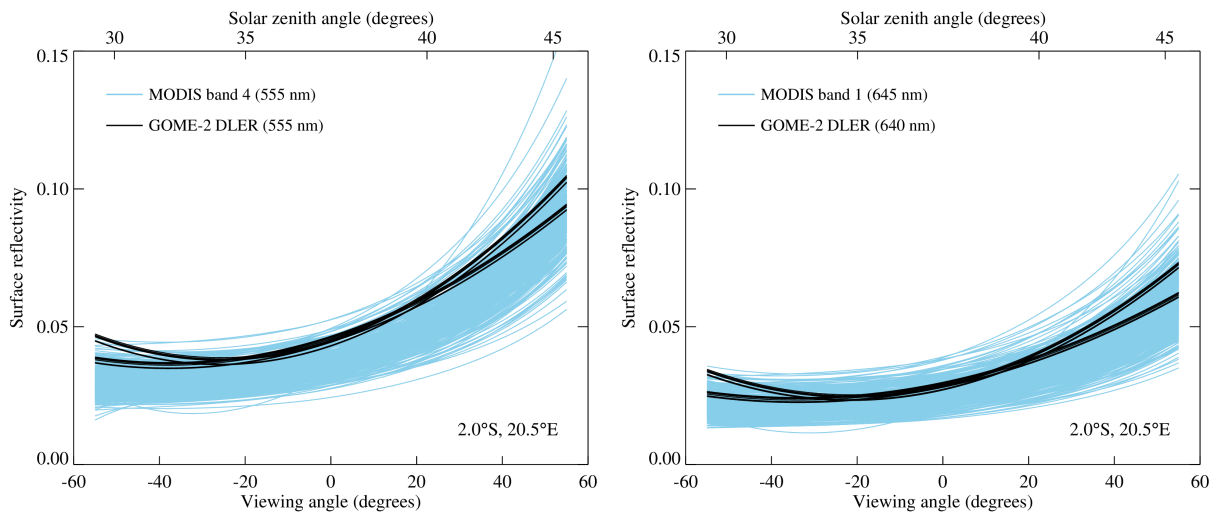


Figure 30: MODIS BRDF versus GOME-2 MSC-DLER for a 1×1 degree latitude/longitude box in Equatorial Africa. The dominating surface type for this region is vegetation.

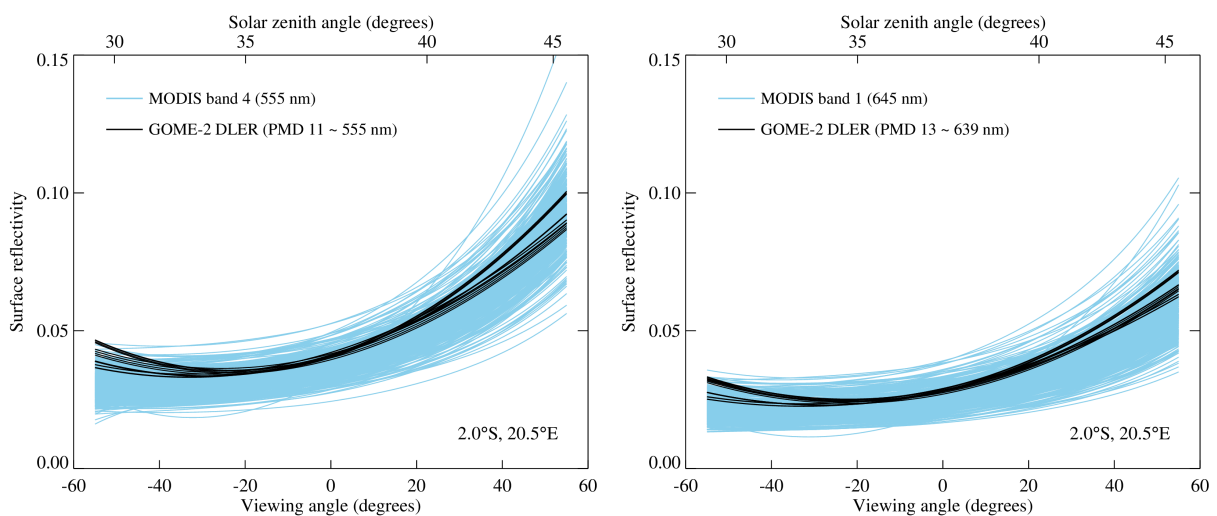


Figure 31: MODIS BRDF versus GOME-2 PMD-DLER for Equatorial Africa.

8.3 Case 3: Libyan desert

Figures 32 and 33 present the results for the Libyan desert. This part of the desert is homogeneous and quite bright. Because of the high surface reflection, light paths which visit the surface more than once are more likely to occur, and this is reflected in a higher mismatch between DLER and BRDF, especially for the shortest wavelengths. As a result of this, the agreement between the MSC-DLER/PMD-DLER on the one side and MODIS BRDF on the other is not much better than reasonable at 555 nm. Around 645 nm, however, the agreement can be considered quite good.

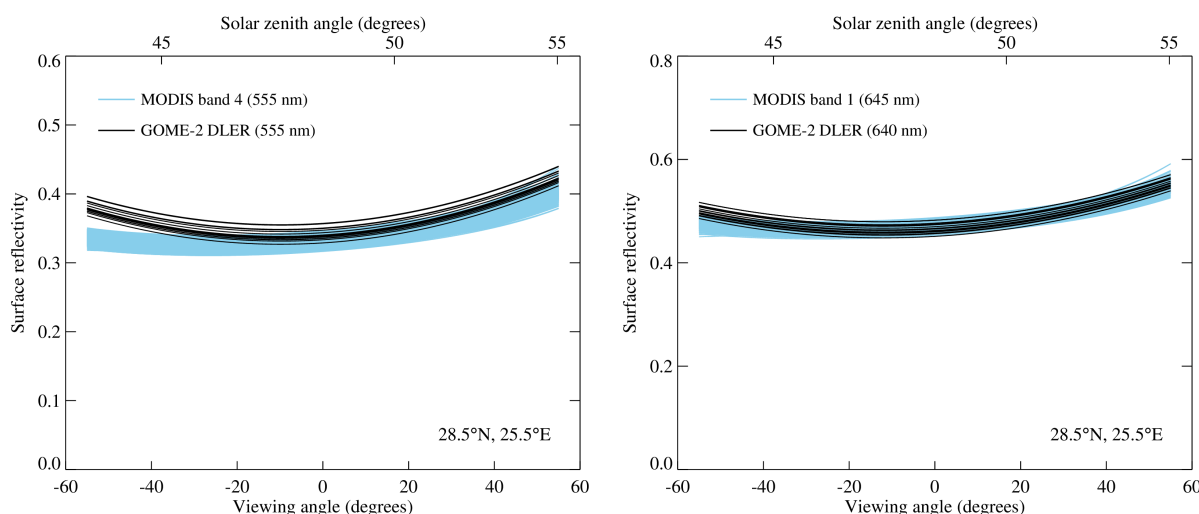


Figure 32: MODIS BRDF versus GOME-2 MSC-DLER for a 1×1 degree latitude/longitude box in the Libyan desert. This part of the desert is quite bright and very homogeneous.

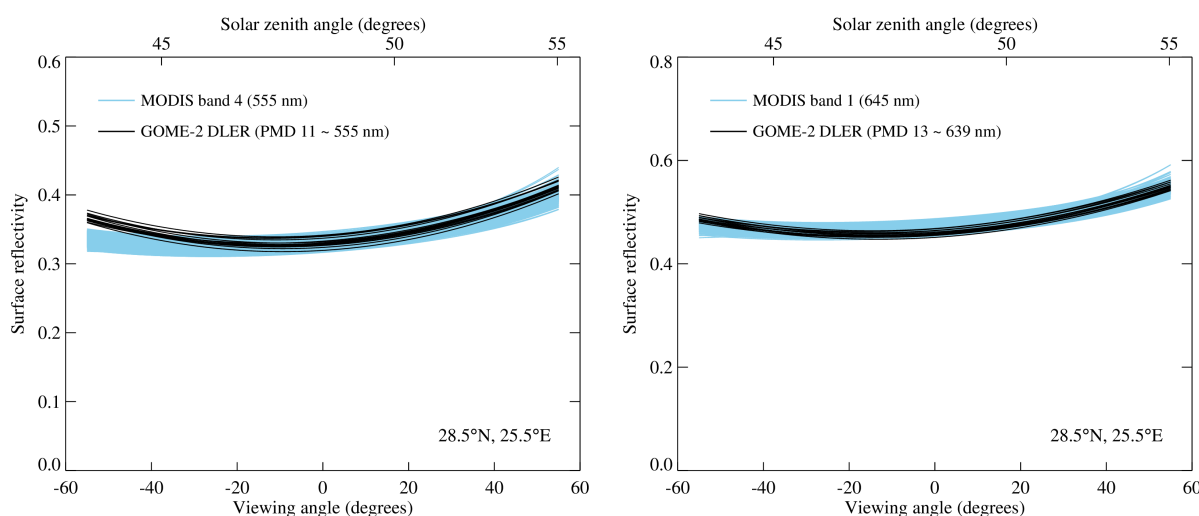


Figure 33: MODIS BRDF versus GOME-2 PMD-DLER for the Libyan desert.

Also for this case there is good agreement between the MSC-DLER and the PMD-DLER. This is as expected. Compared to the MODIS BRDF at 645 nm, the PMD-DLER seems to agree a little less than the MSC-DLER. This may be due to the fact that PMD 13 is quite a broad PMD band [EUMETSAT, 2021; Tilstra et al., 2024a]. However, the differences are very small.

8.4 Summary

The comparisons that were shown in this chapter cannot be considered as part of a validation study, because DLER and BRDF are fundamentally different properties. However, by restricting ourselves to conditions where DLER and BRDF should not differ too much we can still perform a meaningful verification. We therefore restricted ourselves to the longer wavelength bands, and focused on homogeneous scenes. For these scenes, the absolute values of the two properties are very similar. Differences are found, but these can be interpreted as the result of the fundamental difference between DLER and BRDF. We therefore wish to conclude that the directional behaviour of the DLER database is supported at least qualitatively by the comparisons with MODIS BRDF.

The MODIS MCD43C1 data product was retrieved from the online Data Pool, courtesy of the NASA Land Processes Distributed Active Archive Center (LP DAAC), USGS/Earth Resources Observation and Science (EROS) Center, Sioux Falls, South Dakota, https://lpdaac.usgs.gov/data_access/data_pool.

9 Comparison with previous version of the database

In this section we compare the current version of the GOME-2 surface LER database with the previous version of the database. The current version of the database is O3M-402.1, created with processor version 4.1, based on data from GOME-2A, GOME-2B, and GOME-2C, and covering the years 2007–2022. The previous version of the database is O3M-402, created with processor version 3.1, based on data from GOME-2A and GOME-2B, and covering the years 2007–2018.

9.1 v4.1 versus v3.1 – Main Science Channels

Figures 34 to 36 present three typical global maps of the differences between the current v4.1 DLER product and the previous v3.1 DLER product. The images apply to the month March and to the 772-nm wavelength band, and are based on the MIN-LER fields inside the MSC versions of the databases. Because the DLER is by definition dependent on the viewing angle, the global maps were determined for viewing angles of -45° , 0° , and $+45^\circ$, indicated by the labels “East”, “Nadir”, and “West”, respectively, in Figures 34 to 36. However, because the DLER is equal to the non-directional LER over the oceans, the parts over the ocean are identical in Figures 34 to 36. Differences over the oceans are quite small and in most cases not visible in Figures 34 to 36. However, some blue colours

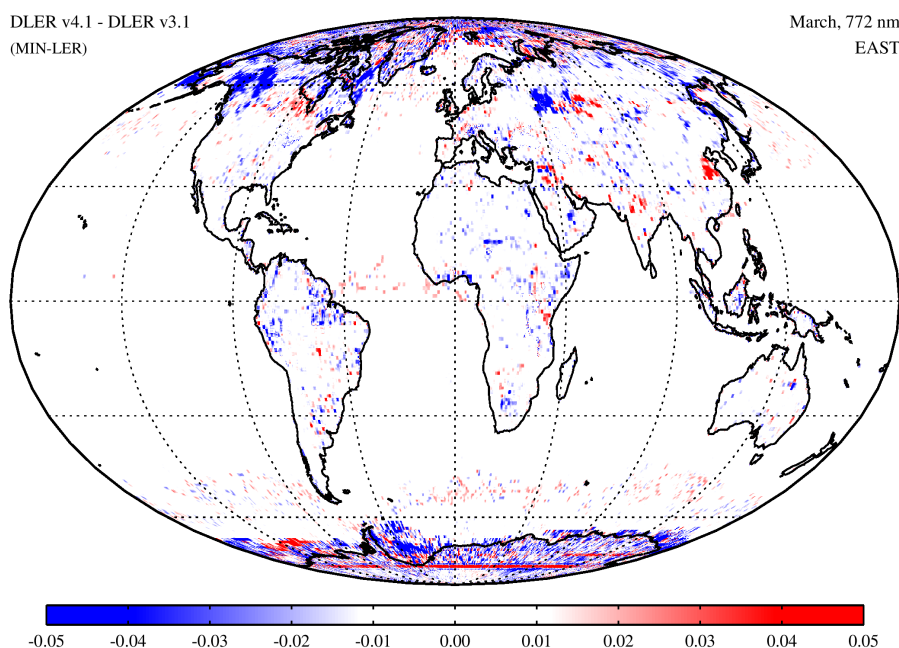


Figure 34: Global map of the v4.1 MSC-DLER minus v3.1 MSC-LER for the month March and for the 772-nm wavelength band. The DLER fields were calculated for a viewing angle of -45° .

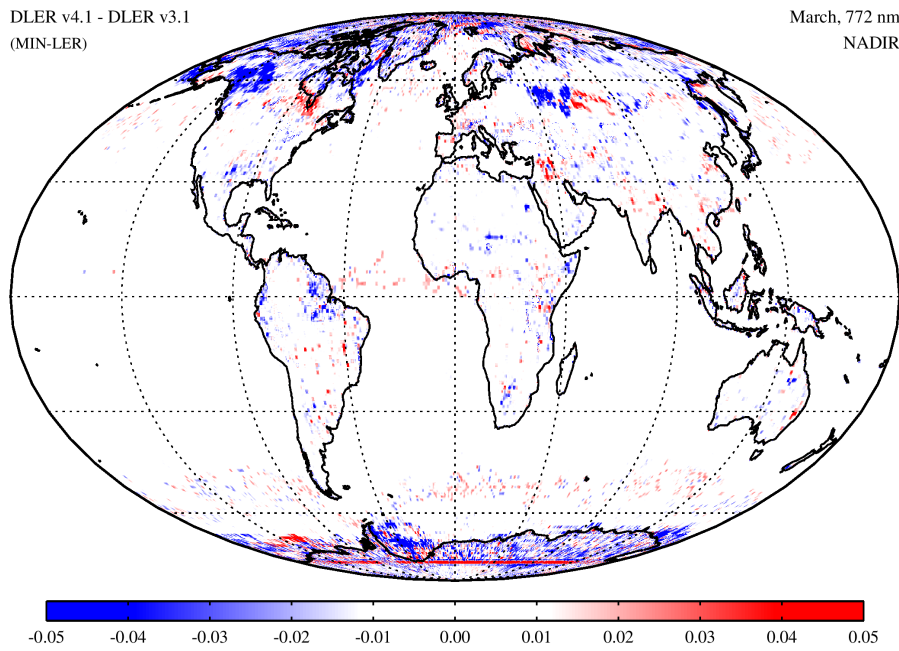


Figure 35: Global map of the v4.1 MSC-DLER minus v3.1 MSC-LER for the month March and for the 772-nm wavelength band. The DLER fields were calculated for a viewing angle of 0°.

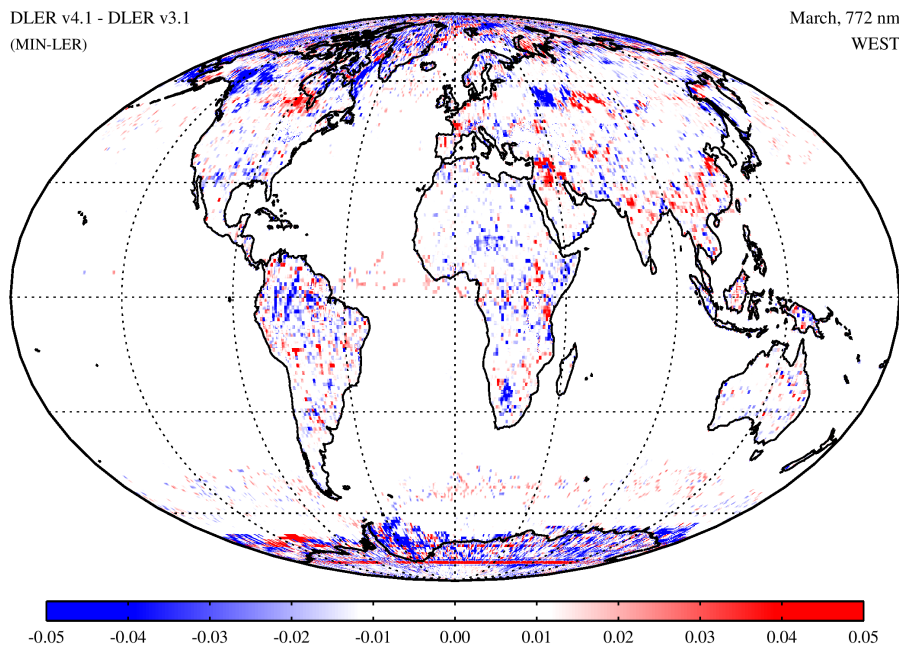


Figure 36: Global map of the v4.1 MSC-DLER minus v3.1 MSC-LER for the month March and for the 772-nm wavelength band. The DLER fields were calculated for a viewing angle of +45°.

are found, which can easily be explained by the fact that the new database suffers less from cloud contamination than the old one. On the other hand, there are also plenty grid cells with red colours.

These red colours are, however, not indicative for cloud contamination in the new database. In fact, the red colours are linked to grid cells which were cloud contaminated in the old database, but not in the new database. The post-processing correction on the old database replaced the surface LER for these grid cells with a replacement surface LER from donor grid cells. This surface LER was the lowest surface LER found in a rectangular region around the grid cell. In many cases, this lowest value is too low, which explains the red colour for these grid cells. So, the new database does better because the new surface LER is not cloud contaminated, while it was in the old database version.

Over land, the differences that we see are larger and different for the three viewing geometries. In general, we see more blue colours than red colours. Red colours are mostly related to differences in snow/ice situations. Much more interesting are the blue colours that are found near the Equator, in the Amazon region, in Africa, and in Indonesia/Borneo. These are typically areas for which cloud contamination is an issue. That the v4.1 DLER is smaller than the v3.1 LER for these regions is caused by the fact that we have combined much more GOME-2 data. The higher amount of available observations reduces the problem of residual cloud contamination for these areas.

9.2 v4.1 versus v3.1 – PMD bands

The same comparison as in the previous section was also performed for the PMD-based databases. In Figures 37 to 39 the results apply to the v4.1 PMD-DLER and to the v3.1 PMD-DLER. The results are again shown for the month March, and we selected PMD 15 because it is closest to the 772-nm MSC-LER wavelength band. In general, the PMD-based plots are very similar to the MSC-based plots shown earlier. Exceptions are found over the ocean, where the differences that are found are clearly smaller for the PMD-LER, and in the much larger blue area for the PMD-LER over Russia. The latter blue area is probably related to differences in snow/ice situation. Note that the PMD-LER misses data from the months March 2007 and March 2008 because the PMD-LER is based on data from 13 March 2008 till August 2022, whereas the MSC-LER is based on data from January 2007 till August 2022. Such differences between MSC-LER and PMD-LER databases due to time period coverage have been discussed before in this VR as well as in previous versions of the VR.

In Figure 37 we can also see the blue regions near the Equator, which illustrate an improvement due to a reduction in terms of residual cloud contamination. The improvement is comparable to that of the MSC-based databases. Note that, like the MSC-LER, the PMD-LER seems to have changed mostly in the “West” viewing direction. That is, the colour blue is more dominant than it is for the “East” and “Nadir” directions. Another thing worth noting is the reddish colour over the desert areas in Northern Africa. This is found for all three viewing directions. It is not clear to us what causes the

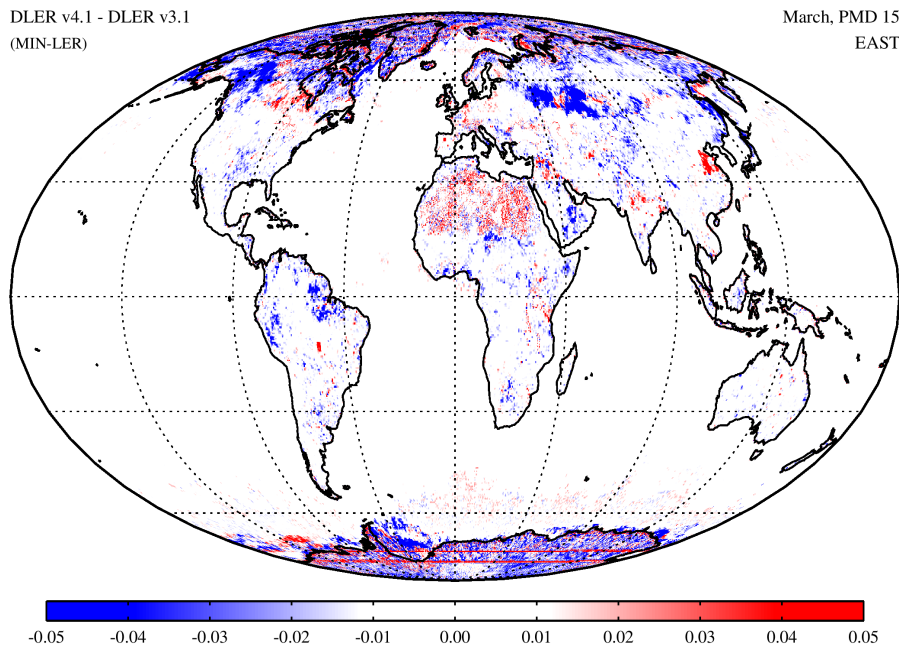


Figure 37: Global map of the v4.1 PMD-DLER minus v3.1 PMD-LER for the month March and for PMD 15. The DLER fields were calculated for a viewing angle of -45° .

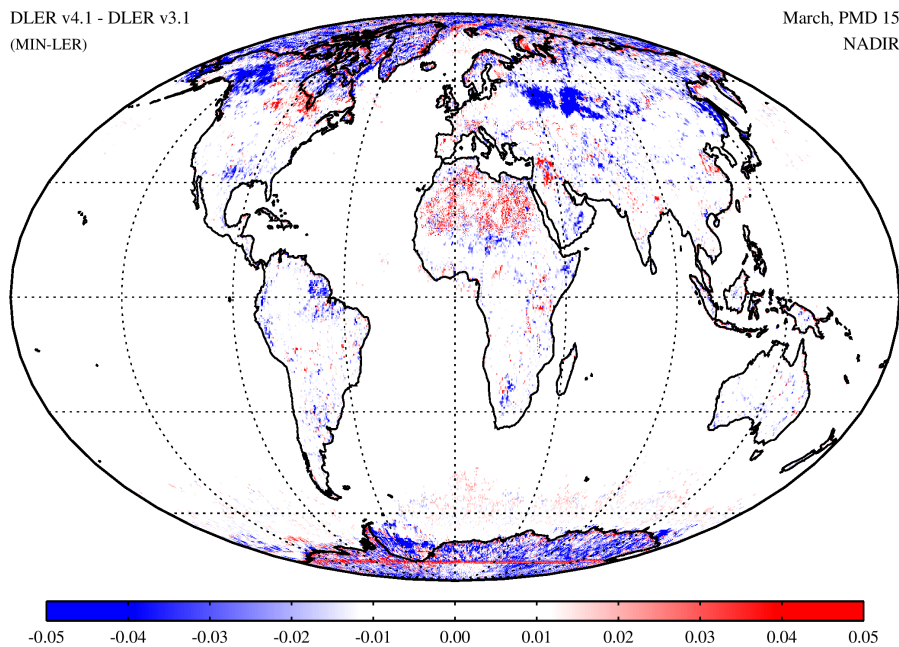


Figure 38: Global map of the v4.1 PMD-DLER minus v3.1 PMD-LER for the month March and for PMD 15. The DLER fields were calculated for a viewing angle of 0° .

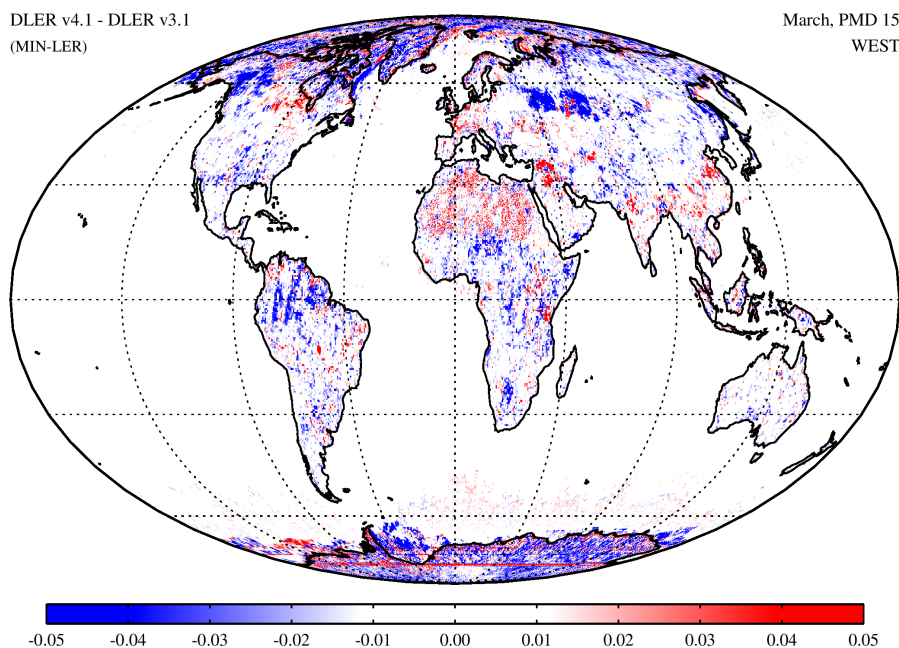


Figure 39: Global map of the v4.1 PMD-DLER minus v3.1 PMD-DLER for the month March and for PMD 15. The DLER fields were calculated for a viewing angle of $+45^\circ$.

differences, but we expect these to be the result of improvements due to the higher amount of data that were used for the new v4.1 database.

Also clear from Figures 34 to 39 is the higher spatial resolution of the PMD-based databases. Although both MSC-LER and PMD-LER fields have a spatial resolution of $0.25^\circ \times 0.25^\circ$, the intrinsic spatial resolution of MSC-LER and PMD-LER are different. The MSC-LER has an intrinsic spatial resolution of $1.0^\circ \times 1.0^\circ$. The PMD-LER has an intrinsic spatial resolution of $0.5^\circ \times 0.5^\circ$.

9.3 Summary

The comparison between the current version of the GOME-2 surface LER database with the previous version of the database shows large differences. This is as expected, because the previous version did not contain the DLER product. At west-viewing geometries the differences are quite large, at east-viewing geometries the differences are small. We showed results for 772 nm and PMD 15. These are long wavelengths, and the effects of surface BRDF are the largest for these cases. We also only showed results for the MIN-LER product. The MODE-LER fields are very similar, however.

10 Summary and conclusions

By direct comparison with the GOME-1 and OMI surface LER databases we conclude that the GOME-2ABC MSC MIN-LER and the GOME-2ABC MSC MODE-LER surface LER products are accurate within 0.01 over the ocean and accurate within 0.04 over snow/ice surfaces. These numbers are valid under the assumption that the most important reference used here (the OMI surface LER product) is perfect. Differences in overpass time and observation geometry have an impact on the retrieved surface LER. From this point of view, the small difference found from the comparisons must be regarded as a clear indication that the GOME-2ABC surface LER product has a high quality.

As for the GOME-2ABC PMD-based surface LER, we were only able to validate the surface LER from the PMD bands up to PMD 9. The results indicate that the PMD-LER is reliable. Over the ocean there appears to be a bias of 0.01, depending on PMD/wavelength. Over land the differences are again higher, as was the case for the MSC-based LER. The differences are most likely caused by the radiometric calibration of the PMDs. The existence of radiometric calibration issues is not speculative as these have already been reported in the past [Tilstra *et al.*, 2011].

A comparison between GOME-2ABC PMD-LER and GOME-2ABC MSC-LER showed that there is a good agreement for the higher PMD bands, but a less good agreement for the lower PMD bands. We attribute the differences that are found mainly to calibration issues. Compared to the previous version of the database there is a considerable improvement for all PMD bands.

The requirements that are set in the AC SAF Product Requirements Document (PRD) [AC SAF Project Team, 2023] are the following. The “threshold”, “target”, and “optimal” levels are set at 0.05 + 10%, 0.03 + 10%, and 0.01 + 5%, respectively. These bias values are in absolute units of surface albedo. The comparisons that were presented in this VR indicate very clearly that at least the “threshold” and “target” levels are reached quite easily. However, also the “optimal” level is reached, albeit more easily for the wavelength bands above 400 nm than for the wavelength bands below 400 nm (see, for instance, Table 6). Note that the requirements that were set in the PRD do not distinguish between land and water surfaces. In appendix A, intercomparison results are shown for land and water surfaces separately. Although land and water surfaces seem to behave somewhat differently, both surface types meet the requirements that were set in the PRD.

Given these results, the conclusion of this VR is that the requirements are met and that the GOME-2 surface DLER database can be used for its original purpose, which is to serve as input for the retrieval of various products of atmospheric composition. It is, however, important to mention the known limitations of the database. Cloud contamination by residual clouds can still occur, although cloud contamination has been reduced considerably with each update of the database. The user should also be aware of the potential impact of aerosol presence. Aerosol filtering is part of the algorithm setup,

but since no filtering is ever perfect, aerosol contamination should be expected, especially for areas which are well known for their aerosol presence.

Instrument degradation was already mentioned as one of the factors that could potentially affect the quality of the database. A correction for instrument degradation is applied to the reflectances, as explained in the ATBD [Tilstra *et al.*, 2024a]. The accuracy of the correction has been studied quite well in the past and the reflectance is corrected to well within the 0.1% level [Tilstra *et al.*, 2012a,b]. Given the error calculations presented in section 8 of the ATBD, this would result in errors in the surface LER values of $\sim 0.01\text{--}0.02\%$. This is very small, if not negligible, compared to the requirements that were mentioned above. We therefore conclude that imperfections in the correction for instrument degradation can only have a negligible impact on the quality of the database.

Another limitation is the usage of data in the polar regions. Due to the phenomenon of polar night, data in the polar regions may consist of donor data taken from neighbouring months. These situations are flagged and users are encouraged to use the flags provided in the database.

A Tables with extended validation results

This appendix contains tables with results from the intercomparisons that were presented earlier, but now for land and water surfaces separately. The results for land and water surfaces are different, but both surface types meet the requirements that were set in the PRD [*AC SAF Project Team, 2023*].

GOME-2ABC versus GOME-1 (MIN-LER)												
Mean surface LER difference ($\times 100$)												
λ (nm)	JAN	FEB	MAR	APR	MAY	JUN	JUL	AUG	SEP	OCT	NOV	DEC
335	0.68	0.77	0.84	-0.27	-0.60	-0.95	0.12	0.27	0.51	0.36	0.49	1.01
380	1.67	1.79	1.66	1.08	0.85	0.77	1.35	1.56	1.57	1.41	1.52	1.77
416	0.30	0.32	0.13	-0.43	-0.48	-0.51	-0.14	-0.05	0.00	-0.12	-0.10	0.30
440	0.07	0.19	0.01	-0.43	-0.50	-0.53	-0.17	-0.04	-0.04	-0.18	-0.13	0.19
463	0.01	0.13	-0.07	-0.43	-0.51	-0.53	-0.15	-0.04	-0.07	-0.23	-0.15	0.11
494	-0.16	-0.07	-0.26	-0.57	-0.66	-0.70	-0.27	-0.16	-0.25	-0.42	-0.31	-0.06
555	-0.54	-0.39	-0.59	-0.85	-1.02	-1.09	-0.58	-0.45	-0.48	-0.67	-0.56	-0.40
610	-0.63	-0.46	-0.66	-0.87	-0.98	-1.04	-0.56	-0.50	-0.55	-0.72	-0.59	-0.46
670	-0.79	-0.61	-0.80	-1.03	-1.14	-1.22	-0.71	-0.66	-0.69	-0.87	-0.74	-0.61
758	-1.05	-0.84	-1.04	-1.26	-1.39	-1.49	-0.99	-0.92	-0.91	-1.08	-0.96	-0.88
772	-1.07	-0.86	-1.05	-1.26	-1.40	-1.49	-1.00	-0.92	-0.93	-1.09	-0.97	-0.89
FWHM of distribution ($\times 100$)												
λ (nm)	JAN	FEB	MAR	APR	MAY	JUN	JUL	AUG	SEP	OCT	NOV	DEC
335	3.48	3.64	3.74	3.27	3.63	3.91	4.02	4.05	3.90	3.65	3.75	3.84
380	2.81	2.82	2.84	2.75	2.90	3.01	2.95	2.75	2.79	2.66	2.79	2.92
416	2.64	2.63	2.64	2.68	2.81	2.86	2.89	2.61	2.54	2.48	2.58	2.58
440	2.59	2.52	2.54	2.63	2.73	2.86	2.85	2.53	2.45	2.40	2.49	2.52
463	2.51	2.41	2.44	2.60	2.70	2.84	2.81	2.48	2.39	2.35	2.42	2.43
494	2.45	2.32	2.36	2.57	2.68	2.82	2.77	2.43	2.37	2.34	2.39	2.37
555	2.48	2.33	2.34	2.48	2.58	2.69	2.65	2.34	2.35	2.37	2.39	2.39
610	2.47	2.31	2.33	2.49	2.56	2.63	2.58	2.32	2.32	2.38	2.39	2.39
670	2.48	2.32	2.35	2.51	2.58	2.64	2.59	2.34	2.33	2.41	2.40	2.41
758	2.56	2.40	2.42	2.55	2.61	2.64	2.64	2.41	2.39	2.48	2.47	2.50
772	2.60	2.43	2.45	2.57	2.63	2.66	2.66	2.43	2.42	2.51	2.50	2.53

Table 11: Mean difference in the surface LER of the GOME-2ABC and GOME-1 surface LER databases, for water surfaces. The FWHM of the distribution is also given. The numbers have been multiplied by 100.

GOME-2ABC versus GOME-1 (MIN-LER)												
Mean surface LER difference ($\times 100$)												
λ (nm)	JAN	FEB	MAR	APR	MAY	JUN	JUL	AUG	SEP	OCT	NOV	DEC
335	1.50	0.62	0.70	0.50	0.30	-0.10	0.43	0.70	0.13	0.31	-0.28	1.50
380	1.61	1.72	1.35	1.16	1.06	1.01	1.34	1.37	1.38	1.34	1.22	1.32
416	0.56	0.55	0.17	-0.01	0.11	0.14	0.26	0.20	0.28	0.26	0.17	0.37
440	0.14	0.22	-0.11	-0.22	-0.10	-0.08	0.05	0.04	0.09	0.07	0.00	0.11
463	-0.08	-0.02	-0.34	-0.39	-0.27	-0.26	-0.09	-0.09	-0.05	-0.08	-0.15	-0.09
494	-0.37	-0.32	-0.62	-0.63	-0.49	-0.50	-0.28	-0.27	-0.29	-0.36	-0.41	-0.34
555	-1.03	-0.91	-1.12	-1.01	-0.91	-1.02	-0.78	-0.72	-0.65	-0.71	-0.90	-0.88
610	-1.60	-1.39	-1.60	-1.48	-1.28	-1.34	-1.02	-0.99	-0.98	-1.07	-1.26	-1.27
670	-2.13	-1.88	-2.09	-2.05	-1.75	-1.76	-1.35	-1.30	-1.33	-1.52	-1.74	-1.70
758	-2.30	-1.70	-1.90	-0.70	-0.90	-0.70	-1.30	-1.10	-1.30	-1.50	-1.30	-1.50
772	-2.30	-2.30	-2.10	-1.10	-2.30	-0.70	-1.10	-1.10	-1.30	-1.50	-1.10	-1.90
FWHM of distribution ($\times 100$)												
λ (nm)	JAN	FEB	MAR	APR	MAY	JUN	JUL	AUG	SEP	OCT	NOV	DEC
335	3.04	6.25	3.04	3.04	3.04	3.04	5.78	3.04	7.21	6.83	8.67	3.04
380	5.08	4.42	4.37	3.91	3.69	3.58	3.56	3.63	3.63	3.93	4.44	4.98
416	4.48	4.10	3.98	3.59	3.27	3.13	3.04	3.03	3.03	3.16	3.62	4.09
440	4.46	4.11	3.91	3.54	3.22	3.13	2.97	2.90	2.92	3.02	3.48	4.08
463	4.51	4.15	3.92	3.59	3.28	3.23	2.99	2.86	2.89	3.00	3.52	4.14
494	4.56	4.21	3.95	3.65	3.34	3.31	3.02	2.83	2.89	3.03	3.56	4.16
555	5.34	5.04	4.73	4.23	3.85	3.95	3.67	3.43	3.45	3.56	4.33	5.00
610	6.41	5.98	5.55	4.90	4.30	4.19	3.91	3.58	3.72	3.97	4.89	5.81
670	7.10	6.60	6.11	5.63	4.87	4.61	4.29	3.88	4.10	4.35	5.38	6.33
758	3.04	3.04	3.04	3.04	3.04	3.04	3.04	3.04	3.04	3.04	3.04	3.04
772	3.04	3.04	3.04	3.04	3.04	3.04	3.04	3.04	3.04	3.04	3.04	3.04

Table 12: Mean difference in the surface LER of the GOME-2ABC and GOME-1 surface LER databases, for land surfaces. The FWHM of the distribution is also given. The numbers have been multiplied by 100.

GOME-2ABC versus OMI (MIN-LER)												
Mean surface LER difference ($\times 100$)												
λ (nm)	JAN	FEB	MAR	APR	MAY	JUN	JUL	AUG	SEP	OCT	NOV	DEC
335	3.00	2.91	2.82	2.24	1.86	1.75	2.03	2.26	2.50	2.64	2.74	2.90
354	2.20	2.17	2.13	1.76	1.44	1.36	1.62	1.79	1.90	1.98	2.05	2.13
367	1.74	1.73	1.72	1.49	1.22	1.16	1.37	1.52	1.54	1.55	1.60	1.69
380	1.82	1.79	1.83	1.70	1.57	1.57	1.78	1.78	1.66	1.61	1.65	1.75
388	1.39	1.37	1.43	1.31	1.20	1.19	1.38	1.38	1.26	1.21	1.25	1.34
416	0.36	0.36	0.40	0.32	0.24	0.25	0.42	0.38	0.24	0.20	0.23	0.30
425	0.35	0.35	0.39	0.35	0.28	0.31	0.48	0.43	0.25	0.20	0.21	0.29
440	0.21	0.23	0.28	0.26	0.21	0.25	0.40	0.33	0.13	0.09	0.11	0.16
463	0.14	0.18	0.22	0.22	0.22	0.28	0.42	0.30	0.07	0.03	0.06	0.10
494	0.01	0.05	0.09	0.13	0.16	0.23	0.35	0.21	-0.04	-0.07	-0.04	-0.01
FWHM of distribution ($\times 100$)												
λ (nm)	JAN	FEB	MAR	APR	MAY	JUN	JUL	AUG	SEP	OCT	NOV	DEC
335	2.13	2.05	2.02	2.10	2.34	2.34	2.20	2.02	2.06	2.02	2.16	2.24
354	2.04	2.00	1.99	1.99	2.10	2.10	2.01	1.93	2.01	1.95	2.06	2.12
367	2.05	2.08	2.13	2.04	1.93	1.93	1.87	1.95	1.99	1.97	2.08	2.13
380	2.09	2.11	2.19	2.22	2.06	2.11	2.12	2.18	2.07	2.02	2.10	2.15
388	1.99	2.03	2.12	2.13	1.97	2.01	1.99	2.04	1.98	1.95	2.03	2.07
416	1.83	1.90	1.99	1.94	1.75	1.78	1.79	1.87	1.80	1.81	1.87	1.92
425	1.81	1.85	1.94	1.94	1.76	1.81	1.83	1.89	1.77	1.77	1.83	1.89
440	1.73	1.78	1.90	1.90	1.77	1.91	1.93	1.90	1.71	1.69	1.74	1.81
463	1.54	1.62	1.73	1.78	1.71	1.93	1.95	1.81	1.54	1.52	1.56	1.63
494	1.42	1.52	1.63	1.69	1.64	1.90	1.93	1.76	1.45	1.40	1.43	1.51

Table 13: Mean difference in the surface LER of the GOME-2ABC and OMI surface LER databases, for water surfaces. The FWHM of the distribution is also given. The numbers have been multiplied by 100.

GOME-2ABC versus OMI (MIN-LER)												
Mean surface LER difference ($\times 100$)												
λ (nm)	JAN	FEB	MAR	APR	MAY	JUN	JUL	AUG	SEP	OCT	NOV	DEC
335	1.94	1.97	1.90	1.60	1.23	1.14	1.39	1.48	1.49	1.51	1.59	1.68
354	1.39	1.44	1.36	1.14	0.82	0.74	0.95	1.03	1.01	1.02	1.11	1.13
367	1.31	1.34	1.28	1.10	0.82	0.75	0.93	0.99	0.96	1.01	1.07	1.07
380	1.49	1.50	1.44	1.28	1.04	0.99	1.14	1.16	1.11	1.17	1.25	1.24
388	1.19	1.21	1.18	1.04	0.82	0.78	0.92	0.92	0.85	0.89	0.96	0.95
416	0.59	0.58	0.51	0.41	0.22	0.17	0.28	0.28	0.30	0.41	0.44	0.42
425	0.56	0.55	0.48	0.40	0.20	0.15	0.26	0.28	0.29	0.40	0.42	0.40
440	0.47	0.45	0.39	0.32	0.14	0.10	0.19	0.20	0.22	0.35	0.36	0.34
463	0.37	0.35	0.29	0.25	0.11	0.06	0.14	0.14	0.16	0.29	0.27	0.25
494	0.20	0.19	0.14	0.14	0.03	-0.01	0.06	0.05	0.06	0.19	0.15	0.11
FWHM of distribution ($\times 100$)												
λ (nm)	JAN	FEB	MAR	APR	MAY	JUN	JUL	AUG	SEP	OCT	NOV	DEC
335	3.93	3.59	3.35	3.17	2.85	3.01	3.10	3.05	3.11	3.70	3.88	3.99
354	3.37	3.23	3.05	2.87	2.54	2.61	2.69	2.67	2.84	3.22	3.24	3.31
367	2.95	2.86	2.74	2.67	2.29	2.30	2.43	2.34	2.53	2.77	2.83	2.90
380	2.79	2.76	2.65	2.54	2.15	2.12	2.25	2.22	2.46	2.61	2.66	2.70
388	2.79	2.75	2.64	2.56	2.16	2.12	2.23	2.19	2.43	2.62	2.65	2.69
416	2.64	2.69	2.69	2.65	2.04	1.98	2.05	1.94	2.09	2.28	2.40	2.48
425	2.66	2.70	2.69	2.62	2.01	1.94	2.00	1.89	2.07	2.28	2.40	2.50
440	2.71	2.74	2.70	2.61	1.99	1.88	1.94	1.85	2.04	2.27	2.40	2.53
463	2.83	2.82	2.74	2.64	2.00	1.87	1.93	1.88	2.03	2.30	2.47	2.64
494	2.90	2.87	2.78	2.68	2.05	1.89	1.96	1.91	2.05	2.34	2.54	2.74

Table 14: Mean difference in the surface LER of the GOME-2ABC and OMI surface LER databases, for land surfaces. The FWHM of the distribution is also given. The numbers have been multiplied by 100.

GOME-2ABC versus OMI (MODE-LER)												
Mean surface LER difference ($\times 100$)												
λ (nm)	JAN	FEB	MAR	APR	MAY	JUN	JUL	AUG	SEP	OCT	NOV	DEC
335	2.71	2.62	2.53	1.97	1.61	1.50	1.78	2.00	2.22	2.35	2.45	2.61
354	1.92	1.89	1.85	1.49	1.20	1.12	1.38	1.54	1.62	1.69	1.77	1.85
367	1.40	1.39	1.38	1.16	0.91	0.85	1.08	1.20	1.20	1.21	1.28	1.36
380	1.47	1.46	1.49	1.35	1.23	1.25	1.47	1.45	1.31	1.27	1.33	1.41
388	1.04	1.04	1.08	0.96	0.86	0.86	1.05	1.04	0.91	0.86	0.92	1.00
416	0.01	0.02	0.04	-0.03	-0.10	-0.09	0.08	0.02	-0.12	-0.16	-0.11	-0.05
425	0.00	0.01	0.03	-0.01	-0.08	-0.04	0.13	0.07	-0.11	-0.16	-0.12	-0.06
440	-0.14	-0.11	-0.08	-0.10	-0.14	-0.10	0.05	-0.03	-0.23	-0.26	-0.22	-0.18
463	-0.20	-0.16	-0.14	-0.13	-0.13	-0.07	0.07	-0.06	-0.28	-0.31	-0.27	-0.24
494	-0.33	-0.28	-0.26	-0.22	-0.19	-0.12	0.00	-0.14	-0.38	-0.41	-0.36	-0.34
FWHM of distribution ($\times 100$)												
λ (nm)	JAN	FEB	MAR	APR	MAY	JUN	JUL	AUG	SEP	OCT	NOV	DEC
335	2.03	1.96	1.89	1.93	2.16	2.16	2.07	1.87	1.91	1.91	2.07	2.14
354	1.93	1.91	1.85	1.83	1.91	1.91	1.86	1.78	1.87	1.85	1.98	2.03
367	1.97	2.01	2.04	1.93	1.79	1.79	1.79	1.86	1.91	1.91	2.05	2.09
380	2.03	2.06	2.12	2.14	1.97	2.06	2.10	2.15	2.01	1.97	2.08	2.12
388	1.95	1.99	2.06	2.06	1.89	1.95	1.97	2.01	1.93	1.90	2.01	2.04
416	1.81	1.89	1.95	1.91	1.71	1.76	1.80	1.87	1.78	1.77	1.85	1.90
425	1.79	1.85	1.91	1.91	1.74	1.81	1.85	1.90	1.76	1.73	1.81	1.88
440	1.72	1.79	1.88	1.88	1.76	1.94	1.97	1.92	1.70	1.67	1.73	1.80
463	1.55	1.65	1.73	1.78	1.72	1.98	2.01	1.84	1.56	1.52	1.56	1.63
494	1.43	1.56	1.64	1.71	1.67	1.96	2.00	1.80	1.46	1.40	1.44	1.51

Table 15: Mean difference in the surface LER of the GOME-2ABC and OMI surface LER databases, for water surfaces. The FWHM of the distribution is also given. The numbers have been multiplied by 100.

GOME-2ABC versus OMI (MODE-LER)												
Mean surface LER difference ($\times 100$)												
λ (nm)	JAN	FEB	MAR	APR	MAY	JUN	JUL	AUG	SEP	OCT	NOV	DEC
335	1.44	1.57	1.46	1.14	0.74	0.68	0.90	0.92	0.80	0.76	0.97	1.15
354	0.87	1.00	0.89	0.66	0.31	0.26	0.45	0.45	0.31	0.30	0.51	0.60
367	0.70	0.81	0.72	0.54	0.22	0.18	0.34	0.33	0.19	0.22	0.39	0.46
380	0.86	0.94	0.85	0.68	0.39	0.35	0.50	0.47	0.32	0.38	0.56	0.60
388	0.53	0.63	0.56	0.42	0.15	0.12	0.25	0.21	0.04	0.08	0.26	0.30
416	-0.17	-0.10	-0.20	-0.26	-0.48	-0.52	-0.39	-0.44	-0.54	-0.41	-0.30	-0.30
425	-0.20	-0.13	-0.24	-0.27	-0.52	-0.55	-0.41	-0.45	-0.55	-0.43	-0.33	-0.34
440	-0.31	-0.24	-0.34	-0.35	-0.58	-0.61	-0.48	-0.53	-0.62	-0.48	-0.39	-0.42
463	-0.42	-0.35	-0.44	-0.42	-0.63	-0.65	-0.53	-0.59	-0.67	-0.53	-0.48	-0.52
494	-0.59	-0.51	-0.58	-0.52	-0.70	-0.72	-0.60	-0.66	-0.75	-0.61	-0.59	-0.65
FWHM of distribution ($\times 100$)												
λ (nm)	JAN	FEB	MAR	APR	MAY	JUN	JUL	AUG	SEP	OCT	NOV	DEC
335	4.81	4.56	4.23	3.78	3.50	3.60	3.66	3.69	3.73	4.37	4.82	4.95
354	4.36	4.28	3.98	3.57	3.24	3.31	3.31	3.31	3.46	3.90	4.19	4.36
367	4.02	3.94	3.74	3.49	3.16	3.12	3.14	3.07	3.32	3.64	3.87	3.99
380	3.95	3.92	3.72	3.46	3.05	2.97	3.00	3.00	3.31	3.56	3.73	3.85
388	3.98	3.94	3.75	3.54	3.11	3.02	3.03	3.01	3.34	3.60	3.75	3.86
416	3.92	3.95	3.85	3.74	3.18	3.02	3.06	2.94	3.15	3.39	3.57	3.65
425	3.98	4.02	3.91	3.77	3.19	3.01	3.06	2.96	3.17	3.43	3.62	3.69
440	4.08	4.14	4.00	3.84	3.21	3.00	3.06	2.97	3.19	3.46	3.66	3.75
463	4.27	4.34	4.15	3.95	3.25	3.01	3.07	3.02	3.24	3.53	3.78	3.90
494	4.44	4.51	4.27	4.07	3.34	3.03	3.10	3.07	3.29	3.59	3.86	4.02

Table 16: Mean difference in the surface LER of the GOME-2ABC and OMI surface LER databases, for land surfaces. The FWHM of the distribution is also given. The numbers have been multiplied by 100.

GOME-2ABC-PMD versus OMI (MIN-LER)												
Mean surface LER difference ($\times 100$)												
PMD	JAN	FEB	MAR	APR	MAY	JUN	JUL	AUG	SEP	OCT	NOV	DEC
4	-0.22	-0.37	-0.45	-0.86	-1.13	-1.32	-1.03	-0.91	-0.78	-0.65	-0.51	-0.27
5	-0.70	-0.82	-0.93	-1.27	-1.52	-1.68	-1.41	-1.32	-1.18	-1.07	-0.95	-0.76
6	0.65	0.63	0.68	0.46	0.21	0.11	0.32	0.42	0.48	0.48	0.53	0.62
7	-0.98	-0.95	-0.89	-1.14	-1.33	-1.40	-1.20	-1.16	-1.12	-1.13	-1.11	-1.05
8	-0.16	-0.10	-0.00	-0.09	-0.20	-0.21	-0.05	-0.07	-0.19	-0.26	-0.25	-0.22
9	-0.55	-0.46	-0.37	-0.37	-0.39	-0.36	-0.26	-0.32	-0.54	-0.60	-0.60	-0.57
FWHM of distribution ($\times 100$)												
PMD	JAN	FEB	MAR	APR	MAY	JUN	JUL	AUG	SEP	OCT	NOV	DEC
4	1.71	1.70	1.82	2.00	2.26	2.47	2.20	1.89	1.89	1.83	1.85	1.79
5	1.72	1.70	1.82	1.97	2.23	2.39	2.14	1.88	1.84	1.79	1.83	1.78
6	1.81	1.83	1.87	1.78	1.85	1.93	1.82	1.74	1.72	1.72	1.80	1.82
7	1.66	1.69	1.69	1.64	1.70	1.77	1.71	1.56	1.51	1.57	1.65	1.66
8	1.76	1.85	1.96	1.81	1.68	1.81	1.82	1.79	1.72	1.70	1.76	1.76
9	1.54	1.66	1.81	1.73	1.61	1.88	1.91	1.83	1.57	1.49	1.50	1.53

Table 17: Mean difference in the surface LER of the GOME-2ABC-PMD and OMI surface LER databases, for water surfaces. The FWHM of the distribution is also given. The numbers have been multiplied by 100.

GOME-2ABC-PMD versus OMI (MIN-LER)												
Mean surface LER difference ($\times 100$)												
PMD	JAN	FEB	MAR	APR	MAY	JUN	JUL	AUG	SEP	OCT	NOV	DEC
4	-1.06	-1.07	-1.05	-1.22	-1.54	-1.63	-1.40	-1.32	-1.34	-1.41	-1.31	-1.19
5	-1.50	-1.47	-1.46	-1.58	-1.87	-1.95	-1.73	-1.67	-1.70	-1.80	-1.73	-1.63
6	0.11	0.12	0.11	0.06	-0.19	-0.25	-0.11	-0.10	-0.11	-0.03	0.02	-0.04
7	-0.93	-0.87	-0.85	-0.87	-1.07	-1.13	-0.99	-1.00	-1.05	-1.07	-1.03	-1.08
8	-0.15	-0.11	-0.12	-0.13	-0.27	-0.32	-0.23	-0.25	-0.28	-0.20	-0.19	-0.27
9	0.03	0.06	0.07	0.09	-0.07	-0.14	-0.08	-0.09	-0.09	0.01	0.01	-0.06
FWHM of distribution ($\times 100$)												
PMD	JAN	FEB	MAR	APR	MAY	JUN	JUL	AUG	SEP	OCT	NOV	DEC
4	4.43	4.33	3.90	3.38	3.14	3.17	3.20	3.13	3.22	3.54	3.88	4.22
5	4.28	4.20	3.78	3.29	3.00	2.99	3.05	2.99	3.07	3.35	3.69	4.02
6	3.06	3.20	2.97	2.76	2.32	2.33	2.39	2.30	2.38	2.52	2.67	2.80
7	2.84	2.93	2.75	2.61	2.15	2.14	2.20	2.09	2.15	2.38	2.58	2.62
8	2.49	2.62	2.48	2.39	1.86	1.78	1.84	1.78	1.88	2.11	2.22	2.28
9	2.63	2.72	2.60	2.58	1.94	1.78	1.83	1.81	1.92	2.17	2.30	2.43

Table 18: Mean difference in the surface LER of the GOME-2ABC-PMD and OMI surface LER databases, for land surfaces. The FWHM of the distribution is also given. The numbers have been multiplied by 100.

GOME-2ABC-PMD versus OMI (MODE-LER)												
Mean surface LER difference ($\times 100$)												
PMD	JAN	FEB	MAR	APR	MAY	JUN	JUL	AUG	SEP	OCT	NOV	DEC
4	-0.50	-0.64	-0.71	-1.12	-1.39	-1.58	-1.30	-1.17	-1.06	-0.94	-0.79	-0.56
5	-0.98	-1.09	-1.19	-1.53	-1.77	-1.92	-1.66	-1.58	-1.46	-1.36	-1.23	-1.05
6	0.31	0.31	0.35	0.13	-0.09	-0.18	0.03	0.11	0.15	0.15	0.22	0.29
7	-1.32	-1.28	-1.22	-1.47	-1.64	-1.71	-1.52	-1.48	-1.45	-1.47	-1.43	-1.38
8	-0.51	-0.44	-0.36	-0.45	-0.55	-0.56	-0.40	-0.42	-0.55	-0.62	-0.59	-0.56
9	-0.88	-0.80	-0.72	-0.72	-0.75	-0.71	-0.61	-0.67	-0.89	-0.94	-0.92	-0.91
FWHM of distribution ($\times 100$)												
PMD	JAN	FEB	MAR	APR	MAY	JUN	JUL	AUG	SEP	OCT	NOV	DEC
4	1.57	1.58	1.67	1.81	2.10	2.31	2.09	1.76	1.72	1.70	1.73	1.65
5	1.59	1.58	1.67	1.78	2.03	2.19	2.01	1.73	1.68	1.67	1.73	1.67
6	1.74	1.76	1.78	1.66	1.69	1.79	1.73	1.65	1.63	1.65	1.77	1.77
7	1.60	1.64	1.63	1.53	1.57	1.65	1.63	1.49	1.44	1.52	1.61	1.61
8	1.74	1.84	1.93	1.78	1.63	1.79	1.83	1.79	1.71	1.67	1.74	1.73
9	1.56	1.70	1.83	1.75	1.63	1.94	1.97	1.89	1.61	1.50	1.50	1.53

Table 19: Mean difference in the surface LER of the GOME-2ABC-PMD and OMI surface LER databases, for water surfaces. The FWHM of the distribution is also given. The numbers have been multiplied by 100.

GOME-2ABC-PMD versus OMI (MODE-LER)												
Mean surface LER difference ($\times 100$)												
PMD	JAN	FEB	MAR	APR	MAY	JUN	JUL	AUG	SEP	OCT	NOV	DEC
4	-1.65	-2.10	-1.50	-1.72	-2.06	-2.08	-1.86	-1.84	-1.97	-2.08	-1.94	-1.78
5	-2.08	-2.10	-1.92	-2.07	-2.37	-2.38	-2.18	-2.18	-2.31	-2.44	-2.33	-2.20
6	-0.51	-0.38	-0.44	-0.53	-0.80	-0.82	-0.65	-0.72	-0.84	-0.76	-0.66	-0.67
7	-1.63	-1.47	-1.48	-1.51	-1.72	-1.74	-1.60	-1.66	-1.81	-1.86	-1.78	-1.76
8	-0.90	-0.76	-0.81	-0.82	-0.98	-1.02	-0.90	-0.96	-1.09	-1.02	-0.96	-1.01
9	-0.78	-0.64	-0.69	-0.66	-0.87	-0.91	-0.81	-0.87	-0.96	-0.84	-0.81	-0.87
FWHM of distribution ($\times 100$)												
PMD	JAN	FEB	MAR	APR	MAY	JUN	JUL	AUG	SEP	OCT	NOV	DEC
4	5.05	3.04	4.72	4.06	3.86	3.99	3.92	3.88	3.99	4.15	4.61	4.90
5	4.85	3.04	4.60	3.94	3.70	3.78	3.73	3.70	3.81	3.95	4.36	4.63
6	4.11	4.27	3.96	3.61	3.20	3.29	3.25	3.22	3.34	3.46	3.62	3.93
7	3.91	4.01	3.73	3.50	3.10	3.11	3.09	3.01	3.14	3.30	3.52	3.69
8	3.80	3.84	3.62	3.46	2.92	2.81	2.88	2.88	3.05	3.25	3.38	3.48
9	4.16	4.17	3.87	3.75	3.07	2.87	3.03	2.98	3.12	3.37	3.56	3.72

Table 20: Mean difference in the surface LER of the GOME-2ABC-PMD and OMI surface LER databases, for land surfaces. The FWHM of the distribution is also given. The numbers have been multiplied by 100.

GOME-2ABC-PMD versus GOME-2ABC (MIN-LER)												
Mean surface LER difference ($\times 100$)												
PMD	JAN	FEB	MAR	APR	MAY	JUN	JUL	AUG	SEP	OCT	NOV	DEC
4	-3.23	-3.27	-3.18	-3.13	-3.10	-3.17	-3.19	-3.21	-3.23	-3.26	-3.25	-3.17
5	-3.10	-3.13	-3.10	-3.02	-2.98	-3.03	-3.07	-3.11	-3.10	-3.13	-3.12	-3.06
6	-1.07	-1.09	-1.04	-0.99	-0.95	-0.98	-0.99	-1.04	-1.03	-1.04	-1.04	-1.02
7	-2.70	-2.72	-2.70	-2.66	-2.63	-2.68	-2.72	-2.73	-2.72	-2.70	-2.70	-2.67
8	-0.52	-0.47	-0.42	-0.39	-0.38	-0.39	-0.40	-0.41	-0.44	-0.46	-0.47	-0.48
9	-0.70	-0.66	-0.62	-0.59	-0.58	-0.59	-0.62	-0.63	-0.64	-0.64	-0.65	-0.66
10	-0.69	-0.66	-0.64	-0.64	-0.63	-0.63	-0.67	-0.67	-0.68	-0.65	-0.67	-0.67
11	-0.38	-0.36	-0.34	-0.34	-0.33	-0.34	-0.37	-0.36	-0.36	-0.35	-0.36	-0.36
13	-0.10	-0.10	-0.10	-0.10	-0.10	-0.11	-0.13	-0.12	-0.11	-0.10	-0.10	-0.10
14	-0.25	-0.26	-0.26	-0.26	-0.26	-0.28	-0.29	-0.28	-0.26	-0.24	-0.25	-0.25
FWHM of distribution ($\times 100$)												
PMD	JAN	FEB	MAR	APR	MAY	JUN	JUL	AUG	SEP	OCT	NOV	DEC
4	1.51	1.60	1.51	1.46	1.53	1.70	1.67	1.45	1.41	1.42	1.51	1.49
5	1.45	1.50	1.43	1.35	1.36	1.53	1.54	1.37	1.34	1.33	1.42	1.42
6	1.01	1.02	0.98	0.95	0.93	1.03	1.02	0.98	0.97	0.94	0.99	1.00
7	1.12	1.16	1.11	1.07	1.01	1.13	1.19	1.10	1.13	1.08	1.11	1.10
8	0.75	0.75	0.69	0.67	0.66	0.70	0.73	0.72	0.73	0.72	0.74	0.74
9	0.61	0.60	0.57	0.54	0.56	0.61	0.63	0.61	0.61	0.57	0.59	0.59
10	0.49	0.48	0.47	0.48	0.48	0.48	0.50	0.50	0.47	0.45	0.47	0.48
11	0.43	0.41	0.37	0.36	0.36	0.38	0.43	0.41	0.40	0.37	0.39	0.39
13	0.35	0.35	0.34	0.33	0.32	0.34	0.36	0.35	0.35	0.34	0.35	0.35
14	0.43	0.42	0.41	0.42	0.46	0.49	0.48	0.46	0.43	0.41	0.43	0.43

Table 21: Mean difference in the surface LER of the GOME-2ABC-PMD and GOME-2ABC surface LER databases, for water surfaces. The FWHM of the distribution is also given. The numbers have been multiplied by 100.

GOME-2ABC-PMD versus GOME-2ABC (MIN-LER)												
Mean surface LER difference ($\times 100$)												
PMD	JAN	FEB	MAR	APR	MAY	JUN	JUL	AUG	SEP	OCT	NOV	DEC
4	-2.96	-3.02	-2.98	-2.85	-2.76	-2.69	-2.69	-2.77	-2.80	-2.80	-2.81	-2.86
5	-2.81	-2.86	-2.86	-2.73	-2.63	-2.56	-2.57	-2.66	-2.65	-2.65	-2.67	-2.73
6	-1.16	-1.19	-1.17	-1.07	-1.03	-0.99	-1.00	-1.08	-1.06	-1.04	-1.06	-1.10
7	-2.35	-2.34	-2.28	-2.17	-2.09	-2.08	-2.10	-2.15	-2.14	-2.22	-2.29	-2.32
8	-0.71	-0.66	-0.60	-0.53	-0.50	-0.48	-0.49	-0.52	-0.56	-0.61	-0.65	-0.70
9	-0.37	-0.30	-0.23	-0.20	-0.21	-0.22	-0.24	-0.26	-0.27	-0.30	-0.35	-0.36
10	-0.92	-0.87	-0.82	-0.77	-0.75	-0.74	-0.75	-0.73	-0.74	-0.79	-0.91	-0.93
11	-0.51	-0.46	-0.43	-0.39	-0.38	-0.36	-0.37	-0.35	-0.36	-0.39	-0.48	-0.51
13	-0.32	-0.27	-0.25	-0.20	-0.17	-0.15	-0.15	-0.14	-0.15	-0.19	-0.27	-0.33
14	-3.87	-3.77	-3.58	-3.47	-3.78	-3.95	-4.02	-3.80	-3.50	-3.25	-3.30	-3.69
FWHM of distribution ($\times 100$)												
PMD	JAN	FEB	MAR	APR	MAY	JUN	JUL	AUG	SEP	OCT	NOV	DEC
4	2.77	2.75	2.28	1.93	2.06	2.14	1.98	1.85	1.86	2.15	2.56	2.77
5	2.55	2.54	2.13	1.79	1.85	1.94	1.84	1.76	1.82	2.08	2.34	2.55
6	1.90	1.79	1.54	1.32	1.37	1.51	1.43	1.33	1.37	1.63	1.69	1.85
7	1.78	1.76	1.51	1.30	1.19	1.26	1.30	1.30	1.33	1.41	1.76	1.80
8	1.28	1.26	1.15	1.06	1.05	1.06	1.03	0.95	0.93	0.95	1.13	1.26
9	1.37	1.31	1.18	1.01	0.90	0.85	0.86	0.88	0.90	0.99	1.26	1.38
10	1.49	1.38	1.18	1.02	0.95	0.92	0.95	0.93	0.92	0.98	1.36	1.55
11	1.53	1.43	1.29	1.11	1.02	0.96	1.00	0.98	0.97	1.01	1.26	1.51
13	1.68	1.57	1.41	1.21	1.12	1.05	1.06	1.05	1.06	1.12	1.34	1.62
14	4.99	4.98	4.80	4.48	4.14	4.24	4.54	4.35	4.00	4.09	3.96	4.43

Table 22: Mean difference in the surface LER of the GOME-2ABC-PMD and GOME-2ABC surface LER databases, for land surfaces. The FWHM of the distribution is also given. The numbers have been multiplied by 100.

GOME-2ABC-PMD versus GOME-2ABC (MODE-LER)												
Mean surface LER difference ($\times 100$)												
PMD	JAN	FEB	MAR	APR	MAY	JUN	JUL	AUG	SEP	OCT	NOV	DEC
4	-3.23	-3.27	-3.18	-3.13	-3.10	-3.17	-3.19	-3.21	-3.23	-3.26	-3.24	-3.17
5	-3.10	-3.13	-3.09	-3.02	-2.98	-3.04	-3.07	-3.11	-3.10	-3.13	-3.12	-3.06
6	-1.07	-1.09	-1.04	-0.99	-0.95	-0.98	-0.99	-1.04	-1.03	-1.04	-1.03	-1.01
7	-2.70	-2.72	-2.70	-2.66	-2.63	-2.68	-2.72	-2.73	-2.72	-2.70	-2.69	-2.67
8	-0.52	-0.47	-0.42	-0.39	-0.38	-0.39	-0.40	-0.41	-0.44	-0.46	-0.46	-0.48
9	-0.70	-0.66	-0.62	-0.59	-0.58	-0.59	-0.62	-0.63	-0.64	-0.64	-0.65	-0.66
10	-0.69	-0.66	-0.63	-0.64	-0.63	-0.63	-0.67	-0.67	-0.67	-0.65	-0.67	-0.67
11	-0.38	-0.36	-0.34	-0.34	-0.33	-0.34	-0.37	-0.36	-0.36	-0.35	-0.36	-0.36
13	-0.10	-0.10	-0.10	-0.10	-0.11	-0.11	-0.13	-0.12	-0.11	-0.10	-0.10	-0.10
14	-0.25	-0.26	-0.26	-0.26	-0.26	-0.28	-0.29	-0.28	-0.26	-0.24	-0.25	-0.25
FWHM of distribution ($\times 100$)												
PMD	JAN	FEB	MAR	APR	MAY	JUN	JUL	AUG	SEP	OCT	NOV	DEC
4	1.51	1.60	1.51	1.46	1.53	1.70	1.68	1.45	1.42	1.41	1.51	1.49
5	1.44	1.50	1.43	1.36	1.36	1.54	1.55	1.37	1.34	1.33	1.41	1.42
6	1.01	1.02	0.98	0.95	0.93	1.03	1.02	0.98	0.97	0.94	0.98	0.99
7	1.12	1.16	1.10	1.07	1.01	1.13	1.19	1.10	1.13	1.07	1.10	1.09
8	0.75	0.75	0.69	0.67	0.66	0.71	0.74	0.72	0.72	0.71	0.74	0.74
9	0.61	0.60	0.57	0.54	0.56	0.61	0.63	0.61	0.60	0.57	0.59	0.59
10	0.49	0.48	0.47	0.48	0.48	0.48	0.50	0.50	0.47	0.45	0.47	0.48
11	0.42	0.41	0.37	0.36	0.36	0.38	0.43	0.41	0.40	0.37	0.39	0.39
13	0.35	0.35	0.34	0.33	0.32	0.34	0.36	0.35	0.34	0.34	0.35	0.35
14	0.43	0.42	0.41	0.42	0.46	0.49	0.48	0.46	0.43	0.41	0.43	0.43

Table 23: Mean difference in the surface LER of the GOME-2ABC-PMD and GOME-2ABC surface LER databases, for water surfaces. The FWHM of the distribution is also given. The numbers have been multiplied by 100.

GOME-2ABC-PMD versus GOME-2ABC (MODE-LER)												
Mean surface LER difference ($\times 100$)												
PMD	JAN	FEB	MAR	APR	MAY	JUN	JUL	AUG	SEP	OCT	NOV	DEC
4	-3.00	-3.03	-2.95	-2.81	-2.73	-2.65	-2.65	-2.71	-2.73	-2.77	-2.82	-2.89
5	-2.86	-2.89	-2.85	-2.70	-2.61	-2.53	-2.54	-2.60	-2.59	-2.63	-2.69	-2.75
6	-1.17	-1.19	-1.18	-1.06	-1.01	-0.96	-0.96	-1.03	-1.01	-1.02	-1.07	-1.11
7	-2.38	-2.36	-2.31	-2.17	-2.10	-2.08	-2.09	-2.13	-2.11	-2.22	-2.31	-2.33
8	-0.71	-0.67	-0.61	-0.54	-0.51	-0.50	-0.51	-0.53	-0.55	-0.61	-0.66	-0.70
9	-0.37	-0.31	-0.25	-0.22	-0.22	-0.23	-0.25	-0.28	-0.27	-0.30	-0.36	-0.36
10	-0.93	-0.88	-0.83	-0.78	-0.77	-0.76	-0.77	-0.74	-0.75	-0.79	-0.92	-0.92
11	-0.52	-0.48	-0.45	-0.40	-0.39	-0.38	-0.38	-0.36	-0.36	-0.39	-0.49	-0.51
13	-0.32	-0.28	-0.26	-0.21	-0.18	-0.15	-0.15	-0.14	-0.15	-0.18	-0.28	-0.33
14	-4.16	-4.17	-3.90	-3.61	-3.95	-4.12	-4.20	-3.96	-3.60	-3.31	-3.47	-3.94
FWHM of distribution ($\times 100$)												
PMD	JAN	FEB	MAR	APR	MAY	JUN	JUL	AUG	SEP	OCT	NOV	DEC
4	2.64	2.70	2.30	1.94	2.07	2.08	1.91	1.79	1.78	2.10	2.49	2.63
5	2.42	2.52	2.16	1.78	1.84	1.88	1.76	1.67	1.70	2.00	2.28	2.42
6	1.89	1.88	1.61	1.34	1.44	1.59	1.48	1.36	1.36	1.64	1.75	1.91
7	1.75	1.79	1.58	1.30	1.23	1.32	1.33	1.29	1.30	1.42	1.77	1.75
8	1.35	1.34	1.21	1.08	1.09	1.12	1.08	0.99	0.95	0.96	1.17	1.32
9	1.44	1.38	1.22	1.03	0.93	0.90	0.92	0.91	0.91	0.99	1.32	1.44
10	1.55	1.47	1.24	1.04	0.97	0.97	1.03	0.99	0.94	0.97	1.41	1.52
11	1.63	1.58	1.36	1.14	1.05	1.02	1.09	1.05	1.00	1.01	1.32	1.55
13	1.76	1.69	1.46	1.24	1.14	1.10	1.12	1.08	1.07	1.10	1.41	1.65
14	5.53	5.59	5.19	4.73	4.37	4.46	4.74	4.54	4.19	4.25	4.34	4.99

Table 24: Mean difference in the surface LER of the GOME-2ABC-PMD and GOME-2ABC surface LER databases, for land surfaces. The FWHM of the distribution is also given. The numbers have been multiplied by 100.

References

- AC SAF Project Team (2023), AC SAF Product Requirements Document, Doc. No. SAF/AC/FMI/RQ/PRD/001, Issue 2.2, 20 December 2023, AC SAF.
- Burrows, J. P., et al. (1999), The Global Ozone Monitoring Experiment (GOME): Mission concept and first scientific results, *J. Atmos. Sci.*, 56(2), 151–175.
- EUMETSAT (2021), GOME-2 Factsheet, Doc. No. EUM/OPS/DOC/10/1299, Issue 4f, 14 December 2021, EUMETSAT, Darmstadt, Germany, <https://www.eumetsat.int/media/47563>.
- Heath, D. F., A. J. Krueger, H. A. Roeder, and B. D. Henderson (1975), The Solar Backscatter Ultraviolet and Total Ozone Mapping Spectrometer (SBUV/TOMS) for NIMBUS G, *Opt. Eng.*, 14(4), 144323, doi:10.1117/12.7971839.
- Herman, J. R., and E. A. Celarier (1997), Earth surface reflectivity climatology at 340–380 nm from TOMS data, *J. Geophys. Res.*, 102(D23), 28,003–28,011, doi:10.1029/97JD02074.
- Kleipool, Q. L., M. R. Dobber, J. F. de Haan, and P. F. Levelt (2008), Earth surface reflectance climatology from 3 years of OMI data, *J. Geophys. Res.*, 113, D18308, doi:10.1029/2008JD010290.
- Koelemeijer, R. B. A., J. F. de Haan, and P. Stammes (2003), A database of spectral surface reflectivity in the range 335–772 nm derived from 5.5 years of GOME observations, *J. Geophys. Res.*, 108(D2), 4070, doi:10.1029/2002JD002429.
- Levelt, P. F., G. H. J. van den Oord, M. R. Dobber, A. Mälkki, H. Visser, J. de Vries, P. Stammes, J.O.V. Lundell, and H. Saari (2006), The Ozone Monitoring Instrument, *IEEE Trans. Geosci. Remote Sens.*, 44(5), 1093–1101, doi:10.1109/TGRS.2006.872333.
- Popp, C., P. Wang, D. Brunner, P. Stammes, Y. Zhou, and M. Grzegorski (2011), MERIS albedo climatology for FRESCO+ O2 A-band cloud retrieval, *Atmos. Meas. Tech.*, 4, 463–483, doi:10.5194/amt-4-463-2011.
- Schaaf, C., and Z. Wang (2015), MCD43C1 MODIS/Terra+Aqua BRDF/AlbedoModel Parameters Daily L3 Global 0.05Deg CMG V006, distributed by NASA EOSDIS Land Processes DAAC, doi:10.5067/MODIS/MCD43C1.006.
- Tilstra, L. G., O. N. E. Tuinder, and P. Stammes (2011), GOME-2 PMD band reflectances – verification report, *KNMI Report KNMI-RP-2011-01*, Issue 2.0, Royal Netherlands Meteorological Institute, De Bilt, The Netherlands.

- Tilstra, L. G., M. de Graaf, I. Aben, and P. Stammes (2012a), In-flight degradation correction of SCIAMACHY UV reflectances and Absorbing Aerosol Index, *J. Geophys. Res.*, *117*, D06209, doi:10.1029/2011JD016957.
- Tilstra, L. G., O. N. E. Tuinder, and P. Stammes (2012b), Introducing a new method for in-flight degradation correction of the Earth reflectance measured by GOME-2, and application to the AAI, in *Proceedings of the 2012 EUMETSAT Meteorological Satellite Conference*, EUMETSAT P.61, Sopot, Poland.
- Tilstra, L. G., O. N. E. Tuinder, P. Wang, and P. Stammes (2017), Surface reflectivity climatologies from UV to NIR determined from Earth observations by GOME-2 and SCIAMACHY, *J. Geophys. Res. Atmos.*, *122*, 4084–4111, doi:10.1002/2016JD025940.
- Tilstra, L. G., O. N. E. Tuinder, P. Wang, and P. Stammes (2021), Directionally dependent Lambertian-equivalent reflectivity (DLER) of the Earth’s surface measured by the GOME-2 satellite instruments, *Atmos. Meas. Tech.*, *14*, 4219–4238, doi:10.5194/amt-14-4219-2021.
- Tilstra, L. G., O. N. E. Tuinder, and P. Stammes (2024a), GOME-2 surface LER product – Algorithm Theoretical Basis Document, *KNMI Report SAF/AC/KNMI/ATBD/003*, Issue 4.3, November 19, 2024.
- Tilstra, L. G., O. N. E. Tuinder, and P. Stammes (2024b), GOME-2 surface LER product – Product User Manual, *KNMI Report SAF/AC/KNMI/PUM/004*, Issue 4.2, November 19, 2024.